

# Technische Universität München

Wissenschaftszentrum Weihenstephan für Ernährung, Landnutzung und Umwelt  
Holzforschung München, Professur für Holz-Bioprozesse

## An investigation of the interaction between filamentous ascomycetes and lignocellulosic substrates

Lara Hassan

Vollständiger Abdruck der von der Fakultät Wissenschaftszentrum Weihenstephan für Ernährung, Landnutzung und Umwelt der Technischen Universität München zur Erlangung des akademischen Grades eines

Doktors der Naturwissenschaften

genehmigten Dissertation.

Vorsitzender: Prof. Dr. Klaus Richter

Prüfer der Dissertation: 1. Prof. Dr. Johan Philipp Benz  
2. Prof. Dr. Caroline Gutjahr

Die Dissertation wurde am 05.06.2019 bei der Technischen Universität München eingereicht und durch die Fakultät Wissenschaftszentrum Weihenstephan für Ernährung, Landnutzung, und Umwelt am 10.09.2019 angenommen.











## Summary

The need to develop renewable raw materials for industrial chemistry as a substitute for oil has been growing over the last decades. In this context, the use of plant biomass is considered a cheaper, less polluting alternative, and a model for adding value to agro-industrial product chains, such as soybeans, sugarcane/sugar beet, and corn but also forestry. These feedstock materials mainly consist of cellulose, which is embedded in a matrix of covalently linked hemicelluloses and lignin. Fungi have the ability to sense the presence of such polymers and rewire their regulatory networks to secrete enzymes that efficiently convert these into fermentable sugars. However, the high degree of cross-linking, the natural heterogeneity and consequent chemical complexity of plant biomass render it recalcitrant to degradation and increase the costs associated with such processes. The key challenge therefore is to make biomass depolymerization more rapid and less costly. The optimization of feedstock materials to better suite fermentation processes and the rational engineering of fungal strains to efficiently produce degrading enzymes will be highly beneficial for biorefinery applications. However, efforts to this end are still hampered by incomplete knowledge of how fungi perceive the substrates and integrate the respective signals to form enzyme cocktails that are tailored to the composition of the biomass in proximity.

This thesis followed a combined approach to decipher the interaction between filamentous ascomycetes and (hemi-)cellulosic substrates. In the first part of the thesis, the model filamentous fungus *Neurospora crassa* and the industrially optimized strain *Trichoderma reesei* RUT-C30 were used to assess the impact of the differences in the physicochemical characteristics of microcrystalline and powdered cellulose substrates on the production of (hemi-)cellulases. The results indicated that particularly crystallinity and hemicellulose content are major determinants of substrate performance. *In vitro* digestions, for example, demonstrated that the powdered cellulose, as the most hemicellulose-contaminated and least crystalline substrate, was the most readily hydrolysable. Intriguingly, while the fungi were able to perceive even small hemicellulosic contents in the substrates, the results indicated that the chemical composition alone does not reflect the fungal response, but other factors, such as substrate bioavailability, are also important. Moreover, only the carbon catabolite de-repressed strain, RUT-C30, was able to take full advantage of the hemicellulose impurities. Nevertheless, comparing carbon catabolite repressed and de-repressed strains of both fungi indicated that the perception differences are not solely due to carbon catabolite de-repression, but are also dependent on the species-specific regulatory networks as well.

The second part of the thesis focused on the fungal perception of the hemicellulose impurities often present in the substrates. The results provided novel insights into the overlap between cellulose and mannan (a major hemicellulose) perception pathways in *N. crassa*. This cross-talk was shown to be competitive both at the level of uptake by cellodextrin transporters and at the level of intracellular signaling, thereby causing a sort of “confusion” that is inhibitive for cellulase production. An intracellular balance between the inducing and inhibiting molecules, cellodextrins and mannodextrins, respectively, was shown to be important for the wildtype cellulolytic response. Importantly, the potential for inhibition was shown to be conserved in the industrially used strains *Myceliophthora thermophila* and *T. reesei* RUT-C30.

In summary, this thesis highlighted key factors to consider when choosing the optimal substrate for lignocellulolytic enzyme production in filamentous fungi. Furthermore, because of the importance of substrate crystallinity and hemicellulose content, they are considered possible targets for enhancing substrate effectiveness in saccharification processes. Additionally, the thesis provided novel insights that advance the fundamental understanding of the cross-talk between perception pathways governing plant cell wall utilization by fungi. The cellulase-inhibitive overlap between mannan and cellulose pathways is important to be addressed. The inhibition relief through rational engineering of mannan-insensitive strains is a critical step in the biotechnological (hemi-)cellulase production process.

## Zusammenfassung

Der Bedarf an nachwachsenden Rohstoffen für die industrielle Chemie als Ersatz für Öl ist in den letzten Jahrzehnten gestiegen. In diesem Zusammenhang wird die Nutzung pflanzlicher Biomasse als billigere, umweltfreundlichere Alternative und als Modell für die Wertschöpfung in agroindustriellen Produktketten wie Sojabohnen, Zuckerrohr/Zuckerrüben, Mais aber auch in der Forstwirtschaft angesehen. Diese Ausgangsstoffe bestehen hauptsächlich aus Cellulose, die in eine Matrix aus kovalent gebundenen Hemizellulosen und Lignin eingebettet ist. Pilze haben die Fähigkeit, das Vorhandensein solcher Polymere zu erkennen und ihre regulatorischen Netzwerke neu zu vernetzen, um Enzyme zu sekretieren, die diese Polysaccharide effizient in fermentierbare Zucker umwandeln. Der hohe Vernetzungsgrad, die natürliche Heterogenität und die damit verbundene chemische Komplexität der pflanzlichen Biomasse machen sie jedoch widerstandsfähig gegen Degradation und erhöhen die mit solchen Prozessen verbundenen Kosten. Die größte Herausforderung besteht daher darin, die Depolymerisation von Biomasse schneller und kostengünstiger zu gestalten. Die Optimierung der Ausgangsstoffe für eine bessere Anpassung der Fermentationsprozesse und die rationale genetische Modifizierung von Pilzstämmen zur effizienten Herstellung von abbaubaren Enzymen werden für Bioraffinerieanwendungen von großem Nutzen sein. Unvollständiges Wissen darüber, wie Pilze die Substrate wahrnehmen und die entsprechenden Signale zu Enzymcocktails integrieren, die auf die Zusammensetzung der Biomasse in der Nähe zugeschnitten sind, erschwert dies jedoch noch.

Diese Arbeit folgte einem kombinierten Ansatz zur Entschlüsselung der Interaktion zwischen filamentösen Ascomyceten und (hemi-)cellulosischen Substraten. Im ersten Teil der Arbeit wurden der filamentöse Pilz und Modellorganismus *Neurospora crassa* sowie der industriell optimierte Stamm *Trichoderma reesei* RUT-C30 verwendet, um die Auswirkungen der Unterschiede in den physikalisch-chemischen Eigenschaften von mikrokristallinen und pulverförmigen Cellulosesubstraten auf die Produktion von (Hemi-)Cellulasen zu beurteilen. Die Ergebnisse zeigten, dass insbesondere Kristallinität und Hemicellulosegehalt wichtige Determinanten der Substrateleistung sind. In-vitro-Fermentationen zeigten zum Beispiel, dass die pulverisierte Cellulose als das am stärksten mit Hemicellulose verunreinigte und am wenigsten kristalline Substrat am leichtesten hydrolysierbar ist. Interessanterweise zeigten die Ergebnisse, dass die chemische Zusammensetzung allein nicht die Pilzreaktion widerspiegelt, obwohl die Pilze selbst kleine hemicelluloseische Inhaltsstoffe in den Substraten wahrnehmen konnten. Stattdessen spielen weitere Faktoren, unter anderem die Bioverfügbarkeit des Substrats, eine wichtige Rolle in der Induktion von lignocellulolytischen Enzymen. Darüber hinaus konnte nur der

von Kohlenstoffkatabolit-Repression befreite Stamm RUT-C30 die Vorteile der Hemicelluloseverunreinigungen voll ausschöpfen. Der Vergleich von Kohlenstoffkatabolismus reprimierten und nicht reprimierten Pilzen zeigte jedoch, dass die zwischen den Pilzen nicht nur auf Unterschiede in der Repression des Kohlenstoffkatabolismus zurückzuführen sind, sondern auch durch die artspezifischen regulatorischen Netzwerke Wahrnehmungsunterschiede beeinflusst werden.

Der zweite Teil der Arbeit konzentrierte sich auf die pilzliche Wahrnehmung der Hemicelluloseverunreinigungen, die häufig in Substraten vorhanden sind. Die Ergebnisse lieferten neue Erkenntnisse über die Überschneidung zwischen Cellulose- und Mannan- (eine der wichtigsten Hemicellulosen) Wahrnehmungspfaden bei *N. crassa*. Die beobachtete Signalwegsüberlagerung konkurrierte sowohl auf der Ebene der Substrataufnahme durch Cellodextrin-Transporter als auch auf der Ebene der intrazellulären Signalübertragung und verursachte damit eine Art "Verwirrung", mit hemmender Wirkung auf die Cellulaseproduktion. Ein intrazelluläres Gleichgewicht zwischen den induzierenden Cellodextrinen und hemmenden Mannodextrinen erwies sich als wichtig für die cellulolytische Reaktion des Wildtyps. Des Weiteren konnte diese Hemmung in den industriell verwendeten Stämmen *Myceliophthora thermophila* und *T. reesei* RUT-C30 ebenfalls nachgewiesen werden.

Zusammenfassend lässt sich sagen, dass diese Arbeit wichtige Faktoren aufzeigt, die bei der Auswahl des optimalen Substrats für die Produktion von lignocellulolytischen Enzymen in filamentösen Pilzen zu berücksichtigen sind. Die Substratkristallinität und der Hemicellulosegehalt gelten aufgrund ihrer Bedeutung als mögliche Ziele für die Verbesserung der Substratwirkung während der Polysaccharid-Depolymerisation. Darüber hinaus lieferte diese Arbeit neue Erkenntnisse über Signalüberlagerungen zwischen Wahrnehmungspfaden, die die Nutzung der Pflanzenzellwand durch Pilze regulieren. Die Cellulaseaktivität-inhibierende Überlappung zwischen Mannan- und Cellulose Signalwegen ist hierbei besonders hervorzuheben. Die Mannan-bedingte Hemmung des Celluloseabbaus kann in nächsten Schritten durch rationale genetische Modifikation zu Stämmen hin gemindert werden, welche unempfindlich für die Mannan-induzierte Inhibition sind. Diese Stämme würden einen entscheidenden Fortschritt für die biotechnologische Produktion von (Hemi-)Cellulasen darstellen.

## Table of contents

<b>Summary</b> .....	<b>I</b>
<b>Zusammenfassung</b> .....	<b>III</b>
<b>List of figures</b> .....	<b>IX</b>
<b>List of tables</b> .....	<b>XI</b>
<b>1. Introduction</b> .....	<b>13</b>
1.1. Importance of lignocellulosic biomass for Bio-based refineries .....	13
1.2. Composition of lignocellulosic biomass .....	13
1.3. Filamentous fungi as lignocellulose degraders .....	17
1.3.1. <i>Neurospora crassa</i> as a model organism .....	18
1.3.2. <i>Trichoderma reesei</i> as an industrial organism .....	19
1.3.3. Brief overview of fungal (hemi-)cellulases .....	20
1.4. Polysaccharide perception and degradation by filamentous fungi .....	21
1.5. Aims of this study .....	24
<b>2. Materials and Methods</b> .....	<b>27</b>
2.1. Materials .....	27
2.1.1. Organisms .....	27
2.1.2. Media and solutions .....	28
2.1.3. Primers .....	31
2.1.4. Instruments and tools .....	31
2.1.5. Consumable .....	33
2.2. Methods .....	37
2.2.1. Preparation of bacterial cellulose .....	37
2.2.2. Propagation of the used organisms .....	37
2.2.3. Growth assays .....	38
2.2.4. Mycelial dry weight .....	38
2.2.5. Crossing of <i>N. crassa</i> strains .....	39
2.2.6. Genomic DNA extraction .....	39
2.2.7. Total RNA extraction .....	40
2.2.8. cDNA synthesis .....	40
2.2.9. Nucleic acid quantification .....	41
2.2.10. Polymerase Chain Reaction (PCR) .....	41
2.2.11. Quantitative real time PCR (qRT-PCR) .....	42
2.2.12. Nucleic acids separation by agarose gel electrophoresis .....	43
2.2.13. Purification of nucleic acids .....	43

2.2.14.	Restriction-ligation cloning .....	43
2.2.15.	<i>E. coli</i> transformation .....	44
2.2.16.	Plasmid DNA miniprep.....	44
2.2.17.	Nucleic acids sequencing .....	44
2.2.18.	<i>N. crassa</i> transformation.....	45
2.2.19.	Glycerol stocks .....	46
2.2.20.	Extraction of intracellular metabolites .....	46
2.2.21.	Extraction of intracellular protein from <i>N. crassa</i> .....	46
2.2.22.	Protein expression and purification from <i>Pichia</i> .....	46
2.2.23.	Bradford assay .....	47
2.2.24.	Cellulase and xylanase assays .....	47
2.2.25.	Sulfuric acid hydrolysis of carbon sources .....	48
2.2.26.	Sugar uptake assay .....	48
2.2.27.	HPAEC-PAD analyses.....	48
2.2.28.	Statistical analyses .....	48
2.2.29.	Sequence retrieval, analysis and domain predictions.....	49
<b>3.</b>	<b>Comparing the physicochemical parameters of three celluloses reveals new insights into substrate suitability for fungal enzyme production .....</b>	<b>51</b>
3.1.	Authors' contributions .....	51
3.2.	Summary.....	51
3.3.	Abstract.....	52
3.4.	Background.....	52
3.5.	Results .....	55
3.5.1.	Substrate characteristics – Surface area and morphology.....	55
3.5.2.	Determination of hemicellulose content of the celluloses.....	56
3.5.3.	Cellulose crystallinity .....	57
3.5.4.	<i>In vitro</i> digestibility of the cellulose substrates .....	58
3.5.5.	Determination of the potential to induce lignocellulolytic gene expression 60	
3.5.6.	Cellulase production in <i>N. crassa</i> and <i>T. reesei</i> RUT-C30.....	61
3.6.	Discussion.....	65
3.7.	Conclusions.....	67
3.8.	Methods .....	68
3.8.1.	Substrates.....	68
3.8.2.	Strains and growth conditions .....	68
3.8.3.	Compositional analyses .....	69

---

3.8.4.	Solid state nuclear magnetic resonance spectroscopy .....	69
3.8.5.	Surface area measurements .....	70
3.8.6.	Scanning electron microscopy.....	70
3.8.7.	Enzymatic assays .....	70
3.8.8.	RNA-extraction and RT-qPCR.....	70
3.8.9.	Statistical analyses.....	71
<b>4.</b>	<b>Cross-talk of cellulose and mannan perception pathways leads to inhibition of cellulase production in several filamentous fungi .....</b>	<b>73</b>
4.1.	Authors' contributions .....	73
4.2.	Summary.....	73
4.3.	Abstract.....	74
4.4.	Introduction .....	74
4.5.	Results .....	76
4.5.1.	Softwood substrates are inhibitory for cellulase production in <i>N. crassa</i> , and GH2-1 is its only $\beta$ -mannosidase.....	76
4.5.2.	The presence of mannodextrins inhibits growth of <i>N. crassa</i> on cellulose 78	
4.5.3.	A delicate intracellular balance between cello- and mannodextrins .....	79
4.5.4.	Cello- and mannodextrins also compete at the level of uptake .....	81
4.5.5.	The inhibitory effect of mannan is conserved in the industrially relevant species <i>Myceliophthora thermophila</i> and <i>Trichoderma reesei</i> .....	83
4.6.	Discussion.....	83
4.7.	Materials and Methods .....	88
4.7.1.	Strains and growth conditions .....	88
4.7.2.	Biomass and enzymatic assays .....	89
4.7.3.	Compositional analysis .....	89
4.7.4.	Nuclear Magnetic Resonance (NMR) analyses .....	89
4.7.5.	GH2-1 heterologous expression.....	90
4.7.6.	Substrate specificity of GH2-1 .....	91
4.7.7.	Contour plot of GH2-1 activity .....	91
4.7.8.	Viscosity measurements .....	91
4.7.9.	Uptake assays .....	92
4.7.10.	Statistical analyses .....	92
<b>5.</b>	<b>General Discussion.....</b>	<b>94</b>
5.1.	Substrate utilization is influenced by crystallinity, hemicellulose content, inducer bioavailability, and fungal regulatory networks .....	94

5.2. Mannan and cellulose perception pathways overlap and this overlap is inhibitive for cellulase production .....	100
5.3. Conclusion and outlook .....	107
<b>6. Appendix.....</b>	<b>110</b>
6.1. Supplementary Methods .....	110
6.1.1. Thermal stability assay.....	110
6.1.2. Microscopy.....	110
6.2. Abbreviations .....	110
6.3. Supplementary Figures .....	112
6.4. Plasmid card .....	116
<b>References .....</b>	<b>117</b>
<b>Acknowledgements .....</b>	<b>135</b>

## List of figures

Figure 1-1. Structure of plant cell wall. ....	14
Figure 1-2. Structural and chemical compositions of (hemi-)cellulosic polysaccharides and the enzymes required for their degradation. ....	16
Figure 1-3. Phylogenetic tree showing the relation of <i>N. crassa</i> and <i>T. reesei</i> to a selection of industrially and scientifically relevant fungal species. ....	17
Figure 1-4. Propagation of <i>N. crassa</i> wild-type strain on sucrose medium. ....	18
Figure 1-5. Propagation of <i>T. reesei</i> RUT-C30 strain on malt extract medium. ....	19
Figure 1-6. Multiple regulatory networks integrate to control fungal lignocellulosic response. ....	22
Figure 3-1. Scanning electron micrographs of cellulose substrates obtained at 8.0 kV accelerating voltage and 100x magnification (Jeol JSM-IT100). ....	56
Figure 3-2. Solid state <sup>13</sup> C NMR spectra of cellulose samples. ....	57
Figure 3-3. Enzymatic digestion of the cellulose substrates <i>in vitro</i> . ....	59
Figure 3-4. Gene expression induction of selected genes used as proxies for the fungal cellulolytic and hemicellulolytic response. ....	61
Figure 3-5. Cellulase and hemicellulase production by <i>N. crassa</i> and <i>T. reesei</i> RUT-C30 on the cellulose substrates. ....	62
Figure 3-6. Total protein secreted by <i>N. crassa</i> (WT and $\Delta cre-1$ ) and <i>T. reesei</i> (QM6a and RUT-C30) on the cellulose substrates. ....	63
Figure 3-7. Cellulase and hemicellulase production by <i>N. crassa</i> (WT and $\Delta cre-1$ ) and <i>T. reesei</i> (QM6a and RUT-C30) on the cellulose substrates. ....	64
Figure 4-1. Characterization of GH2-1. ....	77
Figure 4-2. High mannan content is inhibitory for cellulase activity. ....	79
Figure 4-3. Cello- and mannodextrins compete intracellularly, and the inhibition is independent of CCR by CRE-1. ....	80
Figure 4-4. Cello- and mannodextrins compete at the level of sugar uptake. ....	82
Figure 4-5. Mannan addition is inhibitory to cellulase production in <i>T. reesei</i> and <i>M. thermophila</i> as well. ....	83
Figure 4-6. A model of the induction (A), inhibition (B) and relief of inhibition (C) of cellulase production in <i>N. crassa</i> . ....	86
Figure 5-1. Factors affecting the polysaccharide digestibility and perception fungi. ....	99
Figure 5-2. Structures of (A) cellobiose and (B) mannobiose. ....	104
SFigure 6-1. Cellulase and hemicellulase expression by <i>N. crassa</i> and <i>T. reesei</i> RUT-C30 on Emcocel with or without additional ball-milling. ....	112
SFigure 6-2. Compositional analysis of the different carbon sources. ....	113

SFigure 6-3. GH2-1 localization and thermostability.....113

SFigure 6-4. CMCase activity and protein secretion of *N. crassa* WT and  $\Delta gh2-1$  strains.  
.....114

SFigure 6-5. Analysis of the intracellular sugars of *N. crassa* WT,  $\Delta gh2-1$ ,  $\Delta gh1-1$ , and  
 $\Delta gh2-1$ ,  $\Delta gh1-1$  strains by NMR. ....115

SFigure 6-6. Map of pTSL126B plasmid. ....116

---

## List of tables

Table 2-1. List of strains.....	27
Table 2-2. List of media and solutions.....	28
Table 2-3. List of selection marker. ....	30
Table 2-4. List of cloning and quantitative real-time PCR (RT-qPCR) primers. ....	31
Table 2-5. List of instruments.....	31
Table 2-6. List of software and online tools. ....	33
Table 2-7. List of used carbon sources and chemicals.....	33
Table 2-8. List of consumables and kits. ....	35
Table 2-9: Phusion polymerase PCR reaction mixture.....	41
Table 2-10: PCR thermocycler program.....	41
Table 2-11: Taq polymerase PCR reaction mixture.....	42
Table 2-12: Taq polymerase PCR thermocycler program. ....	42
Table 2-13: Restriction digest reaction components.....	43
Table 2-14: T4 DNA ligase reaction components. ....	43
Table 3-1. Results of sugar analysis of the celluloses after sulfuric acid hydrolysis (in %). .....	57
Table 3-2. Major physical characteristics of the used substrates (manufacturer's information).....	68
Table 3-3. Sequences of primers used for RT-qPCR. ....	71

---

# 1. Introduction

## 1.1. Importance of lignocellulosic biomass for Bio-based refineries

The ever-increasing energy demands resulting from population growth and socio-economic development, as well as the continuously rising price of fossil fuels, necessitate the reformation of global energy policies in support of cleaner sources (Vaz Jr 2017). For instance, liquid transportation fuels, such as ethanol and biodiesel, are the most popular biomass-based energy alternatives (Demirbas 2009). Bio-based refineries, thus, are gaining importance because of their potential for supplying eco-friendly fuels, products, and value-added chemicals (Hatti-Kaul *et al.* 2007; Nigam and Singh 2011). The economic feasibility of biorefineries demands the use of non-edible, renewable, and cheap substrates (Ragauskas *et al.* 2006; Somerville *et al.* 2010). Lignocellulose is the most abundant biomass on Earth (Kuhad and Singh 1993), and its degradation has significant impacts on agriculture, biofuel production, and the environment (Ragauskas *et al.* 2006; Isikgor and Becer 2015; Vaz Jr 2017). More than 150 billion tons of plant biomass (carbon) are produced each year through photosynthesis. Eventually, those materials are mineralized by microorganisms into CO<sub>2</sub> that is released into the atmosphere (Demirbas and Arin 2002). In agricultural practices, decomposition of crop residues in fields is critical to soil productivity and fertility (Bationo and Mokwunye 1991). In industry, lignocellulosic feedstock is an environmentally friendly fossil fuel alternative for the production of next generation biofuels (Naik *et al.* 2010). The industrial utilization of lignocellulosic material requires its degradation into simple fermentable sugars (Mussatto and Teixeira 2010). However, the high degree of cross-linking, the natural heterogeneity and consequent chemical complexity of plant biomass render it recalcitrant to degradation and increase the costs associated with such processes (Sun and Cheng 2002; Himmel *et al.* 2007; Zhou *et al.* 2011; Zhao *et al.* 2012). Multiple approaches have been developed for more effective lignocellulose degradation in order to reduce the cost of biofuel production. Several efforts went into the directions of 1) the enhancement of substrates via pretreatment (Arevalo-Gallegos *et al.* 2017), 2) the development of industrial strains for efficient bioconversion of biomass (Kumar *et al.* 2008), and 3) the improvement of enzymatic activity by means of protein engineering (van Beilen and Li 2002; Zhang *et al.* 2006).

## 1.2. Composition of lignocellulosic biomass

The exact composition of lignocellulosic biomass differs greatly. Different factors contribute to this variability, including plant species, growth environment, harvesting method, storage conditions, densification, and pretreatment techniques (Tumuluru *et al.* 2011; Kenney *et al.*

2013; Williams *et al.* 2016). However, lignocellulosic biomass mainly consists of cellulose, which is embedded in a matrix of covalently linked hemicelluloses and lignin that provide strength and mechanical support to the plant tissues (Somerville *et al.* 2004; Zhong and Ye 2014; Lampugnani *et al.* 2018). The biopolymers are differentially distributed across the plant cell wall layers (Figure 1-1). For instance, the middle lamella is a highly lignified outer layer. It connects the different cells to each other. Inside it is the primary cell wall, a thin layer of highly lignified cellulose fibrils oriented in all directions and embedded in a matrix of hemicelluloses and pectin (Mohnen 2008; Lampugnani *et al.* 2018). The secondary cell wall is less lignified and segmented into three different layers, a thin outer and inner layers, and a thick middle layer. The thicker layer makes up the major part of the cell wall and comprises the major part of the carbohydrates (Gibson 2012).

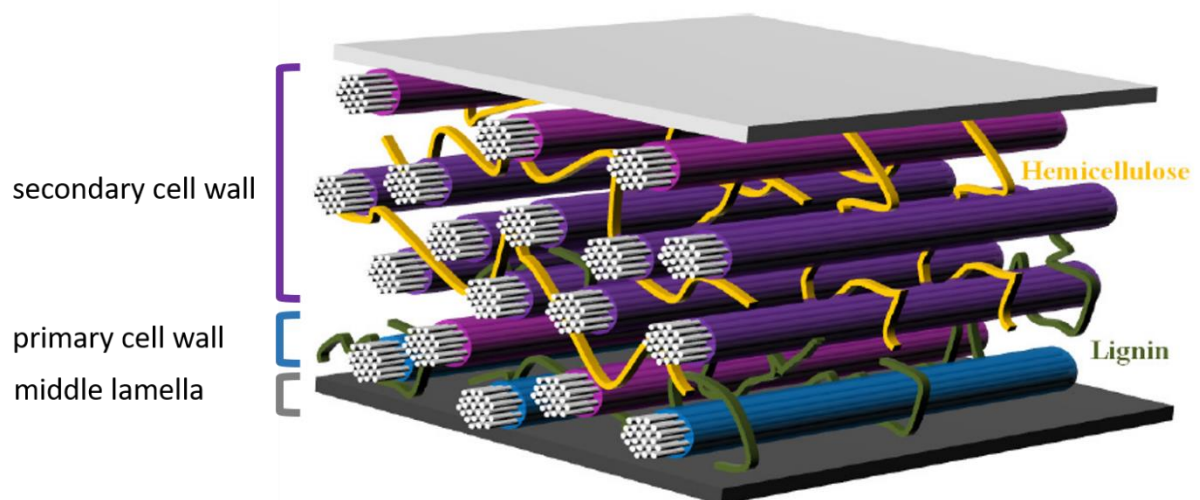


**Figure 1-1. Structure of plant cell wall.**

Plant cell wall structure showing the middle lamella, the primary cell wall, and the secondary cell wall. The latter is constructed between the primary cell wall and the plasma membrane. It typically consists of more arranged cellulose microfibrils, hemicellulose, and lignin, the complex phenolic polymer. This figure was modified from Palmqvist 2014.

Cellulose is the most abundant organic compound on earth (Klemm *et al.* 2005). It has a simple structure which is made up of repeating D-glucose monomers linked together by  $\beta$ -(1,4)-glycosidic bonds and forming linear unbranched chains (Fig 1-2) (Frey-Wyssling 1954). The degree of polymerization (DP) of cellulose extends between 2000 to 14000 residues (Joseleau and Pérez 2016). These linear polymer chains form sheets due to strong hydrogen bonding (Gardner and Blackwell 1974). The sheets are held together by hydrogen bonding and hydrophobic interactions (O'sullivan 1997). These sheets aggregate to form microfibrils containing both crystalline and amorphous (para-crystalline) regions (Payne *et al.* 2015; Joseleau and Pérez 2016). The microfibrils are then packed together to form fibrils which in turn form the cellulose fiber (Payne *et al.* 2015).

On the contrary to cellulose, hemicelluloses are a heterogeneous group of complex polysaccharides. This category of biopolymers includes xyloglucans, xylans, mannans, and glucomannans. Xylans, the major hemicelluloses in hardwood (Timell 1967), are a diverse group of polysaccharides with the common feature of a backbone of  $\beta$ -(1,4)-linked D-xylose residues (Bastawde 1992). Xylan polymers can be substituted and branched with D-galactose, L-arabinose, and (4-O-methyl-)glucuronic acid residues to form other polymers such as arabinoxylans and glucuronoxylans (Figure 1-2) (Scheller and Ulvskov 2010). On the other hand, mannans are the major hemicelluloses in softwoods (Timell 1967) and are mainly made up of  $\beta$ -(1,4)-linked D-mannose chains. The linear backbone of mannan and galactomannan consists entirely of D-mannose residues, while it is often interrupted by D-glucose residues in (galacto-)glucomannan (Kato and Matsuda 1969; Teramoto and Fuchigami 2000). Galactomannan and galactoglucomannan polymers are further branched by  $\alpha$ -linked D-galactose residues.

Pectins are a family of complex polysaccharides with D-galacturonic acid as the main monomeric component (Figure 1-2). They branch into four substructures: homogalacturonan, xylogalacturonan, and rhamnogalacturonan I and II (Mohnen 2008). Homogalacturonan has a linear backbone chain of  $\alpha$ -linked D-galacturonic acid residues. In addition to the  $\alpha$ -linked D-galacturonic chain, xylogalacturonan contains  $\beta$ -linked D-xylose residues as side chains. Rhamnogalacturonan I (RG-I) has a backbone of mixed D-galacturonic acid and L-rhamnose residues with side chains of D-galactose and L-arabinose linked to the L-rhamnose residues. Branched polymers such as arabinogalactan and arabinan can also form side chains of rhamnogalacturonan I, which therefore are often referred to as the “hairy” structures of pectin (Schols *et al.* 1990). Rhamnogalacturonan II consists of a D-galacturonic acid backbone decorated with approximately 12 different monomers (reviewed in Willats *et al.* 2006; Joseleau and Pérez 2016).

Lignin is a polyaromatic, highly branched, biopolymer consisting of phenylpropane compounds (Vanholme *et al.* 2010). Although 15–25% of total biomass dry matter is made up of lignin (Kenney *et al.* 2013), lignin content and composition vary within the different cell types in the plants (Hatakeyama and Hatakeyama 2009). Besides cellulose, hemicelluloses, pectin, and lignin, the biomass also contains many other compounds, for example, fats, resin acids, proteins, and inorganic compounds, but in lower mass fractions than the above-mentioned polymers.

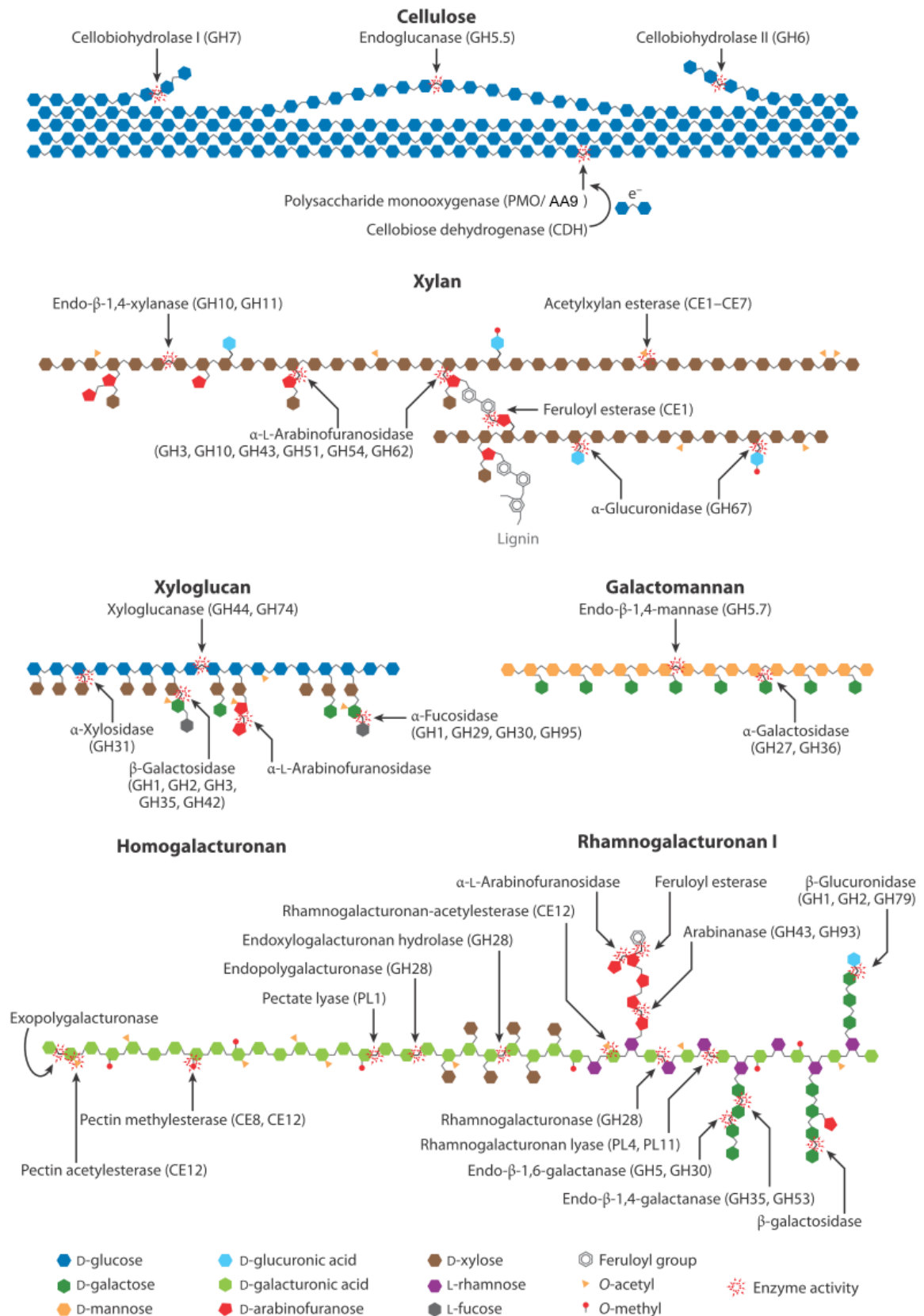


**Figure 1-2. Structural and chemical compositions of (hemi-)cellulosic polysaccharides and the enzymes required for their degradation.** Enzyme activities are represented by major CAZy classes. This figure was modified from Glass *et al.* 2013.

### 1.3. Filamentous fungi as lignocellulose degraders

Many microorganisms have evolved strategies to utilize lignocellulosic biomass as a nutritional source for growth. Lignocellulolytic organisms are found throughout the bacterial and the fungal kingdoms. Filamentous fungi are efficient degraders of polysaccharides (Figure 1-3). They have the ability to sense the presence of such substrates and rewire their regulatory networks to secrete enzymes that efficiently degrade the polymers in their proximity (Glass *et al.* 2013; Tani *et al.* 2014; Benocci *et al.* 2017). Several fungal species such as *Aspergilli* and *Trichoderma reesei* are being used for enzyme production on an industrial scale (Cullen 2007; Schuster and Schmoll 2010; Meyer *et al.* 2011). In recent years, multiple transcriptomic and proteomic analyses of cellulolytic fungi, such as *Neurospora crassa*, served to promote the understanding of the mechanisms that are involved in cellulose degradation and utilization (Znameroski and Glass 2013; Roche *et al.* 2014; Huberman *et al.* 2016; Seibert *et al.* 2016).

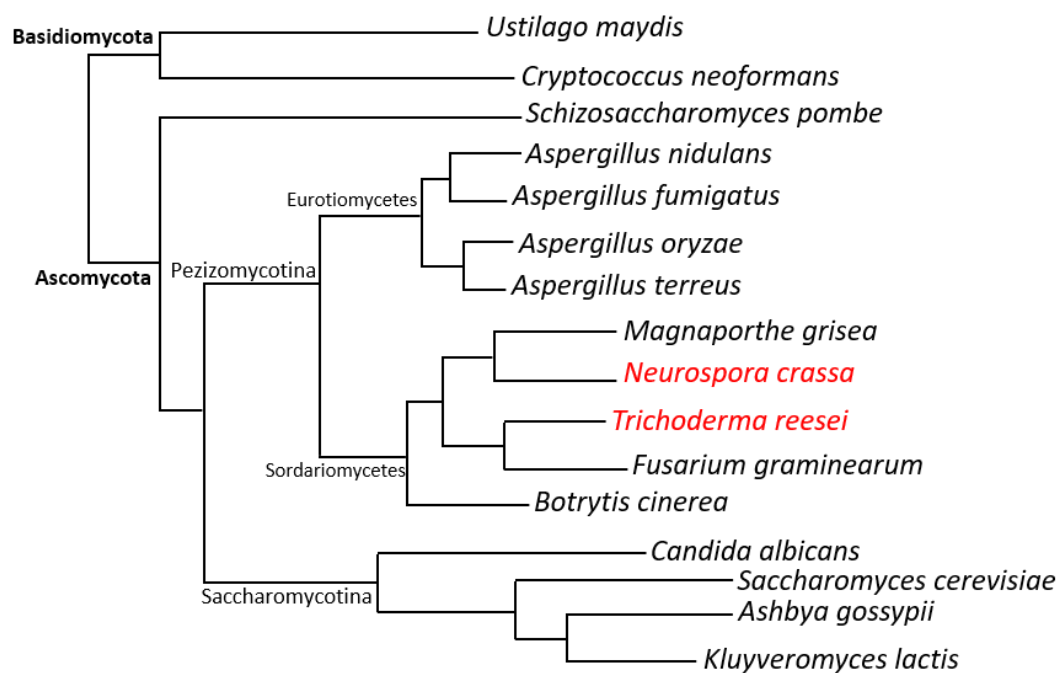


**Figure 1-3. Phylogenetic tree showing the relation of *N. crassa* and *T. reesei* to a selection of industrially and scientifically relevant fungal species.**

This figure was modified from Seibert *et al.* 2016.

### 1.3.1. *Neurospora crassa* as a model organism

*Neurospora crassa* (Figure 1-4) is a filamentous fungus of the ascomycete subphylum that has been studied for decades. It is easy to grow, has a haploid life cycle, and creates an ordered arrangement of products in meiosis facilitating genetic analysis (Dunlap *et al.* 2007). The fungus first received major attention in 1843, upon a *Neurospora* infestation in French bakeries (Davis and Perkins 2002). *N. crassa* is known as a saprotroph, and most of its isolates have been obtained from vegetation or trees after a forest fire (Jacobson *et al.* 2004). However, the exact lifestyle of the fungus is still under investigation (Kuo *et al.* 2014; Gladioux *et al.* 2015). Recent observations suggest that the lifestyle of *N. crassa* may change in adapting to changing environments. For instance, the isolation of *Neurospora* from Amur maple (*Acer ginnala*) in China proposed an endophytic lifestyle for the fungus (Qi *et al.* 2012). Additionally, some field observations and experimental inoculations of pine seedlings (*Pinus sylvestris*) also suggested that the fungus may be living as an endophyte or a saprotroph (Jacobson *et al.* 2004; Kuo *et al.* 2014).

*Neurospora* is considered a model filamentous fungus. It has been the subject of extensive investigations and developments since its selection by Beadle and Tatum to develop the “one gene-one enzyme” hypothesis (Beadle and Tatum 1941). The rise of modern molecular biology techniques and transformation of genetic



**Figure 1-4. Propagation of *N. crassa* wild-type strain on sucrose medium.**

material in *Neurospora* led to the discovery of gene silencing and improved DNA manipulation and sequencing technology (reviewed in Roche *et al.* 2014). *N. crassa* was the first filamentous fungus to have the whole genome sequenced (Galagan *et al.* 2003). The development of molecular tools for targeted gene disruption and integration of recombinant DNA during the recent years enabled the production of a whole genome deletion library for *N. crassa* (Colot *et al.* 2006; Dunlap *et al.* 2007). The invaluable genetic resource is publicly available at the Fungal Genetics Stock Center (FGSC) (McCluskey *et al.* 2010).

*N. crassa* is capable of degrading plant cell wall material and use its sugars as primary carbon sources. The first systematic analysis of *N. crassa* during growth on (hemi-)cellulosic materials was conducted in 2009 (Tian *et al.* 2009). Since then, *N. crassa* has been used as a model organism for understanding how filamentous fungi degrade and utilize plant cell

walls (reviewed in Seibert *et al.* 2016 and Chen *et al.* 2018). *Neurospora* can secrete various functional groups of proteins including enzymes for plant cell wall deconstruction such as carbohydrate-active enzymes (CAZymes) (Figure 1-2), oxidoreductases, proteases, and lipases (Glass *et al.* 2013).

### 1.3.2. *Trichoderma reesei* as an industrial organism

*N. crassa* and *T. reesei* (Figure 1-5) are phylogenetically related, as both belong to the class of Sordariomycetes (Figure 1-3) (Fitzpatrick *et al.* 2006).

*Trichoderma reesei* (*Hypocrea jecorina*) is a mesophilic filamentous fungus that is widely used in industry as a source of (hemi-)cellulases for the hydrolysis of plant cell wall polysaccharides. It was first recognized during World War II through the deterioration of cotton fabrics of the United States Army. The strain QM6a was isolated from the cotton canvas of an army tent on the Solomon Islands. The fungus was put under quarantine in the eponymous Quartermaster collection of the US army. The isolated strain was later named after its principal investigator Elwyn T. Reese (Reese 1976). The whole-genome sequence of the strain QM6a was published in 2008 (Martinez *et al.* 2008).



**Figure 1-5. Propagation of *T. reesei* RUT-C30 strain on malt extract medium.**

After the fungus was recognized as cellulase producer (Mandels and Reese 1957), strain development programs were initiated using random mutagenesis of the wild-type strain QM6a in order to isolate mutants with high cellulase production (Mandels *et al.* 1971). The successful mutant, QM9414, had an extracellular protein and cellulase production levels two to four times that of the wild-type but was still under catabolic repression. Consequently, a plate screening method for high cellulase activity and catabolite derepression was used in conjunction with UV and chemical mutagenesis to generate more efficient mutants (Montenecourt and Eveleigh 1977; Montenecourt and Eveleigh 1977). The hypercellulolytic strain RUT-C30 was then obtained at Rutgers University, New Jersey, through a three-step mutagenesis procedure (reviewed in Peterson and Nevalainen 2012).

Comparative studies between RUT-C30 and QM6a genome revealed several genetic changes in RUT-C30, among which are a truncation in the gene of the key transcription regulator of carbon catabolite repression (CCR) in fungi, *cre1* (Ilmen *et al.* 1996; Seidl *et al.* 2008; Le Crom *et al.* 2009; Rassinger *et al.* 2018) (see also section 1.4). Another mutation

is a large genomic lesion of 85 kb, affecting 29 genes, including transcription factors and enzymes of the primary metabolism (Seidl *et al.* 2008; Le Crom *et al.* 2009).

### 1.3.3. Brief overview of fungal (hemi-)cellulases

Many fungal species have the ability to degrade cellulose by producing extracellular cellulose-degrading enzymes including endo-cleaving (endoglucanases) and exo-cleaving (cellobiohydrolases) enzymes (Goyal *et al.* 1991; Payne *et al.* 2015). Endoglucanases hydrolyze the internal glycosidic bonds of the cellulose chains whereas cellobiohydrolases preferentially act on chain ends (Figure 1-2). The products of the enzymatic hydrolysis of cellulose are mostly the disaccharide cellobiose and, to a lesser extent, cello-oligosaccharides. These sugar dimers and oligomers are further hydrolyzed by the third group of enzymes called  $\beta$ -glucosidases (Payne *et al.* 2015). Cellulases mostly have a small independently folded carbohydrate binding module (CBM) which is connected to the catalytic domain by a flexible linker. The CBMs are responsible for binding of the enzyme to the crystalline cellulose and thus enhance the enzyme activity (Bayer *et al.* 1998). Additionally, a newly categorized class of enzymes called lytic polysaccharide monooxygenases (LPMOs) employ copper, oxygen, and a reducing agent to oxidatively cleave cellulose (Phillips *et al.* 2011; Horn *et al.* 2012).

The major enzymes involved in the hydrolysis of linear mannans and glucomannans are  $\beta$ -mannanases,  $\beta$ -mannosidases, and  $\beta$ -glucosidases (Van Zyl *et al.* 2010). The  $\beta$ -mannanases are endo-acting hydrolases that attack the internal glycosidic bonds of the mannan backbone chain, releasing short  $\beta$ -(1,4)-manno-oligosaccharides.  $\beta$ -Mannosidases, on the other hand, are exo-acting hydrolases that attack the terminal linkage at the non-reducing end to release mannose from the oligosaccharide. Also,  $\beta$ -mannosidases cleave mannobiose into mannose units. The  $\beta$ -glucosidases remove the (1,4)-glucopyranose units at the non-reducing end of the oligomers during the degradation of (galacto-)glucomannans (Moreira 2008). Xylan hemicelluloses, on the other hand, are degraded by the action of xylanases including endo-xylanases that cleave inside the backbone of the polymer, and  $\beta$ -xylosidases that cleave xylose oligomers into xylose residues (Collins *et al.* 2005; Polizeli *et al.* 2005).

For pectin degradation, endo- and exo-polygalacturonases act on the homogalacturonan backbone of the polymer by cleaving either inside it or at the non-reducing ends, respectively. Endo-polygalacturonases release oligogalacturonides, while exo-polygalacturonases generate galacturonic acid monosaccharides through enzymatic hydrolysis. The de-esterification of pectin into pectate and methanol is carried out through

the action of pectin methylesterases. Pectate and pectin lyases perform an eliminative cleavage of either pectate or pectin, respectively (van den Brink and de Vries 2011). The rhamnogalacturonan-I backbone is hydrolyzed by the action of rhamnogalacturonan lyases, rhamnogalacturonan acetylerases, and unsaturated rhamnogalacturonyl hydrolases (van den Brink and de Vries 2011).

#### **1.4. Polysaccharide perception and degradation by filamentous fungi**

Fungi have the ability to sense the presence of carbon sources and rewire their regulatory networks to utilize them efficiently (Glass *et al.* 2013; Tani *et al.* 2014; Huberman *et al.* 2016; Benocci *et al.* 2017). In the presence of an easily metabolizable substrate, such as glucose, the fungus represses the production of lignocellulosic enzymes to prevent wasting energy and enters a state of CCR (Ronne 1995; Ruijter and Visser 1997; Ebbole 1998; Gancedo 1998). CCR is mainly mediated by the well conserved Mig1/CRE-1/Cre1/CreA zinc finger transcription factor (TF) (Bailey and Arst 1975; Strauss *et al.* 1995; Ilmen *et al.* 1996; Ebbole 1998; de Vries *et al.* 1999; Portnoy *et al.* 2011; Sun and Glass 2011). CRE-1 and its orthologs repress the induction of genes involved in (hemi-)cellulose degradation by binding to motifs in the promoter region of those genes and probably interfering with the binding of the positive regulator (Sun and Glass 2011). Additionally, different transcription regulator genes have CRE-1/Cre1/CreA binding sites in their promoter regions, among which multiple have shown to be directly regulated by this TF (Tamayo *et al.* 2008; Portnoy *et al.* 2011; Sun and Glass 2011; Antoniêto *et al.* 2014). For the induction of the (hemi-)cellulolytic response, genes encoding enzymes must be both released from repression and activated by TFs that are regulated specifically by components of the nearby plant biomass. A recent study described two TFs, vegetative incompatibility blocked (VIB-1) and colonial 26 (COL-26), to act at the induction stage of the cellulolytic response as negative regulators of CRE-1-mediated CCR (Figure 1-6) (Xiong *et al.* 2017). VIB-1 and COL-26 were initially described as regulators of extracellular protease secretion in response to both carbon and nitrogen starvation (Xiong *et al.* 2014) and to be involved in glucose sensing and starch degradation (Xiong *et al.* 2014; Xiong *et al.* 2017), respectively.

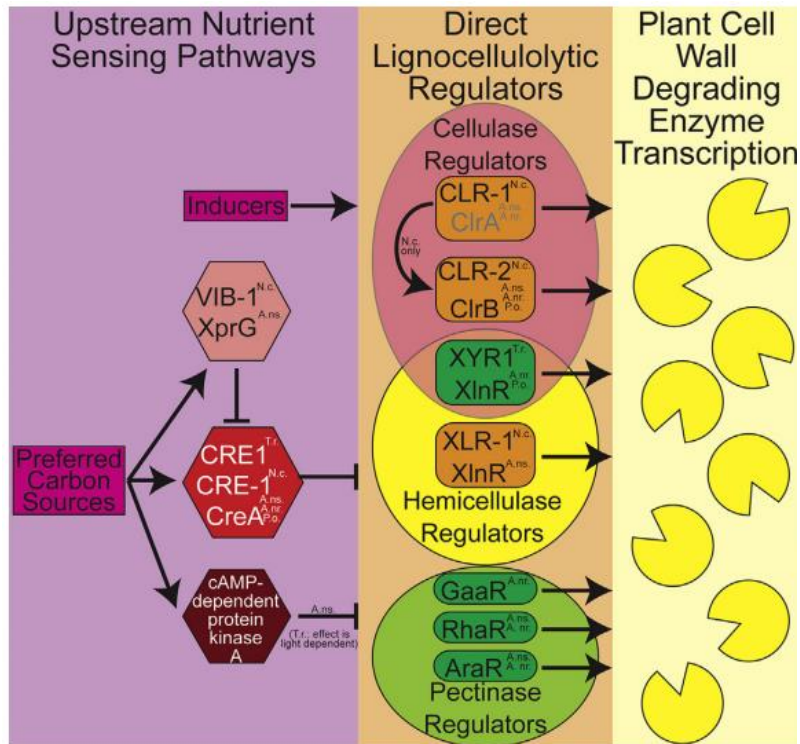


**Figure 1-6. Multiple regulatory networks integrate to control fungal lignocellulosic response.**

At the nutrient-sensing pathways: The fungus utilizes preferable C-sources through the transcription factor CRE-1/CreA/CRE1, which is regulated in part by VIB-1/XprG. When activated, the TF represses transcription of the (hemi-)cellulolytic regulators and enzymes. The cAMP-dependent protein kinase A (PKA) also plays a role in nutrient sensing, although its effect is species dependent. The presence of inducer molecules, liberated by the action of scouting enzymes on the polysaccharides, activates the (hemi-)cellulolytic regulators. At the level of direct lignocellulolytic regulators: In *T. reesei* and *A. niger* XYR1/XInR activates transcription of genes of both the cellulolytic and hemicellulolytic pathways. In *N. crassa* and *A. nidulans*, XLR-1/XInR only regulates transcription of hemicellulase genes. Cellulase gene transcription in *N. crassa*, *A. nidulans*, and *A. niger* is regulated by CLR-1/ClrA and CLR-2/ClrB. In *N. crassa*, CLR-1 activates transcription of some genes necessary for cellulose utilization as well as the main transcriptional activator of cellulase transcription, CLR-2. The CLR-2 homolog, ClrB is involved in cellulase transcription in *A. nidulans* and *A. niger*. Pectin utilization is regulated by several transcription factors: GaaR regulates galacturonic acid utilization, RhaR regulates rhamnose utilization, and AraR regulates arabinose utilization. (A.nr.: *Aspergillus niger*, A.ns.: *Aspergillus nidulans*, N.c.: *Neurospora crassa*, P.o.: *Penicillium oxalicum*, and T.r.: *Trichoderma reesei*). This figure was modified from Huberman *et al.* 2016.

In the general model of polysaccharide perception by fungi, it is proposed that when the preferred C-source is depleted, the fungus gets into a starvation state. During this state, a small set of hydrolases and sugar transporters are expressed. The hydrolases, called scouting enzymes, are then secreted into the extracellular environment. Scouting enzymes then initiate a small-scale digestion of the available substrates to liberate small quantities of sugar monomers and oligomers. These molecules, in turn, are transported by sugar transporters into the hyphae where they act as inducers (Znameroski *et al.* 2012; Znameroski and Glass 2013), triggering the tailored large-scale induction of the fungal

lignocellulosic degradative machinery (Melo *et al.* 1997; Delmas *et al.* 2012; Benz *et al.* 2014; van Munster *et al.* 2014; Xiong *et al.* 2014; Daly *et al.* 2016).

The majority of plant cell wall degradation regulators belong to the zinc cluster family and are conserved in ascomycetes (Coradetti *et al.* 2012; Benocci *et al.* 2017). This TF family is characterized by the presence of zinc finger(s) in their binding domains. In *N. crassa*, the cellulolytic response is mainly regulated by two transcription factors: cellulose degradation regulators CLR-1 and CLR-2 (Coradetti *et al.* 2012; Coradetti *et al.* 2013). In the absence of an inducer, the activity of CLR-1 is repressed by the repressor CLR-3 (Huberman *et al.* 2017). In the presence of cellulose, the polymer is degraded potentially by the action of scouting enzymes, into smaller oligomers such as cellobiose. Cellobiose molecules are transported into the cytosol via the cellodextrin transporters CDT-1 and CDT-2 (Galazka *et al.*, 2010). In the presence of the cellobiose acting as inducer molecule (Znameroski *et al.*, 2012), unknown mechanisms govern the release of CLR-1 from repression (Huberman *et al.* 2017). CLR-1 induces the expression of several cellulolytic genes including CDT-2,  $\beta$ -glucosidases, and CLR-2 (Coradetti *et al.* 2012; Coradetti *et al.* 2013; Craig *et al.* 2015). Homologs of CLR-1 and CLR-2 are present in almost all genomes of filamentous ascomycetes, however, their roles in plant cell wall degradation seem to be different from what was described for *N. crassa* (Figure 1-6) (Coradetti *et al.* 2013 and reviewed in Benocci *et al.* 2017). Recently, CLR-4 was described as a new regulator of the (hemi-)cellulolytic response in *N. crassa* and *Myceliophthora thermophila*, regulating both, genes of the cAMP signaling pathway and genes encoding the (hemi-)cellulolytic TFs *clr-1*, *Mtclr-2*, and *Mtxyr-1* (Liu *et al.* 2019).

The major regulator of the xylanolytic response is the Zn binuclear cluster transcription factor xylan degradation regulator XLR-1. In *N. crassa*, XLR-1 induces the expression of xylanases (Sun *et al.* 2012). The orthologs of this TF in *T. reesei* and some Aspergilli species, XYR1 and XlnR, respectively, additionally regulate genes of the cellulolytic pathway (Figure 1-6) (van Peij *et al.* 1998; van Peij *et al.* 1998; Gielkens *et al.* 1999; Marui *et al.* 2002; Hasper *et al.* 2004; Stricker *et al.* 2006; Mach-Aigner *et al.* 2008; Stricker *et al.* 2008; Noguchi *et al.* 2009). Additional positive regulators of the cellulolytic and xylanolytic responses in *T. reesei* are the activators of cellulase expression ACE2 and ACE3 (Aro *et al.* 2001; Häkkinen *et al.* 2014). On the contrary, ACE1 acts as a repressor of both cellulase and xylanase genes (Aro *et al.* 2003; Wang *et al.* 2012) and the hemicellulase regulator HCR-1 acts as a repressor of xylanase genes in *N. crassa* (Li *et al.* 2014).

Among the transcription factors that are involved in pectin degradation, RhaR regulates rhamnose utilization in Aspergilli (Gruben *et al.* 2014). Also, in *Aspergillus niger*, the

transcription factor GaaR is the regulator of homogalacturonan degradation and galacturonic acid utilization (Alazi *et al.* 2016). AraR, Ara1, ARA-1, and ARA1 are the regulators of the arabinolytic response and arabinose catabolism in *A. niger*, *M. oryzae*, *N. crassa* and *T. reesei*, respectively (Battaglia *et al.* 2011; Klaubauf *et al.* 2016; Thieme *et al.* 2017; Benocci *et al.* 2018; Thieme 2019). Recently, the pectin degradation regulators PDR-1 and PDR-2 were characterized in *N. crassa*. PDR-1 and PDR-2, being homologs of RhaR and GaaR, respectively, regulate the transcription of genes involved in pectin degradation, rhamnose catabolism and galacturonic acid catabolism (Thieme *et al.* 2017; Thieme 2019).

### 1.5. Aims of this study

The employment of plant biomass as renewable raw materials has been considered the most successful strategy to produce biorefinery products due to their abundance and convertibility into fermentable sugars. Due to the heterogeneity and complexity of these feedstock materials, they are of high natural recalcitrance towards decomposition. Yet, plant cell wall polysaccharides are considered applicable substrates for lignocellulose-degrading fungi because of their high carbohydrate content. Fungi have the ability to sense the presence of such substrates and rewire their regulatory networks to secrete enzymes that efficiently degrade the polysaccharides in their proximity. Thus, the optimization of the performance of lignocellulosic polysaccharides as substrates and the rational and targeted engineering of fungal production strains, is a major desire. However, the knowledge of how fungi perceive the substrate and regulate their enzymatic production to fit the composition of the biomass at hand is still incomplete. To address these issues, this thesis work focused on two approaches:

- 1) The first approach aimed to analyze both the physicochemical and molecular biological aspects of cellulase production in filamentous fungi when grown on different cellulosic substrates. For this, the physicochemical properties of three representative celluloses, a hardwood- and a softwood-derived MCC, as well as a hardwood-derived powdered cellulose, were to be examined. To this end, the specific surface area, hemicellulose content, and the crystallinity of the substrates were to be recorded and compared. In addition, the model filamentous fungus *N. crassa* and the industrially optimized strain *T. reesei* RUT-C30 were to be used to assess the impact of the differences in the physicochemical characteristics of the substrates on (hemi-)cellulase production. To assess the fungal performance, cellulase and xylanase productivity, as well as the molecular response were to be recorded.
- 2) The second approach focused on the fungal perception of the hemicellulose (mannan) impurities often present in plant substrates. Indications for potential overlaps between

cellulose and mannan perception pathways were to be investigated. Additionally, using the genetic toolbox available for *N. crassa* alongside biochemical and rheological approaches and uptake studies, the possible sites of overlap were to be determined. In addition to *N. crassa*, the two industrially relevant strains *M. thermophila* and *T. reesei* RUT-C30 were to be used to assess the effect of mannan presence on the cellulolytic production by the fungi.

---

## 2. Materials and Methods

### 2.1. Materials

#### 2.1.1. Organisms

Table 2-1. List of strains.

strain	stock number	name	genotype	source
<i>N. crassa</i>	1	WT	oak ridge (OR) 74 (Colot <i>et al.</i> 2006)	FGSC <sup>a</sup> #2489
	3	<i>clr-2 oex</i> (PC2)	<i>his-3::Pccg-1-clr-2 rid-1 Δsad-1; Δclr-2</i>	EBI <sup>b</sup> , Glass lab (Coradetti <i>et al.</i> 2013)
	5	<i>Δcdt-1</i>	<i>ΔNCU00801::hph</i>	FGSC <sup>a</sup> #16575
	6	<i>Δcdt-2</i>	<i>ΔNCU08114::hph</i>	FGSC <sup>a</sup> #17868
	7	<i>Δclr-1</i>	<i>ΔNCU07705::hph</i>	FGSC <sup>a</sup> #11028
	8	<i>Δclr-2</i>	<i>ΔNCU08042::hph</i>	FGSC <sup>a</sup> #15834
	9	<i>Δcdt-1 Δcdt-2</i>	<i>ΔNCU00801::hph, ΔNCU08114::hph</i>	PhB <sup>c</sup>
	10	<i>3βG</i>	<i>ΔNCU00130::hph, ΔNCU04952::hph, ΔNCU08755::hph</i>	EBI <sup>b</sup> , Glass lab
	11	<i>Δqko</i>	<i>ΔNCU00130::hph, ΔNCU04952::hph, ΔNCU08755::hph, ΔNCU0890::hph</i>	PhB <sup>c</sup>
	12	<i>Δgh5-7</i>	<i>ΔNCU08412::hph</i>	FGSC <sup>a</sup> #23488
	15	<i>gh2-1-gfp</i>	<i>pCSR/GPD::NCU00890cDNA-GFP</i>	PhB <sup>c</sup>
	22	WT, <i>his-</i>	<i>his-3, mat A</i>	FGSC <sup>a</sup> #6103
	61	<i>Δgh1-1</i>	<i>ΔNCU00130::hph</i>	FGSC <sup>a</sup> #
	62	<i>Δgh2-1</i>	<i>ΔNCU00890::hph</i>	FGSC <sup>a</sup> #
	68	<i>Δcre-1</i>	<i>ΔNCU08807::hph</i>	EBI <sup>b</sup> , Glass lab
	70	<i>Δclr-1 Δclr-2</i>	<i>ΔNCU07705::hph, ΔNCU08042::hph</i>	this study
	75	<i>clr-1 oex</i> (PC1)	<i>ΔNCU07705::hph, csr1-::Pgpd1-clr-gDNA</i>	this study
	83	<i>Δgh2-1 Δgh1-1</i>	<i>ΔNCU00890::hph, ΔNCU00130::hph</i>	this study
88	<i>Δgh2-1 clr-2 oex</i>	<i>his-3::Pccg-1-clr-2 rid-1 Δsad-1; Δclr-2, ΔNCU00890::hph</i>	this study	
118	<i>Δgh2-1 Δcre-1</i>	<i>ΔNCU00890::hph, ΔNCU08807::hph</i>	this study	
136	<i>gh2-1-comp</i>	<i>ΔNCU00890, pCSR-knockin/native prom::NCU00890gDNA</i>	PhB <sup>c</sup>	
<i>T. reesei</i>	16	QM6a	ATCC 13631	AIT <sup>d</sup> , M. Schmolll
	18	RUT-C30	ATCC 56765	AIT <sup>d</sup> , M. Schmolll
<i>P. pastoris</i>	111	<i>Pichia_gh21-1</i>	<i>pGAPZ-B, NCU00890cDNA</i>	PhB <sup>c</sup>

<b><i>E. coli</i> DH5<math>\alpha</math></b>	-	F- $\Phi$ 80 <i>lacZ</i> $\Delta$ M15 $\Delta$ ( <i>lacZYA-argF</i> ) U169 <i>recA1 endA1 hsdR17</i> (rK-, mK+) <i>phoA supE44</i> $\lambda$ - <i>thi-1gyrA96</i> <i>relA1</i>	Thermo Fisher Scientific (Waltham, USA)
--	---	---	---

<sup>a)</sup> Fungal Genetics Stock Center (FGSC; <http://www.fgsc.net/>), (McCluskey *et al.* 2010); <sup>b)</sup> Energy Biosciences Institute, Berkeley, USA; <sup>c)</sup> generated by Prof. Dr. J. Philipp Benz; <sup>d)</sup> AIT Austrian Institute of Technology GmbH, Vienna

## 2.1.2. Media and solutions

Double distilled water (ddH<sub>2</sub>O) was used to dissolve the substances used for media preparation.

**Table 2-2. List of media and solutions.**

name	Substances	concentration
<b>D-biotin stock solution</b>	D-biotin	0.1 mg/ml
	filter sterilize	
<b>Vogel's trace elements stock solution</b>	citric acid monohydrate	60.0 mM
	zinc sulfate heptahydrate	42.0 mM
	ammonium iron(II) sulfate hexahydrate	6.5 mM
	copper (II) sulfate pentahydrate	2.5 mM
	manganese (II) sulfate monohydrate	0.75 mM
	boric acid	2.0 mM
	sodium molybdate dihydrate	0.52 mM
	filter sterilize	
<b>50x Vogel's solution (Vogel 1956)</b>	trisodium citrate dihydrate	0.43 M
	potassium dihydrogen phosphate	1.84 M
	ammonium nitrate	1.25 M
	magnesium sulfate heptahydrate	40.0 mM
	calcium chloride dihydrate (pre-dissolve in water)	34.0 mM
	D-biotin stock solution (0.1 mg/ml)	0.25% (v/v)
	trace elements stock solution	0.50% (v/v)
	filter sterilize	
<b>Vogel's Minimal Medium (MM)</b>	Sucrose	2.0% (w/v)
	50x Vogel's solution	2.0% (v/v)
	agar-agar (only solid medium)	1.5% (w/v)
<b>10x FIGS solution</b>	L-sorbose	20.0% (w/v)
	D-fructose	0.5% (w/v)
	D-glucose	0.5% (w/v)
	filter sterilize	
<b>bottom agar (BA)</b>	50x Vogel's solution	2.0% (v/v)
	agar-agar (only solid medium)	1.5% (w/v)
	autoclave, then add 10x FIGS solution	10.0% (v/v)
<b>top agar (TA)</b>	50x Vogel's solution	2.0% (v/v)
	agar-agar (only solid medium)	1.0% (w/v)

	autoclave, then add 10x FIGS solution	10.0% (v/v)
<b>2x Westergaard's solution (Westergaard and Mitchell 1947)</b>	potassium nitrate	0.2% (w/v)
	di-potassium phosphate	0.14% (w/v)
	potassium dihydrogen phosphate	0.1% (w/v)
	magnesium sulfate heptahydrate	0.1% (w/v)
	sodium chloride	0.02% (w/v)
	calcium chloride dihydrate (pre-dissolve in water)	0.02% (w/v)
	D-biotin stock solution (0.1 mg/ml)	0.01% (v/v)
	trace elements stock solution	0.02% (v/v)
	filter sterilize	
<b>Westergaard's medium</b>	2x Westergaard's solution	50.0% (v/v)
	Sucrose	1.5% (w/v)
	agar-agar	2.0% (w/v)
<b>Lysogeny Broth (LB) Medium (Bertani 1951)</b>	yeast extract	0.5% (w/v)
	tryptone/peptone	1.0% (w/v)
	sodium chloride	1.0% (w/v)
	agar-agar (only solid medium)	1.5% (w/v)
<b>LB low salt medium (Bertani 1951)</b>	yeast extract	0.5% (w/v)
	tryptone/peptone	1.0% (w/v)
	sodium chloride	0.5% (w/v)
	agar-agar (only solid medium)	1.5% (w/v)
<b>super optimal broth with catabolite repression (SOC) medium (Hanahan 1983)</b>	yeast extract	0.5% (w/v)
	tryptone/peptone	2.0% (w/v)
	sodium chloride	10.0 mM
	potassium chloride	2.5 mM
	magnesium chloride	10.0 mM
	magnesium sulfate monohydrate	10.0 mM
	set pH to 7.0 and autoclave	
	D-glucose	20.0 mM
<b>Mandels Andreotti trace element solution</b>	iron(II) sulfate heptahydrate	250 mg/l
	manganese(II) sulfate monohydrate	85 mg/l
	zinc sulfate heptahydrate	70 mg/l
	cobalt(II) chlorate dihydrate	100 mg/l
<b>Mandels Andreotti buffer (citrate phosphate buffer)</b>	citric acid	0.2 M
	adjust the pH to 5.0 with disodium phosphate dihydrate	0.2 M
<b>Mandels Andreotti Medium (Mandels and Andreotti 1978)</b>	ammonium sulfate	2.8 g/l
	dipotassium phosphate	4.0 g/l
	magnesium sulfate heptahydrate	0.6 g/l
	calcium chloride dihydrate	0.8 g/l
	peptone	1 g/l
	urea (5mM)	0.3 g/l

	phosphate-Citrate Buffer	480 ml
	trace element solution	20ml
<b>YPD medium</b>	yeast extract	1% (w/v)
	peptone	2% (w/v)
	D-glucose	20.0 mM
	agar-agar	2%(w/v)
<b>5x Taq buffer</b>	Tris HCl pH 8.5	0.25 M
	sodium chloride	0.1 M
	magnesium chloride hexahydrate	10.0 mM
	Ficoll 400	12.5% (w/v)
	BSA	0.25% (w/v)
	Xylene Cyanol FF	0.1% (w/v)
<b>50x Tris Acetate EDTA (TAE) stock solution</b>	Tris	2.0 M
	acetic acid 100%	1.0 M
	EDTA disodium salt dihydrate	50.0 mM
<b>citrate phosphate buffer</b>	citric acid monohydrate	50.0 mM
	adjust the pH to 5.0 with sodium phosphate dibasic	
<b>gDNA extraction lysis buffer</b>	sodium hydroxide	50.0 mM
	EDTA disodium salt dihydrate	1.0 mM
	Triton X-100	1.0% (v/v)
<b>cells lysis buffer</b>	monosodium phosphate	50 mM
	sodium chloride	300 mM
	PMFS	1 mM
	Lysozyme (dissolved in 15 mM NaH <sub>2</sub> PO <sub>4</sub> )	20 mg/ml
<b>spore solution</b>	sodium chloride	0.4%
	Tween 80	0.025%
<b>mycelia lysis buffer</b>	trisodium phosphate	50 mM
	EDTA disodium salt dehydrate pH 7.5	1 mM
	Glycerol	5 %
	PMSF	1mM
<b>elution buffer</b>	sodium dihydrogen phosphate	50 mM
	sodium chloride	300 mM

**Table 2-3. List of selection marker.**

All additives and supplements were sterile filtered.

<b>name</b>	<b>selection markers</b>	<b>concentration</b>
1000x Ampicillin stock solution	Ampicillin sodium salt	100 mg/ml
1000x Cyclosporin A stock solution	Cyclosporin A	5 mg/ml
100x histidine stock solution	L-histidine	20 mg/ml
500x Hygromycin B stock solution	Hygromycin B Gold	200 mg/ml
1000x Kanamycin stock solution	Kanamycin sulfate	30 mg/ml
1000x Zeocin stock solution	Zeocin	25 mg/ml

### 2.1.3. Primers

**Table 2-4. List of cloning and quantitative real-time PCR (RT-qPCR) primers.**

Restriction sites are underlined and with boldface letters. The oligonucleotides were purchased from Eurofins Genomics (Ebersberg, Germany).

purpose	name	sequence	Tm
short fragment of <i>actin</i> (NCU04173)	qPCR_actin_fwd 2	CATCGACAATGGTTCCGGGTATGT G	58.0 °C
	qPCR_actin_rev 2	CCCATACCGATCATGATACCATG ATG	56.9 °C
short fragment of <i>cbt-1/clp-1</i> (NCU05853)	5853RT-Fwd	CGCCCTGACCTACACCTAC	56.0 °C
	5853RT-Rev	GGCCAAACGACCAAAGAGC	56.3 °C
short fragment of <i>D-xylulose kinase</i> (NCU11353)	11353RT-Fwd	GGCACATCATCGCTTCACTG	55.8 °C
	11353RT-Rev	CAAGGGAGATGCGCGAGG	57.9 °C
short fragment of <i>ce16-1</i> (NCU09416)	9416RT-Fwd	GGTGCTGCTCCCATCTACTAC	56.7 °C
	9416RT-Rev	GTA <del>CTTGGCGATGGCGAC</del>	54.9 °C
<i>clr-1</i> overexpression in CSR locus, Sbfl and Pacl restriction sites	clr-1_CSR-GPD_F	ATCG <b>CCTGCAGG</b> ATGTCGCCGTCTT CCAAC	68.8 °C
	clr-1_CSR-GPD_R	AGTCT <b>TAATTA</b> AATCAACCACTCAGG AACGTTTCG	60.5 °C

### 2.1.4. Instruments and tools

**Table 2-5. List of instruments.**

name	model	manufacturer
autoclave	Varioklav 135 S	Thermo Fisher Scientific (Waltham, USA)
ball mill	MM 200	Retsch (Haan, Germany)
BeadBug homogenizer	24 D1030	Süd-Laborbedarf (Gauting, Germany)
confocal laser scanning microscope	TCS SP5	Leica Microsystems (Wetzlar, Germany)
electroporator	Eporator	Eppendorf (Hamburg, Germany)
gel imaging system	Fusion solo S	Vilber Lourmat (Eberhardzell, Germany)
heating block	TSC ThermoShaker	Analytik Jena (Jena, Germany)
heating block with cover	ThermoMixer C	Eppendorf (Hamburg, Germany)
high-performance anion-exchange chromatography with pulsed amperometric detection (HPAEC-PAD)	Dioncex ICS-3000	Thermo Fisher Scientific (Waltham, USA)
Incubator 30 °C	Heratherm IGS100	Thermo Fisher Scientific (Waltham, USA)
Incubator 37 °C	IR 1500	Flow Laboratories (Inglewood, USA)
Incubator shaking	Excella 24	New Brunswick Scientific (Edison, USA)

## Materials and Methods

---

laboratory bead mill	BeadBug 24 D1030	Süd-Laborbedarf Gauting (Gauting, Germany)
large scale centrifuge	Megafuge 40R	Heraeus (Hanau, Germany)
light Incubator 25 °C	BK 5060 EL	Heraeus (Hanau, Germany)
light incubator shaking	Innova 42	New Brunswick Scientific (Edison, USA)
Microwave	MW 7803	Severin, Sundern
oven	Jouan	Thermo Fisher Scientific (Waltham, USA)
pH-meter	SevenEasy	Mettler Toledo (Columbus, USA)
Pipettes	Research plus	Eppendorf (Hamburg, Germany)
plate incubator	INCU-Mixer MP	Benchmark Scientific (Edison, USA)
plate reader	Infinite 200 PRO NanoQuant reader	Tecan (Männedorf, Switzerland)
Real-time PCR System	Mastercycler® ep realplex	Eppendorf (Hamburg, Germany)
rocking machine	RT 26	Analytik Jena (Jena, Germany)
sequencing system	MiSeq	Illumina (San Diego, USA)
stereo microscope	S8AP0	Leica Microsystems (Wetzlar, Germany)
sterile bench	BDK-S	BDK Luft- und Reinraumtechnik (Sonnenbühl-Genkingen, Germany)
tabletop centrifuge	Centrifuge 5424	Eppendorf (Hamburg, Germany)
tabletop centrifuge (cooled)	Centrifuge 5427 R	Eppendorf (Hamburg, Germany)
thermocycler	ProfessionalTRIO	Analytik Jena (Jena, Germany)
thermocycler gradient	peqStar 2x Gradient	VWR (Radnor, USA)
tube revolver	Rotator	Analytik Jena (Jena, Germany)
Water bath	1083	GFL, Burgwedel
water purifier	mini-UP+	Berrytec (Grünwald, Germany)

**Table 2-6. List of software and online tools.**

<b>name</b>	<b>Purpose</b>	<b>manufacturer</b>
AnnHyb V4.946	determination of primer melting temperatures	Olivier Friard (Torino, Italy)
Basic Local Alignment Search Tool (BLAST)	search for and comparison of nucleotide and amino acid sequences, determination of sequence identity	National Center for Biotechnology Information (NCBI) (Bethesda MD, USA)
Chromeleon Chromatography Data System V7.2 SR3	recording and analysis of HPAEC-PAD data	Thermo Fisher Scientific (Waltham, USA)
fungal and oomycete genomics resources (FungiDB)	nucleotide and protein sequence retrieval, homology searches	National Institute of Allergy and Infectious Diseases (NIAID) (Maryland, USA) and University of California, Riverside (Riverside, USA)
Fungal Genetics Stock Center (FGSC)	collection of <i>N. crassa</i> strain information, navigation for the <i>N. crassa</i> deletion strain stock collection	Kansas State University, Department of Plant Pathology (Manhattan KS, USA)
Microsoft Office and excel 2013	statistical analysis, manuscript preparation	Microsoft (Redmond, USA)
Plotly 2015	Plotly	Plotly Technologies Inc. (Montreal, QC)
Realplex 2.2	RT-qPCR results analysis	Eppendorf (Hamburg, Germany)
Rstudio 1.1.453 (2016)	statistical analysis, figure preparation	RStudio: Integrated Development for R. RStudio, Inc.
Rstudio 1.1.453 (2016)	statistical analysis, figure preparation	RStudio: Integrated Development for R. RStudio, Inc.
SnapGene Viewer V3.2.1	primer design, <i>in silico</i> plasmid assembly	GSL Biotech LLC (Chicago, USA)

### 2.1.5. Consumable

**Table 2-7. List of used carbon sources and chemicals.**

<b>name</b>	<b>order number</b>	<b>Manufacturer</b>
Avicel PH-101	11365	Merck (Darmstadt, Germany)
D-glucose anhydrous	X997	Carl Roth (Karlsruhe, Germany)
sucrose	S7903	Merck (Darmstadt, Germany)
glucomannan	37220-7-0	Konjac Foods
mannan	-	Megazyme (ivory nut)
mannobiose	O-MBI	Megazyme
acetic acid 100%	3738	Carl Roth (Karlsruhe, Germany)
agar-agar, Kobe I	5210	Carl Roth (Karlsruhe, Germany)
agar-agar, bacteriological	2266	Carl Roth (Karlsruhe, Germany)
agarose	AG02	Nippon Genetics Europe (Dueren, Germany)
ammonium chloride	5470	Carl Roth (Karlsruhe, Germany)

ammonium iron(II) sulfate hexahydrate	P728	Carl Roth (Karlsruhe, Germany)
ammonium nitrate	K299	Carl Roth (Karlsruhe, Germany)
ammonium sulfate	5606	Carl Roth (Karlsruhe, Germany)
Ampicillin sodium salt	HP62	Carl Roth (Karlsruhe, Germany)
D-biotin	3822	Carl Roth (Karlsruhe, Germany)
bovine serum albumin (BSA) fraction V	8076	Carl Roth (Karlsruhe, Germany)
calcium chloride dihydrate	5239	Carl Roth (Karlsruhe, Germany)
citric acid monohydrate	20276	VWR (Radnor, USA)
copper (II) sulfate pentahydrate	23174	VWR (Radnor, USA)
Cyclosporin A	100507	VWR (Radnor, USA)
di-potassium phosphate	P749	Carl Roth (Karlsruhe, Germany)
di-sodium phosphate	4984	Carl Roth (Karlsruhe, Germany)
ethylenediaminetetraacetic acid (EDTA) disodium salt dihydrate	X986	Carl Roth (Karlsruhe, Germany)
ethanol >96%	T171	Carl Roth (Karlsruhe, Germany)
ethanol >99%	9065	Carl Roth (Karlsruhe, Germany)
Ficoll 400	F2637	Merck (Darmstadt, Germany)
D-fructose	4981	Carl Roth (Karlsruhe, Germany)
glycerol	3783	Carl Roth (Karlsruhe, Germany)
L-histidine	H5659	Merck (Darmstadt, Germany)
hydrochloric acid	4625	Carl Roth (Karlsruhe, Germany)
4-hydroxybenzhydrazide	H-9882	Megazyme (Bray, Ireland)
Hygromycin B Gold	ant-hg-1	Thermo Fisher Scientific (Waltham, USA)
Kanamycin sulfate	T832	Carl Roth (Karlsruhe, Germany)
magnesium chloride hexahydrate	M2670	Merck (Darmstadt, Germany)
magnesium sulfate heptahydrate	P027	Carl Roth (Karlsruhe, Germany)
manganese (II) sulfate monohydrate	25303	VWR (Radnor, USA)
potassium acetate	T874	Carl Roth (Karlsruhe, Germany)
potassium chloride	P9333	Merck (Darmstadt, Germany)
potassium dihydrogen phosphate	3904	Carl Roth (Karlsruhe, Germany)
potassium nitrate	P021.1	Carl Roth (Karlsruhe, Germany)
2-propanol	6752	Carl Roth (Karlsruhe, Germany)
Roti-phenol/chloroform/isoamyl-mix	A156	Carl Roth (Karlsruhe, Germany)
Roti-Quant 5x	K015	Carl Roth (Karlsruhe, Germany)
sodium acetate anhydrous	6773	Carl Roth (Karlsruhe, Germany)
sodium chloride	3957	Carl Roth (Karlsruhe, Germany)
sodium dihydrogen phosphate dihydrate	T879	Carl Roth (Karlsruhe, Germany)
sodium hydroxide solution 50%	87938290	VWR (Radnor, USA)

sodium molybdate dihydrate	0274	Carl Roth (Karlsruhe, Germany)
sodium nitrate	A136	Carl Roth (Karlsruhe, Germany)
sodium sulfate decahydrate	T108	Carl Roth (Karlsruhe, Germany)
sodium thiosulfate anhydrous	APPCA6830	VWR (Radnor, USA)
D-sorbitol	S6021	Merck (Darmstadt, Germany)
sulfuric acid 96%	4623	Carl Roth (Karlsruhe, Germany)
trifluoroacetic acid (TFA)	T6508	Merck (Darmstadt, Germany)
Tris(hydroxymethyl)-aminomethane	AE15	Carl Roth (Karlsruhe, Germany)
trisodium citrate dihydrate	3580	Carl Roth (Karlsruhe, Germany)
Triton X-100	T8787	Merck (Darmstadt, Germany)
tryptone/peptone from casein	8952	Carl Roth (Karlsruhe, Germany)
Tween 20	P9416	Merck (Darmstadt, Germany)
yeast extract	2363	Carl Roth (Karlsruhe, Germany)
Zeocin	ant-zn-1	Thermo Fisher Scientific (Waltham, USA)
zinc sulfate heptahydrate	29253236	VWR (Radnor, USA)

**Table 2-8. List of consumables and kits.**

<b>name</b>	<b>order number</b>	<b>Manufacturer</b>
100 bp Quick-Load DNA ladder	N0467	New England Biolabs (Ipswich, USA)
24 deep well plate	742926	Biozym (Hessisch Oldendorf, Germany)
CarboPac PA20 analytical column for HPAEC-PAD	60142	Thermo Fisher Scientific (Waltham, USA)
CarboPac PA200 column for HPAEC-PAD	62895	Thermo Fisher Scientific (Waltham, USA)
Deoxynucleotide solution set	N0447	New England Biolabs (Ipswich, USA)
DNA ladder 1 kb	N3232	New England Biolabs (Ipswich, USA)
DNase I (RNase-Free)	M0303	New England Biolabs (Ipswich, USA)
ELISA 96 well micro test plate, F	82.1581	Sarstedt (Nümbrecht, Germany)
Filtropur BT 50, 0.2 µm filter	83.1823.101	Sarstedt (Nümbrecht, Germany)
GeneJet RNA Purification Kit	K0731	Thermo Fisher Scientific (Waltham, USA)
glass fiber filter 1	5056823	Schubert & Weiss Omnilab (Marktobersdorf, Germany)
High Capacity cDNA Reverse Transcription Kit	10400745	Thermo Fisher Scientific (Waltham, USA)
Hi-Yield Plasmid Mini Prep DNA Isolation kit	30 HYDF100	Süd-Laborbedarf Gauting (Gauting, Germany)
Midori Green Advance	MG04	Nippon Genetics Europe (Dueren, Germany)
One Taq DNA polymerase	M0480	New England Biolabs (Ipswich, USA)
Pacl restriction enzyme	R0547	New England Biolabs (Ipswich, USA)
PeqGOLD Trifast DNA/RNA/protein-purification kit	30-2010DE	VWR (Radnor, USA)
Phusion High-Fidelity PCR Kit	E0553	New England Biolabs (Ipswich, USA)
qPCR BIO SyGreen Mix Separate-ROX	PB20. 14	Nippon Genetics Europe (Dueren, Germany)

## Materials and Methods

---

quartz cuvette, 10 mm layer thickness	Z276650	Merck (Darmstadt, Germany)
Sbfl restriction enzyme	R3642	New England Biolabs (Ipswich, USA)
Sealing Film, for 96 and 384 Well Microplates	CORNBF400S	Schubert & Weiss Omnilab (Marktobendorf, Germany)
syringe filter 0.2 µm Filtropur S	83.1826.001	Sarstedt (Nümbrecht, Germany)
syringe filter Millex 5 µM	10054850	Thermo Fisher Scientific (Waltham, USA)
T4 DNA Ligase	M0202	New England Biolabs (Ipswich, USA)
Vivaspin 20 centrifugal concentrators, 10 kDa	Z614602	Merck (Darmstadt, Germany)
Wizard SV Gel and PCR Clean-up System	A9281	Promega (Fitchburg, USA)
Zero Blunt cloning Kit	440302	Thermo Fisher Scientific (Waltham, USA)
Zirkonium beads (Ø = 0.5 mm)	24 D1132-05	Süd-Laborbedarf Gauting (Gauting, Germany)

## 2.2. Methods

### 2.2.1. Preparation of bacterial cellulose

For the preparation of bacterial cellulose, the commercially available Nata de coco was purchased. The latter is a jelly-like food produced by the fermentation of coconut water by *Komagataeibacter xylinusbacteria*. The gel-like parts of the substrate were soaked overnight in ddH<sub>2</sub>O and then washed extensively again with ddH<sub>2</sub>O. The gel-like parts were then grinded, and the grinded material were washed again with ddH<sub>2</sub>O and collected through vacuum filtration. The substrate underwent extensive rounds of grinding, washing, and filtering. After the last round, the filtered particles were collected and subjected to freeze drying. The resulting powder substrate was used as a C-source in growth experiments.

### 2.2.2. Propagation of the used organisms

#### *Neurospora crassa*

Slanted tubes containing 2 ml of solid Vogel's Minimal Medium (MM) (Vogel 1956) were inoculated with conidia either from previously growing *N. crassa* strains or glycerol stocks. The slants were then incubated for 2 days at 30 °C and in dark. Afterwards, the tubes were further incubated for additional 5 to 8 days at 25 °C and in light. For the preparation of conidial solution, 1 ml ddH<sub>2</sub>O were added to the slant, followed by vigorous vortexing. The conidial suspension was then transferred to a 1.5 ml reaction tube and centrifuged for 1 min at 1000 rpm then the supernatant was discarded. Lastly, 0.5 ml ddH<sub>2</sub>O were used to resuspend the conidia.

#### *Trichoderma reesei*

*Trichoderma reesei* QM6a and RUT-C30 strains were grown on solid malt extract medium plates for 3 days at 30°C and then incubated for additional 5 days at 25 °C and in dark. For the preparation of conidial solution, 2 ml of spore solution (Table 2-2) was distributed over the *T. reesei* plates. The solution was gently mixed with the spores, then it was recollected and filtered through sterile glass wool into new reaction tubes. The reaction tubes were centrifuged for 1 min at 1000 rpm then the supernatant was discarded. Lastly, 0.5 ml ddH<sub>2</sub>O were used to resuspend the spores.

#### *Pichia pastoris*

*Pichia pastoris* X-33 strain was used as protein expression system. The maintenance of *Pichia* strain was done as described in the Invitrogen expression in *Pichia* protocol ([https://assets.thermofisher.com/TFS-Assets/LSG/manuals/pgapz\\_man.pdf](https://assets.thermofisher.com/TFS-Assets/LSG/manuals/pgapz_man.pdf)).

### 2.2.3. Growth assays

#### Starting from conidia

Ten days old *N. crassa* or *T. reesei* conidia were used to inoculate 1% (w/v) C-source in 1x Vogel's solution or 1x Mandels-Andreotti solution (Mandels and Andreotti 1978), respectively. A concentration of  $1 \times 10^6$  conidia/ml was used for the inoculation. A Tecan plate reader was used to measure the concentration of the conidia at 600 nm. The volume of conidial suspension necessary to achieve the required concentration was calculated using the equation below:

$$V_{conidia\ suspension} = \frac{0.0123}{OD_{600} \times dilution} \times V_{total}$$

Where:

- 0.0123: a constant that was determined by cell counting with a hemocytometer and correlating to a standard series of cell counts with measured optical densities at 600 nm
- $V_{total}$ : 3 ml medium in 24 deep-well plates and 100 ml in 250 ml flasks.

The *N. crassa* (at 25 °C) and *T. reesei* (at 30 °C) strains were incubated at the indicated temperatures, 200 rpm, and in constant light in the corresponding C-source. The incubation was terminated after the indicated number of days, and biomass and culture supernatants were harvested afterwards for further analysis.

#### Two-step cultivation

For this mode of cultivation, *N. crassa* and *T. reesei* were pre-incubated in 50 ml of MM or 2% (w/v) glucose with Mandels-Andreotti solution, respectively, as described above (2.2.2). The cultures were incubated for 3 days in constant light, 200 rpm and at 25°C (*N. crassa*) and 30°C (*T. reesei*). The cultures were collected through vacuum filtration and about 0.5 g of mycelia were added to 100 ml 1% (w/v) C-source with 1x Vogel's or 1x Mandels-Andreotti medium and then the cultures were further incubated at 25°C and 200 rpm for two days (*N. crassa*) or at 30°C and 200 rpm for three days (*T. reesei*), respectively. For *N. crassa* cultures to be used in RT-PCR or uptake assays, the cultures were incubated for 16 h at 25 °C, 200 rpm and constant light. *N. crassa* mycelia were then collected and washed three times in 1x Vogel's no carbon for 15 min. Afterwards, Mycelia were transferred to the indicated C-sources and incubated for additional 4 h for induction. Biomass and samples of culture supernatants were collected at the end of the assays.

### 2.2.4. Mycelial dry weight

After the end of incubation time, *N. crassa* mycelia were collected and washed once with ddH<sub>2</sub>O. The excess liquid was removed by shortly putting the mycelia over a tissue. The

mycelia were then transferred to pre-weighted aluminum pans and dried for 16 h at 105 °C. After drying, the aluminum pans containing the mycelia were weighted again and the differences between both measurements were calculated.

### **2.2.5. Crossing of *N. crassa* strains**

*N. crassa* crossing were performed using one of the crossing partners as female crossing partner and inoculated on a Westergaard's medium plate. Subsequently, the other crossing partner was used as male and inoculated on MM slants (2.2.20). Both strains were incubated for 2 days at 30 °C in dark then transferred to RT in daylight. After additional incubation over 9 to 14 days, stereo microscope was used to confirm the formation of protoperithecia of the female crossing partner. Then, the conidia of the male crossing partner were harvested by adding 1 ml ddH<sub>2</sub>O to the slants and vortexing. Afterwards, about 150 µl of the conidial suspension was pipetted on the Westergaard's medium plate with the female crossing partner. The suspension was spread equally over the plate by moving it with a pipette tip. The crossed strains on the plate were then incubated for additional 2 to 3 weeks, until the ascospores were visualized. Subsequently, the ascospores were harvested by adding about 2 ml ddH<sub>2</sub>O on the petri dish and transferring the ascospore suspension into a 1.5 ml reaction tube. The spores were stored at 4 °C. After dilution, an amount of 250 to 500 ascospores were heat activated for 30 min at 59 °C and plated on a MM plate with hygromycin (200 µg/ml each). The plates were incubated for 16 h at RT. Germinated ascospores were picked under the stereo microscope, and incubated on slanted tubes containing 2 ml of MM with hygromycin (2.2.2). The genotype of the crossed strains were confirmed by selection on media with Hygromycin, with/without L-histidine. Lastly, gDNA of the positive candidates were extracted from conidia (2.2.6) and genotyping PCR was performed (2.2.10).

### **2.2.6. Genomic DNA extraction**

The isolation of genomic DNA was performed using 7 to 10 days old conidia. First, the cells were resuspended and grinded in 400 µl gDNA lysis buffer (Table 2-2) in a 2 ml screw cap reaction tube where 250 mg 0.5 mm silica beads were added. The grinding was done using a laboratory bead mill at maximum speed for three times 30 s with a resting period of 30 s in between. The cells-buffer samples were incubated for 30 min at 65 °C and vortexed three times in between. The lysis reaction was then stopped by adding 80 µl of 1 M Tris HCl pH 7.5 and inverting the reaction tubes several times. The samples were centrifuged for 1 min at 13,000 x g and RT. Afterwards, the supernatant was transferred to a new 1.5 ml reaction tube. A volume of phenol:chloroform:isoamylalcohol (25:24:1) equal to the sample

volume was added to the supernatant and mixed by vortexing. Phase separation was allowed by centrifugation for 10 min at 13,000 x g and RT. The upper aqueous phase containing DNA was transferred to a new reaction tube, where about three sample volumes of ice cold 95% (v/v) ethanol was added and immediately mixed by inversion to precipitate the DNA. After 10 min incubation at RT, the samples were centrifuged again for 15 min at 13,000 rpm and RT. The supernatant was discarded and the DNA pellet was washed with 600 µl 70% (v/v) ethanol. The reaction tubes were centrifuged for 5 min at 13,000 rpm and RT. Residual ethanol was removed by air drying under the laminar flow sterile bench. About 50 µl of ddH<sub>2</sub>O were used to dissolve the DNA pellet.

### **2.2.7. Total RNA extraction**

Mycelia of *N. crassa* strains used for RT-qPCR were harvested after the induction on respective C-sources. The following steps were performed on ice or in centrifuges cooled to 4 °C. About 250 mg of wet-weight biomass was transferred into a 2 ml screw cap tube together with 250 mg 0.5 mm silica beads and 1 ml PeqGOLD Trifast DNA/RNA/protein-purification solution or TRIzol Reagent. The mycelia were lysed using a laboratory bead mill at maximum speed for two times 30 s with a resting period of 30 s in between. The samples were gently shaken for 10 min at RT. Afterwards, 200 µl chloroform was added to the cell lysate and mixed by vortexing. The mixture was incubated for 3 min at RT and then centrifuged for 15 min at 12,000 x g. The samples' supernatants were transferred to a new reaction tube where 0.5 ml 2-propanol was added. The mixtures were directly mixed by inversion. The samples were then incubated for 10 min at RT to allow precipitation of RNA, followed by 10 min centrifugation at 12,000 x g. The samples' supernatants were decanted and the RNA pellets were washed using 1 ml 75% (v/v) ethanol. The reaction tubes were then centrifuged for 5 min at 7,500 x g. Residual ethanol was removed completely by pipetting. The RNA pellets were air dried to remove additional residual ethanol. The pellets were resuspended in 45 µl RNase-free ddH<sub>2</sub>O. The RNA samples were then digested with DNase I (RNase Free) according to the manufacturer's instructions and subsequently purified using the GeneJet RNA Purification Kit. Lastly, the purified samples were stored at -80 °C until use.

### **2.2.8. cDNA synthesis**

For cDNA synthesis, 1 µg of purified RNA was used as a template. The cDNA synthesis was performed using and the High Capacity cDNA Reverse Transcription Kit.

## 2.2.9. Nucleic acid quantification

### Quantification by spectrophotometry

The concentrations of DNA and RNA samples were quantified with correspondence to the light observance at a specific wave length (260 and 280 nm, respectively). A Tecan Infinite® 200 PRO NanoQuant reader was used to perform the measurements. The ratio of the absorption of DNA to the absorption of protein (260/280) and the ratio of absorption of DNA to the absorption of oligosaccharides were considered to determine the purity of DNA. Positive amounts of DNA were considered for values between 1.8 and 2 and values greater than 2, respectively.

### Quantification by agarose gel electrophoresis

To determine the concentration of DNA and RNA samples, a certain volume of DNA was gel electrophoresed (02.2.12) and the corresponding band color intensity was compared to the intensities of the bands of known concentrations of the marker used.

## 2.2.10. Polymerase Chain Reaction (PCR)

The standard PCR technique was carried out as described by Mullis and Faloona (Mullis and Faloona, 1987). The desired amplicon was amplified from the respective plasmid DNA, gDNA or cDNA by PCR. A “low fidelity” *Thermus aquaticus* (Taq) polymerase was used for genotyping and colony PCRs, while a “high fidelity”, *Pyrococcus furious*-like, Phusion (Pfu) polymerase was used for cloning purposes. The PCR mixtures and thermocycler runs were prepared and performed as described by the manufacturer. The following components (Table 2-9 and Table 2-11) and PCR programs (Table 2-10 and Table 2-12) were used for amplification.

**Table 2-9: Phusion polymerase PCR reaction mixture.**

component	volume (µl)	final concentration
ddH <sub>2</sub> O	33.0	-
5x Phusion HF buffer	10.0	1x
10 mM dNTPs	1.0	200.0 µM
10 µM forward primer	2.5	0.5 µM
10 µM reverse primer	2.5	0.5 µM
template DNA	1.0	500 ng gDNA or 0.5 ng plasmid DNA
Phusion DNA polymerase	0.5	1.0 unit

**Table 2-10: PCR thermocycler program.**

Step	temperature (°C)	time	cycles
initial denaturation	98.0	30 s	-
denaturation	98.0	10 s	35
annealing	lowest T <sub>m</sub> of primer pair + 2 °C	30 s	
Elongation	72.0	30 s per kb	

final elongation	72.0	7 min	-
Hold	16.0	unlimited	-

**Table 2-11: Taq polymerase PCR reaction mixture.**

component	volume ( $\mu$ l)	final concentration
ddH <sub>2</sub> O	8.5	-
5x Phusion HF buffer	3.0	1x
10 mM dNTPs	0.3	200.0 $\mu$ M
10 $\mu$ M forward primer	1.0	0.7 $\mu$ M
10 $\mu$ M reverse primer	1.0	0.7 $\mu$ M
template DNA	1.0	500 ng gDNA or 0.5 ng plasmid DNA
Taq DNA polymerase	0.2	1.0 unit

**Table 2-12: Taq polymerase PCR thermocycler program.**

step	temperature	time	cycles
initial denaturation	95.0 °C	5 min	-
denaturation	95.0 °C	30 s	35
annealing	lowest T <sub>m</sub> of primer pair in °C	30 s	
elongation	72.0 °C	1 min per kb	
final elongation	72.0 °C	7 min	-
hold	16.0 °C	unlimited	-

### 2.2.11. Quantitative real time PCR (qRT-PCR)

For the RT-qPCR reactions, 100 ng of cDNA was used either in the mix of the qPCR BIO SyGreen Mix Separate-ROX kit or sensiFAST SYBR No-ROX kit as described by the manufacturers. The reactions were performed in a Mastercycler ep realplex<sup>2</sup>. The primers were designed with the following parameters: melting temperatures (T<sub>m</sub>) of 60  $\pm$ 2°C, primer lengths of 20-24 nucleotides, guanine-cytosine (GC) content of 45-55%, and PCR amplicon lengths of 100-200 base pairs.

RT-qPCR was performed as described before (Benz *et al.* 2014). The *act* gene (NCU04173, actin variant) was used as endogenous control to normalize the expression values of the target genes. To determine the expression of target genes in *N. crassa* WT strain, 16 h MM pre-grown cultures were washed three times for 15 min each in 1x Vogel's no carbon solution and then transferred to an induction solution of 1x Vogel's solution plus the respective induction C-source. The expression levels were compared in the induced strains versus the non-induced ones. Relative expression levels were determined and analyzed using the realplex 2.2 software.

### 2.2.12. Nucleic acids separation by agarose gel electrophoresis

For the separation and detection of DNA and RNA samples, agarose gels in 1x TAE buffer were prepared. The percentages (0.7 - 2%) of agarose varied inversely with the expected size of the bands. For the detection of DNA under UV light, Midori green was used in gel preparation. The samples were prepared by mixing with a suitable volume of 10x loading buffer. Depending on the percentage of the gel and the size of DNA/RNA fragments, running time of the gel was adjusted to 30-40 minutes at 140 V and 50 mA. The molecular weight markers were used to determine the size of the different fragments. Visualization of the bands and pictures of gel were taken using the gel imaging system Fusion solo S.

### 2.2.13. Purification of nucleic acids

#### Purification of DNA fragments from agarose gel

After agarose gel electrophoresis of PCR samples, the desired amplicons of the size ranges from 250 bp to 5 kb were excised from the gel, and weighed. The DNA bands were purified using the Promega Wizard SV Gel and PCR Clean-up System, according to the manufacturer's instruction manual.

#### Purification of PCR product

The purification of the PCR product was done using Wizard SV Gel and PCR Clean-up System (Promega; Fitchburg, USA) following the manufacturer's manual.

### 2.2.14. Restriction-ligation cloning

For the production of *clr-1* mis-expression strain (*clr-1 oex*), the *clr-1* gene was amplified from gDNA using the primers *clr-1\_CSR-GPD\_F* and *clr-1\_CSR-GPD\_R* (Table 2-4). Both, the PCR product and the pTSL126B plasmid (SFigure 6-6) were subjected to restriction digest for 16 h at 37 °C with the restriction enzymes *Sbfl* and *Pacl* (Table 2-8). Consequently, both digested PCR product and plasmid were purified (2.2.13) and ligated, for 30 min to 1 h at RT, using T4 DNA ligase with the reaction mixture described below:

**Table 2-13: Restriction digest reaction components.**

component	amount
10x Cutsmart reaction buffer	5 µl
restriction enzyme 1	2 units
restriction enzyme 2	2 units
template DNA	up to 2 µg
ddH <sub>2</sub> O	fill up to 50 µl

**Table 2-14: T4 DNA ligase reaction components.**

component	amount
10x T4 DNA ligase buffer	1 $\mu$ l
digested DNA fragment (insert)	3-5x the equimolar mass of used plasmid
digested plasmid (vector)	50 ng
T4 DNA ligase	5 units
ddH <sub>2</sub> O	fill up to 10 $\mu$ l

The DNA fragment to be used in the ligation reaction was calculated using the formula below:

$$m_{insert} = \frac{m_{vector} \times l_{insert} \times Y}{l_{vector}}$$

Where:

- $m_{insert}$ : the insert mass to be used in the ligation reaction
- $l_{insert}$  and  $l_{vector}$ : the length of the fragment and vector in bp, respectively,
- $Y$ : constant standing for the concentration factor of the insert to vector ratio
- $m_{vector}$ : vector mass used in the ligation reaction

After ligation, the assembled constructs were transformed into *E. coli* DH5 $\alpha$  strains (2.2.15).

### 2.2.15. *E. coli* transformation

Shortly before transformation, 45  $\mu$ l of chemical competent *E. coli* DH5 $\alpha$  cells were thawed on ice for 5 min followed by the addition of 5  $\mu$ l of DNA solution and incubation on ice for 30 min. The DNA-cells suspension was moved to a heating block heat shocked for 30 s at 42  $^{\circ}$ C. The suspension was then cooled down for 3 min on ice, followed by the addition of 450  $\mu$ l of SOC medium. The cells were then incubated for 60 min at 37  $^{\circ}$ C and 250 rpm. Consequently, 50  $\mu$ l of the cell suspension were plated on solid agar LB plates with the appropriate selective marker and incubated for 16 h at 37  $^{\circ}$ C. On the next day, transformed colonies were picked and transferred to new LB plates and genotyping was performed by colony PCR.

### 2.2.16. Plasmid DNA miniprep

Plasmid mini prep HiYield Plasmid Mini Kit was used, according to the manufacturer's instructions, for the extraction of plasmid constructs from *E. coli* cells.

### 2.2.17. Nucleic acids sequencing

Purified plasmid samples PCR products were premixed with the forward primer and sequenced via the Eurofins Genomics (Ebersberg), following their specification. Glycerol stocks were prepared from *E. coli* strain with positive constructs (2.2.19).

### 2.2.18. *N. crassa* transformation

Confirmed plasmid construct was used for *N. crassa* transformation. For this,  $\Delta clr-1$  deletion strain was grown in 250 ml flasks with 50 ml of solid MM (2.2.2), then the conidia were harvested by the addition of 50 ml of cold and sterile 1M D-Sorbitol. After vortexing, the conidial suspension was filtered through a sterile gauze into a 50 ml sterile falcon tube and filled up till 50 ml with cold 1M D-Sorbitol. The falcon tube was then centrifuged for 5 min at 2000 rpm and 4 °C. The supernatant was discarded and the cells were washed again twice with 50 ml D-sorbitol and centrifugation for 5 min at 1500 rpm. Afterwards, the supernatant was removed and cells were resuspended in 5 ml D-sorbitol. Lastly, the cells suspension was measured at an optical density of 600 nm, the suspension was centrifuged for 3 min at 1500 rpm and the supernatant was discarded. The final volume was adjusted so that the concentration is  $2.5 \times 10^9$  conidia/ml was calculated as follows:

$$V_{final} = V_{suspension} \div \left( \frac{OD_{measured} \times dilution}{0.0123 \times 1000} \right)$$

Where:

- $V_{final}$  : volume of 1 M sorbitol that was used for the resuspension after the final centrifugation step
- $V_{suspension}$  : volume of conidia suspension previous to the final centrifugation step

Then, 40  $\mu$ l of the conidia suspension were mixed with 1  $\mu$ g to 2  $\mu$ g of purified expression construct in 10  $\mu$ l ddH<sub>2</sub>O. An only 10  $\mu$ l ddH<sub>2</sub>O sample was used as a negative control. After 30 min incubation on ice, the suspension was transferred into a pre-cooled electroporation cuvette (1 mm gap size) and then the cells were electro-transfected at 1500 V with an Eppendorf electroporator. Then, 950  $\mu$ l of cold 1 M D-Sorbitol were directly used and the mixture was transferred into a 15 ml falcon tube and mixed with 2 ml MM. Following a 60 min incubation at 30 °C, the conidial suspension was centrifuged for 3 min at 1500 rpm. 2 ml of the supernatant were discarded and the conidia were resuspended in the remaining 1ml solution. The latter was split into 250  $\mu$ l and 750  $\mu$ l aliquots that were transferred into new 15 ml falcons. Both tubes were then filled up to 10 ml with top-agar (at 55 °C) and mixed by inversion. The mixtures were poured over previously prepared bottom-agar plates. As a selection marker, Cyclosporin A was added to both, bottom- and top-agar media. The agar plates were incubated for 3 days at 30 °C in dark. Lastly, grown colonies were picked and grown on new tubes with 2 ml of slanted MM. Positive transformed strains were confirmed by genotyping PCR (2.2.10), after the extraction of gDNA (2.2.6).

### **2.2.19. Glycerol stocks**

Glycerol stocks were prepared by mixing 750 µl of *N. crassa* conidial suspension or bacteria cultures (after overnight growth in LB medium supplemented with antibiotics) with 250 µl of a sterile filtered 75% (v/v) glycerol solution. The mixtures were vortexed and directly frozen in liquid nitrogen. The glycerol stocks were labeled properly and stored at -80°C.

### **2.2.20. Extraction of intracellular metabolites**

After the incubation on the indicated C-source, *N. crassa* mycelia were collected and their intracellular metabolites were extracted using a protocol modified from Tambellini *et al.* (Tambellini *et al.* 2013). First, the mycelia were washed three times with ddH<sub>2</sub>O. Then about 500 mg of the mycelia were grinded where 24 ml of cold CH<sub>3</sub>Cl:MeOH (1:1) and 6 ml ddH<sub>2</sub>O were added to the mycelia. The samples were incubated for 30 min on ice. Afterwards, the samples were centrifuged for 15 min, at 4000 rpm and 4 °C. Supernatants were collected and re-centrifuged for 30 minutes at 12000 rpm and 4 °C. The samples were stored at 4 °C for further analysis.

### **2.2.21. Extraction of intracellular protein from *N. crassa***

After incubation of *N. crassa* on the indicated C-source, the mycelia were harvested by using a Buchner funnel and a glass fiber filters, washed three times by 50 ml 1x Vogel's solution. The mycelia were then frozen in liquid nitrogen. Frozen mycelia were grinded into powder using freezing-milling method. Afterwards, about 250 mg of frozen mycelia were lysed by adding 750 µl mycelia lysis buffer (Table 2-2). Samples were incubated for 30 min at -20 °C, then centrifuged for 10 minutes at 1300 rpm and 4 °C. Protein concentration was measured as described below (2.2.23) and the samples were stored at 4 °C for further analysis.

### **2.2.22. Protein expression and purification from *Pichia***

The growth of the *Pichia* strain with positive expression constructs and the preparation of cell lysate were done according to the Invitrogen expression in *Pichia* protocol ([https://assets.thermofisher.com/TFS-Assets/LSG/manuals/pgapz\\_man.pdf](https://assets.thermofisher.com/TFS-Assets/LSG/manuals/pgapz_man.pdf)). Briefly, strains were incubated on YPD plates with 25 µl/100 ml zeocin for 4 days at 30°C. Single colonies were used to inoculate 15 ml YPD media with 1 µg/ml Zeocin. The cultures were incubated for 16 h at 30°C and 250 rpm. Afterwards, the pre-culture was used to inoculate 50 ml YPD media containing 0.5 µg/ml zeocin in 250 ml flasks. The cultures were further incubated for 4 days at 23°C and 250 rpm. The cultured were then centrifuged in a pre-cooled centrifuge and the cells were harvested. For cell lysis, 25 ml cell lysis buffer were

added to the cells. The suspensions were incubated for 15 min in a 37°C water bath. Afterwards, 12.5 µl DNase I was added to the mixture that was further incubated for 30 min. Cells were then centrifuged for 20 min at 16,000 xg and 4°C. The cell lysate supernatant was then used for GH2-1 purification by immobilized metal-affinity chromatography (IMAC) of the histidine affinity tag (Bornhorst and Falke 2000). Elution of the enzyme was performed via a pH gradient of 5.5, 5.0, and 4.5 of the same elution buffer (Table 2-2). Protein concentration was measured as described below.

### **2.2.23. Bradford assay**

Bradford assay was performed to determine the total amount of purified protein, intracellular protein, as well as in culture supernatants. Dilution series of BSA as standard (Bradford, 1976) was prepared. Roti®-Quant reagent was diluted 1:5 with ddH<sub>2</sub>O. Afterwards, 200 µl of the 1x Roti-Quant was mixed with 10 µl of protein sample. The mixtures were incubated for 5 min at RT. Afterwards, the samples' absorbance at 595 nm was measured using a Tecan Infinite® 200 PRO NanoQuant reader. The linear regression of the BSA standards was calculated and used as a reference to calculate the protein concentration of the samples.

### **2.2.24. Cellulase and xylanase assays**

For the analyses of cellulase and xylanase production by the fungi, samples were collected from culture supernatant. The samples were centrifuged for 10 min at 11000 rpm. The supernatant was then carefully transferred into a new reaction tube and stored at 4 °C. Azo-CMCase and Azo-xylanase activity assays were carried out according to the protocols of the manufacturer (Megazyme, Ireland; S-ACMC and S-AXBL). The assays were slightly modified so that the reaction mixture was reduced to a quarter of the original volume.

### **2.2.25. Sulfuric acid hydrolysis of carbon sources**

To determine the constituent sugars of different C-sources a chemical hydrolysis with H<sub>2</sub>SO<sub>4</sub> was performed ref. The samples were first dried for 16 h at 60 °C, then about 5 mg of dried material were swollen in 50 µl of 72% (v/v) H<sub>2</sub>SO<sub>4</sub> at RT for 1 to 4 h depending on the recalcitrance of the sample. After incubation, 1.45 ml ddH<sub>2</sub>O was to the sample, and the mix was further incubated for 1 h at 121 °C. Followed by a centrifugation step for 5 min at 13,000 x g to remove residual solids. The supernatants were transferred to new reaction tubes, and stored at 4 °C, until the compositional analysis proceeds.

### **2.2.26. Sulfuric acid hydrolysis of carbon sources**

To determine the constituent sugars of different C-sources a chemical hydrolysis with H<sub>2</sub>SO<sub>4</sub> was performed ref. The samples were first dried for 16 h at 60 °C, then about 5 mg of dried material were swollen in 50 µl of 72% (v/v) H<sub>2</sub>SO<sub>4</sub> at RT for 1 to 4 h depending on the recalcitrance of the sample. After incubation, 1.45 ml ddH<sub>2</sub>O was to the sample, and the mix was further incubated for 1 h at 121 °C. Followed by a centrifugation step for 5 min at 13,000 x g to remove residual solids. The supernatants were transferred to new reaction tubes, and stored at 4 °C, until the compositional analysis proceeds.

### **2.2.27. Sugar uptake assay**

The uptake of monosaccharides by *N. crassa* was determined as published previously (Galazka *et al.*, 2010; J. Benz *et al.*, 2014). For detailed description, see section 4.7.9.

### **2.2.28. HPAEC-PAD analyses**

The evaluation of sugars present in the samples were analyzed using an ICS-3000 liquid chromatography system (Dionex, Thermo Scientific), equipped with a pulsed amperometric detector, as follows:

#### *For the compositional analysis of complex*

The H<sub>2</sub>SO<sub>4</sub> hydrolyzed samples were diluted to concentrations below 10 µg/ml. For the analysis of neutral monosaccharides containing samples, a CarboPac® PA20 3x150 mm column was used. The samples were eluted using 5 mM NaOH as the mobile phase isocratic. While for the analysis of uronic acids and disaccharides containing samples, a CarboPac PA200 column was used. The samples were eluted using 0.1 M NaOH and 0.1 M NaOH/1 M NaAc. The following gradient was used in this case: 2 min 0% 0.1 M NaOH/1 M NaAc, 10 min 0-10% 0.1 M NaOH/1 M NaAc and 3 min 0% 0.1 M NaOH/1 M NaAc. In both columns, samples were eluted for 15 min, at 30 °C column temperature, and a flow rate of 0.4 ml/min.

### **2.2.29. Statistical analyses**

Experiments were done in biological triplicate, and statistical significance was determined by applying analysis of variance (ANOVA) followed by a post-hoc Tukey test using the statistical computing software R (Team 2013). Values of bars and lines in bar and line graphs, respectively, are the mean of the biological replicates, and error bars in all figures are standard deviations (n=3).

**2.2.30. Sequence retrieval, analysis and domain predictions**

FungiDB was used to retrieve *N. crassa* DNA, mRNA, and amino acids sequences (<http://fungidb.org/fungidb/>) in FASTA file format. For the visualization of DNA and mRNA sequences, SnapGene software (from GSL Biotech; <https://www.snapgene.com/>) was used.

---

### **3. Comparing the physicochemical parameters of three celluloses reveals new insights into substrate suitability for fungal enzyme production**

Lara Hassan, Manfred J. Reppke, Nils Thieme, Steffen A. Schweizer, Carsten W. Mueller, and J. Philipp Benz

#### **3.1. Authors' contributions**

L.H., M.J.R., N.T., S.A.S., and C.W.M. performed the experiments and acquired the data. L.H., M.J.R., N.T., C.W.M. and J.P.B. analyzed and interpreted the data. L.H. and J.P.B. drafted the initial manuscript. All authors reviewed and approved the final version of the manuscript.

#### **3.2. Summary**

Lignocellulosic feedstocks are a rich source of simple sugars that are used in biorefinery and green chemistry. The key step here is the degradation of such feedstocks by the action of lignocellulosic enzymes produced by microorganisms, such as bacteria or filamentous fungi. However, the recalcitrant and heterogeneous nature of lignocellulosic materials complicates their digestion by such enzymes. Hence, pretreatment techniques and extraction methods lead to the presence of less heterogeneous purified cellulosic substrates such as microcrystalline celluloses (MCCs). In addition to their use as cellulase-inducing substrates, MCCs have been used as binding agents and fillers in the pharmaceutical and food industries, respectively. Although the purity and availability of such substrates render them easy to use, various products have been shown to differ in their characteristics regarding crystallinity, chemical composition, and particle size. These differences may have an influence on the fermentation processes and the production of enzymes by fungi. Therefore, in this study, the physicochemical parameters (e.g. morphology, surface area, particle size, crystallinity, and chemical composition) of three cellulosic substrates, two MCCs and one powdered cellulose, were compared. Moreover, the effect of such parameters on the production of (hemi-)cellulases by the industrial strain *T. reesei* RUT-C30 and the model strain *N. crassa* was analyzed. The results indicated that particularly crystallinity and hemicellulose content are major determinants of substrate performance. However, the results also indicated that the chemical composition alone does not reflect the fungal response, but other factors, such as substrate bioavailability, carbon catabolite de-repression, and species-specific regulatory networks are also important.

### 3.3. Abstract

The industrial applications of cellulases are mostly limited by the costs associated with their production. Optimized production pathways are therefore desirable. Based on their enzyme inducing capacity, celluloses are commonly used in fermentation media. However, the influence of their physicochemical characteristics on the production process is not well understood. In this study, we examined how physical, structural and chemical properties of celluloses influence cellulase and hemicellulase production in an industrially-optimized and a non-engineered filamentous fungus: RUT-C30 and *Neurospora crassa*. The performance was evaluated by quantifying gene induction, protein secretion and enzymatic activities.

Among the three investigated substrates, the powdered cellulose was found to be the most impure, and the residual hemicellulosic content was efficiently perceived by the fungi. It was furthermore found to be the least crystalline substrate and consequently was the most readily digested cellulose *in vitro*. *In vivo* however, only RUT-C30 was able to take full advantage of these factors. When comparing carbon catabolite repressed and de-repressed strains of *T. reesei* and *N. crassa*, we found that *cre1/cre-1* is at least partially responsible for this observation, but that the different wiring of the molecular signaling networks is also relevant.

Our findings indicate that crystallinity and hemicellulose content are major determinants of performance. Moreover, the genetic background between WT and modified strains greatly affects the ability to utilize the cellulosic substrate. By highlighting key factors to consider when choosing the optimal cellulosic product for enzyme production, this study has relevance for the optimization of a critical step in the biotechnological (hemi-)cellulase production process.

### 3.4. Background

Due to their wide applicability, the demand for cellulases and hemicellulases is constantly increasing. Currently, these enzymes are used in the processing of food and animal feed, in the textile and laundry industries, for pulping and paper production, as well as for the biofuels industry (Kuhad *et al.* 2011). The overall technical enzymes market is projected to reach a value of 1.27 billion USD in 2021, with the bioethanol application predicted to be the fastest-growing section (Report 2016). The goal here is to efficiently convert sustainably produced lignocellulosic feedstocks to fermentable sugars for the production of biofuels, but also other products of the biorefinery. Due to the high recalcitrance of cellulose, this process requires high enzyme loadings, warranting research efforts aiming to increase enzyme yields and decrease the production costs.

Cellulose is composed of unbranched chains with repeating  $\beta$ -1,4-linkages of only D-glucose units. Many parallel glucan chains form tight microfibrils held together by hydrogen bonds, rendering the surface of cellulose highly hydrophobic and recalcitrant to enzymatic attack (Matthews *et al.* 2006; Himmel *et al.* 2007; Habibi *et al.* 2010; PÉrez and Samain 2010). Traditionally, the fine structure of cellulose is described in a simplistic two-phase model, in which highly ordered regions are classified as crystalline and less well-ordered regions as amorphous (Harada H 1985). Moreover, cellulose in the natural setting is embedded in a matrix of hemicelluloses and lignin, adding structural support and protection (Somerville *et al.* 2004; Ding and Himmel 2006). The major hemicelluloses in hardwoods and grasses are xylans and mixed-linkage glucans, while (galacto-)glucomannans dominate in softwoods (Timell 1967; Pettersen 1984; Harada H 1985).

Cellulases are commonly produced by fermentation of lignocellulosic substrates with microorganisms, such as bacteria or filamentous fungi. Microcrystalline celluloses (MCCs) have been used as excipients in the pharmaceutical industry for decades, but are also used as cellulase-inducing substrates due to their purity, availability and ease of use. MCCs are usually prepared by treatment of cotton linters or wood pulp with dilute mineral acid to hydrolyze and extract the amorphous regions of cellulose as well as hemicelluloses, lignin and pectin (Battista and Smith 1961; Hanna *et al.* 2001). The result is a partially depolymerized cellulose with a limited degree of polymerization in the form of colloidal crystallites that can aggregate and agglomerate to particle sizes of usually between 20 – 200  $\mu$ M (Adel *et al.* 2011). MCCs are derived from various sources, such as hardwoods and softwoods. Various products from the international market have been shown to differ in their characteristics regarding crystallinity, monosaccharide composition, and particle size (Baehr and Puls 1991; Landin *et al.* 1993; Landin *et al.* 1993; Newman 1994). Moreover, batch-to-batch variability has been shown to have an equally strong impact on the MCC properties (Rowe *et al.* 1994).

The filamentous ascomycete *T. reesei* (teleomorph *Hypocrea jecorina*) has become the preferred organism for the production of cellulases (Seiboth *et al.* 2011; Viikari *et al.* 2012; Paloheimo *et al.* 2016), one of the best known and publicly available strains being RUT-C30 of the Rutgers lineage derived from screens for hyper-cellulase production after rounds of classical mutagenesis (Le Crom *et al.* 2009; Peterson and Nevalainen 2012).

*T. reesei* has also been instrumental in the elucidation of the molecular factors underlying the perception and degradation of cellulose in filamentous fungi (Kubicek 2013). The general principle of induction and repression governing the response is conserved as in all microorganisms, but varies in its implementation between fungi (for a review, see Glass *et al.* 2013). In *T. reesei* (and species of the genus *Aspergillus*), the transcription factor (TF) XYR1/XInR is the major regulator of the cellulolytic and hemicellulolytic response, even

though recently ACE3 was described in *T. reesei* as a novel master regulator of cellulase expression and a modulator of xylan degrading enzyme expression (Hakkinen *et al.* 2014). In other fungi, such as in the genetic model system *N. crassa*, the XYR1 homologs only modulate production of cellulases and are mainly required for the induction of hemicellulases (for recent reviews, see Huberman *et al.* 2016; Seibert *et al.* 2016). Instead, two other conserved TFs in tandem govern the response to cellulose: CLR-1 and CLR-2 (Coradetti *et al.* 2012; Craig *et al.* 2015). The function of CLR-2 does not seem to be strictly conserved in *T. reesei* (Hakkinen *et al.* 2014), but is in other fungi such as in *A. nidulans* (Coradetti *et al.* 2012).

Other than the induction pathways, carbon catabolite repression (CCR), a mechanism enabling microorganisms to prefer easily metabolizable carbon sources over polymeric or recalcitrant substrates, seems strictly conserved in filamentous fungi (Glass *et al.* 2013). A central mediator of CCR is the zinc-finger TF CreA/Cre1 (Bailey and Arst 1975; Ilmen *et al.* 1996; de la Serna *et al.* 1999; Sun and Glass 2011), which acts in a double-lock mechanism on both the target genes as well as the regulatory TFs (Huberman *et al.* 2016). In *T. reesei* RUT-C30, a truncated version of the *cre1* gene is present (Mello-de-Sousa *et al.* 2014), leading to a cellulase de-repressed phenotype (Ilmen *et al.* 1996).

The production of cellulases in filamentous fungi is furthermore dependent on the presence of specific inducer molecules. In case of cellulose, the relevant signaling molecules are short cellodextrins such as cellobiose, which are released from cellulose by the action of cellulases, or metabolic derivatives, such as sophorose (Sternberg and Mandels 1979; Zhou *et al.* 2012; Znameroski *et al.* 2012).

According to the aforementioned points it is clear, therefore, that multiple factors will affect the production of cellulases in microorganisms: 1) the composition of the substrate, 2) the accessibility of the cellulose to enzymatic attack, 3) the overall enzymatic complement produced by the organism, 4) the nature and amount of inducer molecules being released, and 5) the wiring of the regulatory networks integrating the perceived signals in the respective production organism employed. MCCs as more pure substrates might appear to be less complex in their applicability than plant biomass, but their effectiveness is subject to the same combination of physical, chemical and biological factors. A huge variety of sources, production methods, as well as batch-to-batch variations (Baehr and Puls 1991; Landin *et al.* 1993; Landin *et al.* 1993; Rowe *et al.* 1994) makes it highly demanding for the user to choose the best substrate and warrant studies to determine the most relevant factors. Despite a plethora of studies on the characteristics of cellulose and their effects on enzyme hydrolysis, the effects of central factors, such as crystallinity and fine structure (surface area; porosity), are still unclear and partly disputed (Fan *et al.* 1980; Fan 1981; Puri 1984; Mansfield *et al.* 1999; Mooney *et al.* 1999; Hall *et al.* 2010; Park *et al.* 2010;

Rollin *et al.* 2011; Peng *et al.* 2013; Li *et al.* 2014; Peciulyte *et al.* 2014). However, with some notable exceptions (e.g. Peciulyte *et al.* 2014) most of these studies used isolated enzyme systems, which is helpful to focus, but is also simplifying, since it ignores the biology of the production organism. To extend our view, we therefore analyzed both the physicochemical and molecular biological aspects of cellulase production in two filamentous fungi when grown on different cellulosic substrates. We chose three representative celluloses: a hardwood- and a softwood-derived MCC as well as a hardwood-derived powdered cellulose, and tested their effectiveness as cellulase-inducing substrates on the hypercellulolytic *T. reesei* strain RUT-C30 and the non-adapted laboratory model strain *N. crassa*. The physicochemical analyses of the substrates were done at several structural levels (acc. to Mansfield *et al.* 1999): fiber (surface area and morphology), fibril (composition, particle size), and microfibril (crystallinity). To assess the fungal performance, cellulase productivity as well as the molecular response were recorded.

## 3.5. Results

### 3.5.1. Substrate characteristics – Surface area and morphology

For this study, three different cellulose products were chosen as cellulase-inducing growth substrates: a hardwood-derived MCC (Emcocel HD90), a softwood-derived MCC (Avicel PH-101) and a hardwood-derived purified cellulose (Alphacel) (see Methods; Table 3-2). The celluloses were initially observed by scanning electron microscopy (SEM) to visualize macromolecular substrate characteristics. In line with the manufacturer's specifications, Emcocel contained the largest particles in comparison to the MCC gold standard Avicel as well as the purified cellulose Alphacel (Figure 3-1 A-C). While Alphacel had the most fibrous appearance (Figure 3-1 B), Emcocel consisted mostly of particle agglomerates that could be broken up by additional ball-milling (Figure 3-1 C & D).

N<sub>2</sub>-BET measurements showed an inverse correlation between the specific surface area of the celluloses and the average particle size. The specific surface area of Emcocel (0.80 m<sup>2</sup>/g) was only about 2/3 the area of Avicel (1.28 m<sup>2</sup>/g) and less than half the area of Alphacel (1.64 m<sup>2</sup>/g). After additional ball-milling, however, the surface area of Emcocel doubled and was comparable to the other substrates (1.58 m<sup>2</sup>/g).

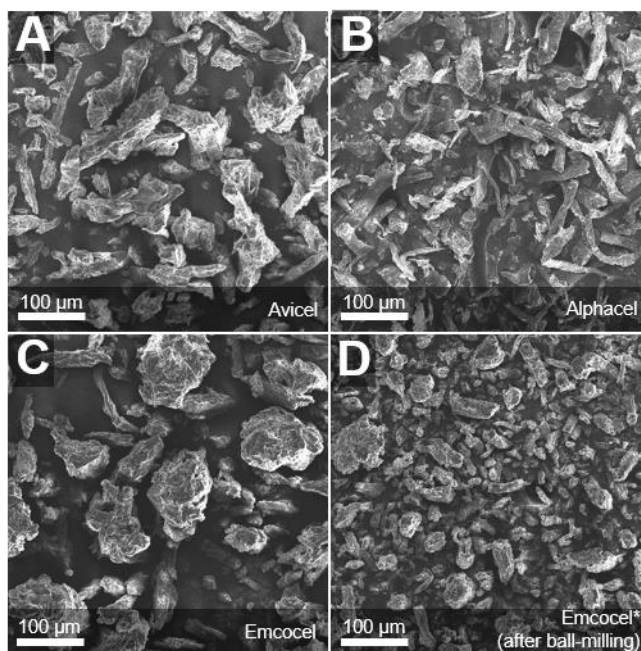


**Figure 3-1. Scanning electron micrographs of cellulose substrates obtained at 8.0 kV accelerating voltage and 100x magnification (Jeol JSM-IT100).**

Scanning electron micrographs of cellulose substrates obtained at 8.0 kV accelerating voltage and 100x magnification (Jeol JSM-IT100). Images show a representative picture for each substrate out of several technical replicates.

### 3.5.2. Determination of hemicellulose content of the celluloses

To determine the purity of the different MCCs regarding hemicellulose contaminations, we performed a compositional analysis after total acid hydrolysis. Bacterial cellulose was used as a hemicellulose contamination-free standard for comparison. For Avicel, Alphacel and the bacterial cellulose, a 1 hour swelling time in 72 %  $\text{H}_2\text{SO}_4$  was sufficient to achieve an almost complete hydrolysis. For Emcocel however, an undissolved residual mass remained after the hydrolysis, indicating that the process had been incomplete (data not shown). For that reason, the hydrolysis of Emcocel was repeated using longer swelling times (4 hours) to give the sulfuric acid more time to completely react with the MCC.

As expected, the bacterial cellulose showed no trace of other monosaccharides other than glucose (Table 3-1). Alphacel on the other hand, was the most unpure cellulose with a particularly high content of xylan. The high xylan:mannan ratio is indicative of its source material being hardwood pulp (acc. to Baehr and Puls 1991). Avicel as a softwood-derived MCC presented a much more moderate xylan:mannan ratio, but still contained considerable amounts of both hemicelluloses. Emcocel proved to be the least hemicellulose-contaminated cellulose in our analysis with xylan and mannan contents of less than 1 % each. This amount was more or less constant at all different swelling times tested (not shown), while the amount of detected glucose increased considerably at four hours,

suggesting that the cellulosic fraction of Emcocel is extremely densely packed and recalcitrant to the hydrolysis. Even after four hours of swelling, ~6-7 % of the mass remained unaccounted for. We did not detect elevated amounts of lignin or extractables in Emcocel however (data not shown), indicating that the residual mass is mainly undissolved cellulose.

**Table 3-1. Results of sugar analysis of the celluloses after sulfuric acid hydrolysis (in %).**

	Avicel <sup>1</sup>	Emcocel <sup>2</sup>	Alphacel <sup>1</sup>	bacterial cellulose <sup>1</sup>
<b>D-glucan</b>	93 ± 5.5	92 ± 0.4	84 ± 5.8	97 ± 4.2
<b>D-xylan</b>	3.5 ± 0.4	0.8 ± 0.08	14.7 ± 1.1	ND
<b>D-mannan</b>	1.8 ± 0.1	0.3 ± 0.01	1.3 ± 0.3	ND

1) 1 hour swelling; 2) 4 hours swelling; ND) none determined

### 3.5.3. Cellulose crystallinity

Crystallinity has been widely used to describe celluloses and woods, since it is a good measure of the inherent degree of structural order and thus may have a major influence on the recalcitrance of the substrate to biochemical attack (e.g. Horii *et al.* 1984; Sterk *et al.* 1987; Newman 2004; Park *et al.* 2010). Due to the differences observed in bioavailability of the celluloses, we decided to measure also the crystallinity of all three substrates. To this end, samples of the celluloses were analyzed by solid-state <sup>13</sup>C nuclear magnetic resonance (NMR) and the crystallinity index (Crl) calculated by the NMR C4 peak separation method (Horii *et al.* 1984; Newman and Hemmingson 1990; Park *et al.* 2010).

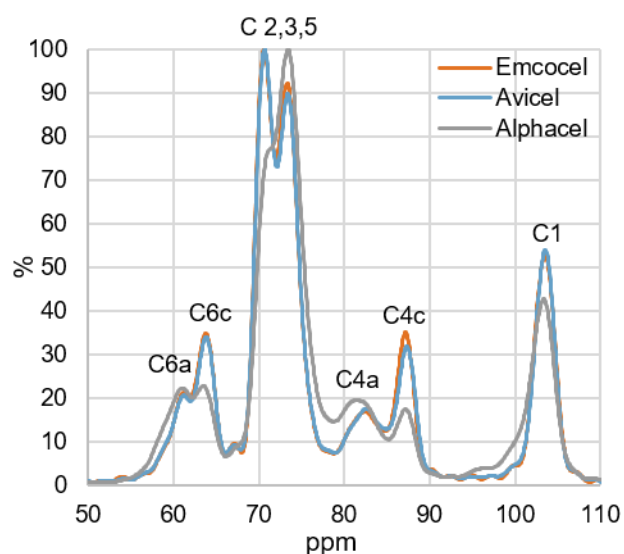


**Figure 3-2. Solid state <sup>13</sup>C NMR spectra of cellulose samples.**

Depicted are normalized spectra between 50 and 110 ppm showing the assignment of peaks to the carbons in a glucopyranose repeat unit. Shown is a single but representative spectrum for each cellulose.

The NMR spectra displayed noticeable differences in height of the C4 peaks between the samples (Figure 3-2). Alphacel showed the lowest crystallinity with 33.1 % compared to Avicel with 54.4 % and Emcocel with 56.7 %. The calculated CrIs therefore allowed for a clear discrimination of the MCCs and the powdered cellulose product Alphacel. Additionally, the results demonstrate that Emcocel was the most crystalline cellulose product in our experiments.

#### **3.5.4. *In vitro* digestibility of the cellulose substrates**

Since the fungal cellulase induction will be highly dependent on the enzymatic digestibility for the liberation of inducer molecules, we next wanted to test this in an *in vitro* assay. To this end, *N. crassa* cellulases were incubated with the cellulose substrates. The liberated sugars were analyzed by HPAEC-PAD, and the residual cellulose harvested for SEM analysis (Figure 3-3).

The chromatograms indicated that mainly glucose and higher cellodextrins accumulated in the assay supernatants after extensive digestion (8 hours; Figure 3-3 A). The quantified amounts of glucose, xylose and mannose at more initial time points (1 hour; Figure 3-3 A; inset) showed that Alphacel was the most readily digested substrate. Similarly, Emcocel was the least digested substrate again, corroborating that it is most recalcitrant of all three substrates to enzymatic or chemical attack.

When observed by SEM, all three celluloses showed a more particulate appearance after 24 hours of enzymatic digestion. This was most prominent for the MCCs, which completely disintegrated into individual fibers (Figure 3-3 B-G). At higher magnifications, it became evident that the surfaces of all digested substrates appeared smoother than the controls (Figure 3-3 H-M). This might indicate that the rough top layers were formed by more amorphous cellulose and/or hemicelluloses. It furthermore suggests that the flat layers exposed after the digest might represent more recalcitrant cellulose-rich areas. Particularly the parallel fibrillar structures visible on the surface of some fibers of Emcocel after the digest (Figure 3-3 I; arrow) seem to represent relatively pure, ordered cellulose fibrils, leaving little contact surface for enzymes to attack.

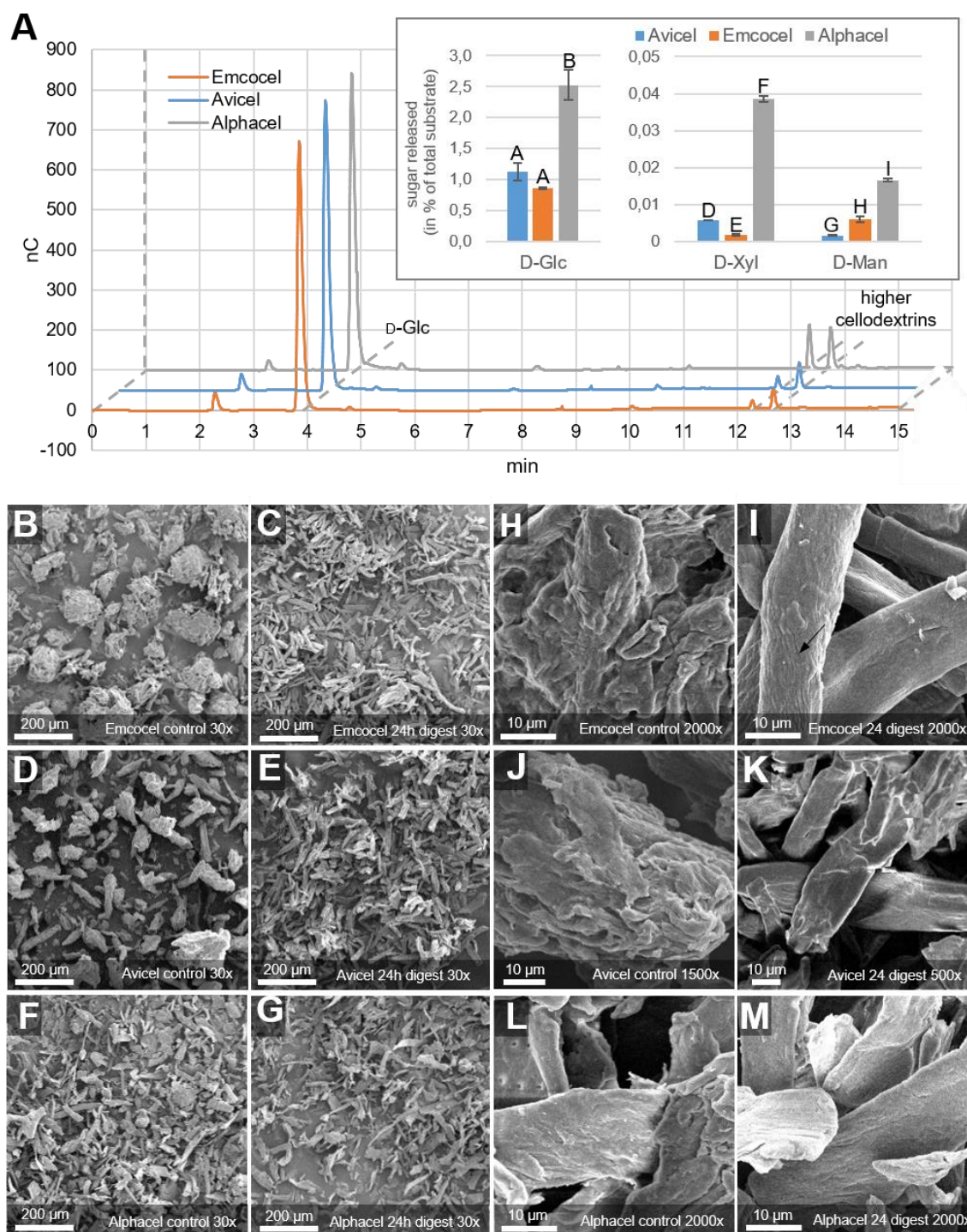


**Figure 3-3. Enzymatic digestion of the cellulose substrates *in vitro*.**

All celluloses were digested by a *N. crassa*-derived cellulase cocktail (filtered culture supernatant after 5 days growth on Avicel) for a total of 24 hours. **(A)** Shown are representative HPAEC-PAD chromatograms of the reaction supernatants after 8 hours as well as the quantification results for monosaccharides at an initial time point (1 hour; inset in A). The peaks of D-glucose (D-Glc) and higher cellodextrins (not quantified) are indicated. Note: in this run (CarboPac® PA200 column), the other monosaccharides will also migrate at the same speed as D-Glc, but the amounts are substantially lower. The quantifications represent means of triplicate reactions. Error bars represent standard deviations (n=3). Different lower and upper case letters indicate significant difference within data groups that are significantly different (one-way ANOVA followed by a post-hoc Tukey's test, p-values < 0.05 were considered significant). **(B-M)** Representative scanning electron micrographs out

of technical triplicates for each cellulose substrate obtained at 8.0 kV accelerating voltage and 30x – 2000x magnification (Jeol JSM-IT100).

### **3.5.5. Determination of the potential to induce lignocellulolytic gene expression**

With a molecular approach, we tested the ability of the cellulose substrates to induce the major cellulolytic and hemicellulolytic pathways on the level of gene expression. Moreover, this analysis was supposed to provide indirect insight into the early bioavailability of inducer molecules, and therefore to what extent fungi will be able to actually perceive the measured differences in the substrate composition. Since the molecular response pathways to cellulose and hemicellulose are more separated in *N. crassa* than in *T. reesei* (see background and reviewed in (Glass *et al.* 2013), we only used *N. crassa* for these assays. Based on a survey of published transcriptomics analyses (Sternberg and Mandels 1979; Tian *et al.* 2009; Coradetti *et al.* 2012; Ogawa *et al.* 2012; Sun *et al.* 2012; Benz *et al.* 2014), we chose three genes that served as proxies for the induction of the cellulolytic, xylanolytic and mannanolytic pathways in *N. crassa*, since they had been shown to be robustly induced by their respective substrates and serve a specific function in those pathways: the cellobionic acid transporter gene *cbt-1/clp-1* (NCU05853), the D-xylulose kinase encoding gene NCU11353, and the putative acetylmannan esterase encoding gene *ce16-1* (NCU09416).

The initial cellulolytic response (as measured by *cbt-1/clp-1*) to Avicel, Emcocel and Alphacel was similar (Figure 3-4 A). Emcocel, however, showed a tendency to respond weaker. Even though it was found to have the lowest cellulose content of all tested substrates, the response to Alphacel tended to be strongest, indicating a better bioavailability of the cellulose microfibrils.

The xylanolytic response (as measured by the *D-xylulose kinase* gene expression) was clearly strongest in the case of Alphacel, which also had the highest content of xylan, and was found to be less intense in the MCC substrates (Figure 3-4 B). Interestingly however, *N. crassa*'s response to the xylan impurities in Avicel and Emcocel was not necessarily proportional to the overall content. Emcocel induced the xylanolytic pathway more strongly, even though the xylan content was lower than in Avicel, again indicating that the bioavailability is not directly proportional to the overall content.

In case of the mannanolytic pathway, the responses to the three substrates were very distinct (Figure 3-4 C). Avicel induced the acetylmannan esterase gene *ce16-1* >7-fold stronger than Emcocel, which roughly reflects the difference in mannan content and might be expectable, since Avicel is derived from softwoods and Emcocel from hardwoods, in which xylans are the dominating hemicellulose. The fact that the strongest response was

again detected on Alphacel, although the overall mannan content was found to be lower than in Avicel might have two reasons: 1) the bioavailability of the plant cell wall sugars in the non-microcrystalline substrate is generally higher, and 2) there is some evidence that the cellulolytic and mannanolytic pathways cross-react in *N. crassa* (as well as in *Aspergillus oryzae*) (Ogawa *et al.* 2013; Craig *et al.* 2015). The strong cellulolytic response to Alphacel might therefore also co-induce the mannanolytic pathway more strongly.

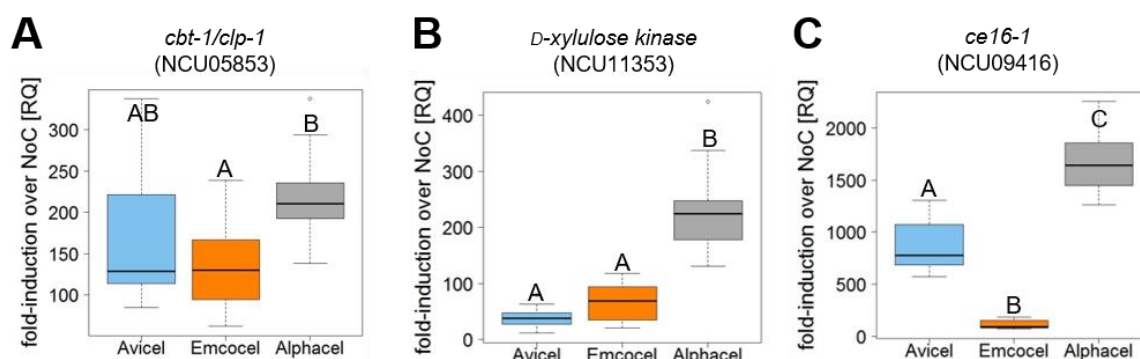


**Figure 3-4. Gene expression induction of selected genes used as proxies for the fungal cellulolytic and hemicellulolytic response.**

Sucrose pre-grown *N. crassa* cultures were exposed to the celluloses or no carbon source for 4 hours before RNA was harvested. Gene induction was measured by RT-qPCR. Shown is the mean fold-induction over the no carbon (No C) starvation condition derived from biological and technical triplicates. Error bars represent standard deviations ( $n=3$ ). Letters indicate significant difference within data groups that are significantly different (one-way ANOVA followed by a post-hoc Tukey's test,  $p$ -values  $< 0.05$  were considered significant).

### 3.5.6. Cellulase production in *N. crassa* and *T. reesei* RUT-C30

The effectiveness of the three celluloses as substrates for cellulase production in filamentous fungi was tested in 100 ml shake flask cultures. We used both the industrially optimized hypercellulolytic *T. reesei* strain RUT-C30, as well as the genetic model system *N. crassa*. The performance was evaluated after 3 and 6 days of growth by three main analyses of the culture supernatants: total secreted protein concentration, endo-glucanase activity and endo-xylanase activity (Figure 3-5). Total and not specific activities (normalized to fungal biomass) are presented, since we aimed to study overall yields on each carbon source. These are therefore representative for the combined effects of bioavailability differences on induction, degradation, metabolism, secretion and growth.

Overall, the data showed that both the softwood-MCC (Avicel) as well as the powdered cellulose (Alphacel) outperformed the hardwood-MCC (Emcocel HD-90) in *N. crassa*, where total secreted protein as well as endo-glucanase and endo-xylanase activities were consistently lowest for Emcocel. While secreted protein, endo-glucanase and endo-xylanase activities were comparable on Avicel and Emcocel (Figure 3-5), Alphacel was

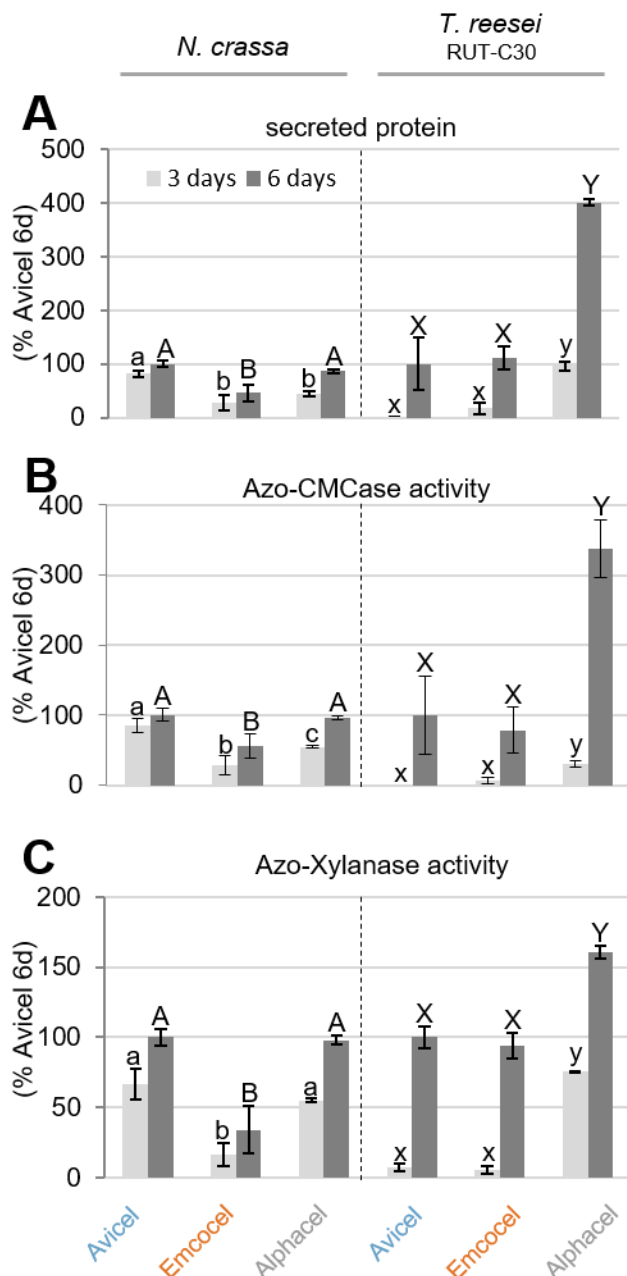


**Figure 3-5. Cellulase and hemicellulase production by *N. crassa* and *T. reesei* RUT-C30 on the cellulose substrates.**

non-engineered organisms such as *N. crassa* and are able to take full advantage of the much less crystalline PCs such as Alphacel. We hypothesized that differences in the genetic configuration in these fungi may play a decisive role to this end. Since one of the major modifications from WT to industrial strain is the reduction or removal of CCR, we tested the effect of this by comparing protein production on the three celluloses of the de-repressed *T. reesei* RUT-C30 strain to its WT strain QM6a as well as by comparing the *N. crassa* WT to a deletion strain of *cre-1*, encoding the major TF mediating CCR (Figure 3-6). To limit the effect of differences in germination speed between the genotypes as much as possible

found to induce cellulases and hemicellulases more strongly in *T. reesei* (Figure 3-5 B and C). Moreover, protein secretion by *T. reesei* RUT-C30 had a longer lag phase (Figure 3-5 A; compare day 3 vs. day 6 data).

Since it seemed likely that the poor performance of Emcocel was at least partly due to the much smaller surface area of the substrate (see above), we also tested the performance of the ball-milled Emcocel (Emcocel\*; *N. crassa* only) with an about doubled surface area compared to the original (Figure 3-1). Surprisingly however, protein production was almost indistinguishable from the unmilled Emcocel, indicating that the specific surface area was not limiting for the performance in the fermentations.

#### WT vs. industrially optimized strains

Combining the physicochemical properties of the celluloses with the fungal performance data, it appears like hypersecreting systems such as the industrially utilized *T. reesei* RUT-C30 strain are less sensitive to small increases at high crystallinities than

(Seiboth *et al.* 2011; Ogawa *et al.* 2013), we modified our experimental setup for these assays and shifted identical amounts of fungal biomass to cellulose cultures after pre-growth on sucrose/glucose (see Material & Methods). Since the starting material was mycelia in this experiment, we shortened the incubation time to two and three days for *N. crassa* and *T. reesei*, respectively.

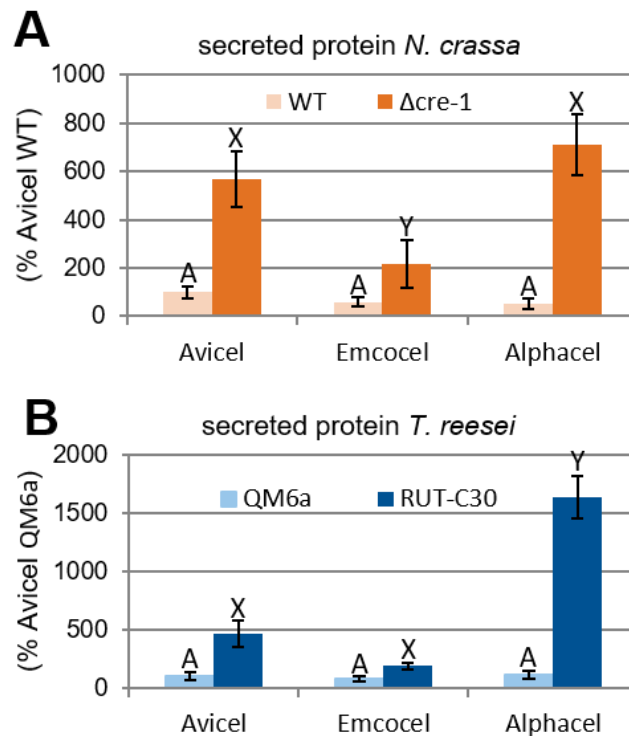
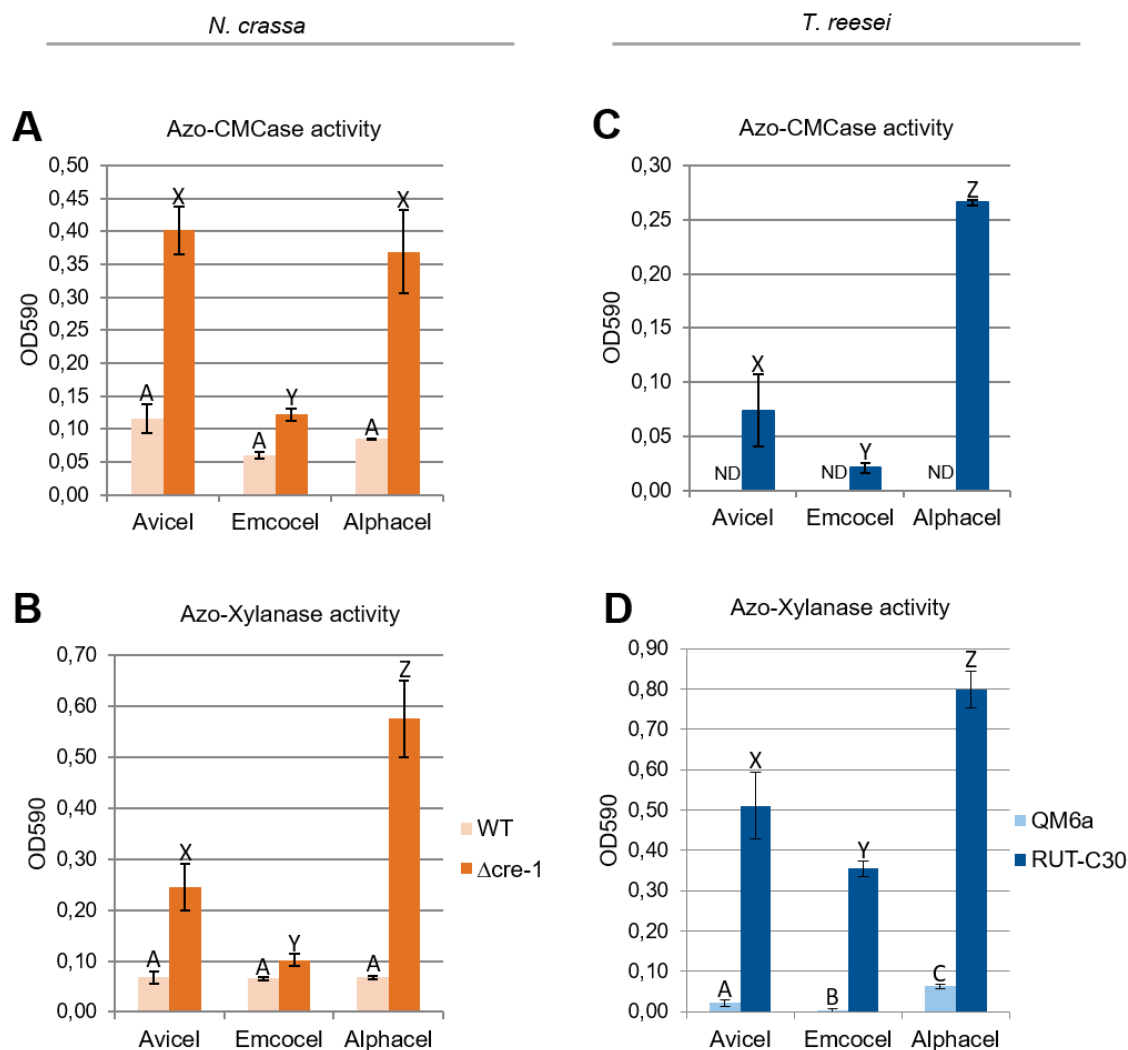


**Figure 3-6. Total protein secreted by *N. crassa* (WT and  $\Delta cre-1$ ) and *T. reesei* (QM6a and RUT-C30) on the cellulose substrates.**

Performance was measured by analysis of culture supernatant aliquots taken after 2 and 3 days, respectively. Protein concentration was measured by Bradford assay as described in Methods. Values are the mean of biological triplicates. Error bars represent standard deviations ( $n=3$ ). Different lower and upper case letters indicate significant difference within data groups that are significantly different (separately for both fungi and sample days; one-way ANOVA followed by a post-hoc Tukey's test,  $p$ -values  $< 0.05$  were considered significant).

Two observations could be made: First, the carbon catabolite de-repressed strains (*T. reesei* RUT-C30 with a truncated *cre1* gene (Mello-de-Sousa *et al.* 2014) and *N. crassa* with a *cre-1* deletion) displayed strongly elevated protein levels in comparison to the respective WT strains (Figure 3-6) which is in line to what was previously shown in both fungi (Tangnu *et al.* 1981; Portnoy *et al.* 2011; Sun and Glass 2011), indicating that CCR has a repressing effect even on highly recalcitrant substrates with low glucose fluxes such as Emcocel (even though the effect there was smallest). And second, also the *T. reesei* WT strain (QM6a) was not able to take full advantage of the low-crystallinity substrates such as Alphacel (Figure 3-6 B, light blue), just as we had found for *N. crassa* (*cf.* Figure 3-5). However, while protein production of *T. reesei* RUT-C30 was roughly inversely proportional

to the substrate crystallinities again (Figure 3-6 B, dark blue), the deletion of *cre-1* in *N. crassa* was not sufficient to phenocopy this, and protein production on the PC Alphacel was only marginally stronger than on the MCC Avicel (Figure 3-6 A, darkorange), mainly due to stronger xylanase expression (Figure 3-7 B) while cellulase expression was similar on the two aforementioned substrates. These observations indicate that other genetic determinants are present in addition to the absence of a fully functional CRE-1 that allows *T. reesei* RUT-C30 to utilize the PC Alphacel better than the other substrates.



### 3.6. Discussion

In our study, we compared three commercial cellulose powders that might be used as substrates for fungal fermentations regarding their effectiveness as inducers for the production of cellulases and hemicellulases. We chose representative substrates that differed either in their source material (i.e. softwood vs. hardwood) or their production process (i.e. hydrolytically degraded MCC vs. mechanically processed powdered cellulose). Analytical comparisons have shown that powdered celluloses have an overall higher hemicellulose content, lower crystallinity and a broader molecular weight distribution than MCCs (Baehr and Puls 1991). The nature of the source material, on the other hand, can influence properties such as the hemicellulose composition (Timell 1967; Harada H 1985; Willför *et al.* 2005; Adel *et al.* 2011). Depending on the application, one or more of these properties become more relevant than others (e.g. Baehr and Puls 1991 and Adel *et al.* 2011). Consequently, all of these properties might have a strong influence on the performance of the cellulose products in cellulase fermentations. While these points are not well understood and were to be tested here, batch-wise variations were not considered since all chosen substrates were used from a single batch.

The hemicellulosic content of the cellulose products was found to be relevant in the context of the cellulase fermentations. The fungi are able to perceive their presence early on, as demonstrated by their effect on gene expression in *N. crassa* after only four hours of induction. In agreement and extension of what was proposed by Baehr *et al.* (Baehr and Puls 1991), even the relatively “pure” MCCs can thus be considered to represent heterogeneous systems in which the non-cellulosic parts affect both structure (and thus enzymatic kinetics/accessibility) as well as the fungal response.

The powdered cellulose (Alphacel) was found to be the most readily digested substrate. In agreement with earlier studies, the analytical results confirmed that the crystallinity of the powdered cellulose was substantially lower than that of the MCCs, and that it was furthermore much less pure, with a hemicellulose content of ~15% (Baehr and Puls 1991). Also among the MCCs, the softwood-derived product (Avicel) outperformed the hardwood-derived one (Emcocel) when *N. crassa* was used and was found to have a lower crystallinity as well as a higher hemicellulose content. These two factors therefore stand out and appear to be dominant for the effectiveness in our study. Crystallinity and hemicellulose-content might also be linked, since the non-removed hemicelluloses are likely tightly associated with the cellulose by intercalation between the cellulose strands (O'sullivan 1997), thereby lowering the overall crystallinity.

Intriguingly, enzyme production was inversely proportional to the differences in substrate crystallinity for *T. reesei* RUT-C30, but not for *N. crassa*, where production on Avicel and

Alphacel were similar, despite this difference. We hypothesized that in absence of a fully functional CRE-1/Cre1 (Le Crom *et al.* 2009), the higher flux of signaling molecules derived from the more readily digested Alphacel would be directly turned into stronger expression. Indeed, the *T. reesei* WT strain QM6a (with functional CCR) was not able to utilize Alphacel equally well as inducing substrate. However, only xylanase production was found to benefit substantially by deletion of the CCR-mediating TF *cre-1* in *N. crassa*, indicating that particularly the XLR-1-dependent hemicellulase production is carbon catabolite repressed in the WT. In the de-repressed mutants, the effect of higher inducing sugar concentrations is then dependent on the regulatory networks present in the fungi (Glass *et al.* 2013). In *T. reesei*, the dominant XYR1 system regulates both cellulase and hemicellulase induction, which might explain why both cellulase and xylanase production are benefiting from the availability of abundant inducing molecules on Alphacel. In *N. crassa* on the other hand, these pathways are much less linked and their regulation is decoupled in a way that CLR-1 and CLR-2 are responsible for the major cellulolytic response while the ortholog of XYR1, XLR-1, is responsible for the xylanolytic response and only modulates the expression of some genes in the cellulose degradation pathway (cf. (Mach-Aigner *et al.* 2008; Coradetti *et al.* 2012; Sun *et al.* 2012) and reviewed in: (Glass *et al.* 2013)). The cross-induction of cellulases by xylan is therefore comparably weak. It is thus feasible that in *N. crassa* the high amount of available xylan in Alphacel will only hyperinduce the XLR-1-dependent hemicellulases, but the inducing effect of the low-crystallinity cellulose is compensated by the lower overall cellulose abundance in Alphacel.

It was also interesting to note that the slightly higher crystallinity of Emcocel compared to Avicel does not seem to allow continuous maximal production capacity despite the similarly strong gene induction measured at four hours. This seems to indicate that even small differences in measured crystallinity in celluloses manifest themselves in substantial performance differences over time due to a positive feedback loop between substrate bioavailability, metabolism and fungal growth – a fact that has to be considered when choosing a substrate for enzyme fermentations.

Besides the cellular systems, the activity of the enzymes on the substrate for the release of inducer molecules and products will be a bottleneck step. Factors that have been described to affect enzyme activity include: reversible & irreversible adsorption (to cellulose or lignin, respectively), end product inhibition, synergism and others (e.g. Mooney *et al.* 1999; Levine *et al.* 2010; Fox *et al.* 2011). Many studies have looked at the interaction of cellulose structure and enzymatic hydrolysis, and particularly structural characteristics such as crystallinity and surface area have been shown to be determining factors (e.g. Fan *et al.* 1980; Fan 1981; Mansfield *et al.* 1999; Mooney *et al.* 1999; Hall *et al.* 2010; Rollin *et al.* 2011; Peng *et al.* 2013; Li *et al.* 2014; Peciulyte *et al.* 2014). It has been pointed out,

however, that the effects of crystallinity and surface area are difficult to be evaluated individually, since they are often highly interrelated (at least when celluloses are mechanically (pre-) treated) (Mansfield *et al.* 1999). In our experiments, surface area did not appear to be limiting, since the performance of Emcocel could not be improved by further ball-milling. This observation is in line with other studies that did not detect any impact of particle size on the rate and extent of sugar release or enzyme binding (Fan *et al.* 1980; Peters *et al.* 1991; Mansfield *et al.* 1999). However, depending on the fermentation condition and molecular crowding, this might change (Levine *et al.* 2010).

Overall, crystallinity seemed to be a major determinant of the effectivity of the celluloses in our study. Digestibility was found to be lower for more crystalline substrates in almost all assays (particularly visible for enzyme production in *T. reesei*). Many previous studies have found that crystallinity critically impacts the enzymatic cellulose hydrolysis (e.g. Fan 1981; Hall *et al.* 2010; Rollin *et al.* 2011; Peng *et al.* 2013; Li *et al.* 2014). We are aware of only one study that was not able to support this finding (Puri 1984). Nevertheless, Park *et al.* cautioned to correlate small differences in CrI, as found between Avicel and Emcocel, with changes in cellulose digestibility, since many other factors might play a role as well, such as for example the distribution of crystalline, para-crystalline and “amorphous” regions in the particles and in relation to the surface area (Park *et al.* 2010). Still, the resistance of Emcocel towards acid hydrolysis, which was considerably stronger than found for Avicel, confirmed that this product is substantially more recalcitrant and suggests that small differences in CrI might have a strong effect at high crystallinities. The CrI of MCCs might therefore not necessarily correlate linearly with digestibility as previously shown (Fan *et al.* 1980) and other variables need to be considered. More studies are needed to determine this in more detail.

### 3.7. Conclusions

We found that both the inherent cellulose crystallinity and the hemicellulose content are major factors determining the suitability of celluloses as substrates for the expression of cellulases in filamentous fungi as production hosts. Crystallinity restricts the enzymatic digestibility and thus also the release of inducer molecules. Moreover, even in MCCs, that are considered relatively “pure”, the residual hemicellulose content is efficiently perceived by the fungi and – depending on the molecular signaling pathways – translated into a corresponding cellulolytic and hemicellulolytic response, which is not necessarily analogous to the overall composition, indicating differences in bioavailability which cannot be resolved analytically.

The cellulolytic response profiles of *N. crassa* and *T. reesei* were similar, but showed also important differences. For example, only *T. reesei* RUT-C30 was able to take full advantage

of the most amorphous cellulose substrate. This effect was not solely due to carbon catabolite de-repression, but is dependent on the species-specific regulatory network. The application of *N. crassa* as an indicator of the activated response pathways therefore seems promising, due to a rapid response time, and since the cellulolytic and hemicellulolytic pathways show a much more limited cross-talk than in *T. reesei* and can thus be individually evaluated.

In conclusion, the presented results provide a set of criteria that can theoretically be applied to broader ranges of substrates and thereby aid in the rational decision for cellulose substrates to be used in enzyme fermentations. Understanding the factors for the performance of cellulose substrates will help to optimize the manufacturing process of lignocellulolytic enzymes from fungi for a number of biotechnological applications, such as for food, feed, textile and biorefinery.

### 3.8. Methods

#### 3.8.1. Substrates

Each used substrate is from a single batch preparation. The major physical characteristics of these substrates as indicated by the manufacturers are summarized in Table 3-2.

**Table 3-2. Major physical characteristics of the used substrates (manufacturer's information).**

	<b>Avicel™ PH-101</b>	<b>EMCOCEL® HD90</b>	<b>Alphacel</b>
<b>Brand</b>	Fluka	JRS Pharma GmbH & Co. KG	ICN Biomedicals, Inc.
<b>Type</b>	Softwood MCC	Hardwood MCC	Hardwood PC
<b>Average particle size (µm)</b>	~ 50	124 *	35 **
<b>Bulk density (g/cm<sup>3</sup>)</b>	0.26 – 0.31	0.41	0.44 – 0.50

\*) by Malvern d50; \*\*) avg. fiber length

#### 3.8.2. Strains and growth conditions

*N. crassa* wild type (FGSC #2489) and the  $\Delta cre-1$  strain (kind gift of N. L. Glass, UC Berkeley, USA) were grown on 2% sucrose Vogel's minimal medium slants in the dark at 30°C for 2 days, and transferred to constant light conditions at 25°C for conidiation. *T. reesei* QM6a and RUT-C30 strains (kind gift of M. Schmoll, AIT, Austria) were propagated on malt extract agar plates in the dark at 28 °C and then switched to 25°C in constant light for conidiation. The first set of growth experiments (Figure 3-5) was performed in flasks containing 100 ml 1% (w/v) cellulose with 1x Vogel's (at 25°C and in constant light) or 1x Mandels-Andreotti medium (at 30°C and in constant light) and at 200 rpm for *N. crassa* and *T. reesei*, respectively (Vogel 1956; Mandels and Andreotti 1978). The second set of growth

experiments (Figure 3-6 and Figure 3-7) was carried out through a two-step cultivation procedure. *N. crassa* and *T. reesei* strains were first grown in 50 ml 2% (w/v) sucrose with 1x Vogel's for 20 hours (at 25°C and in constant light) or 50 ml 2% (w/v) glucose with 1x Mandels-Andreotti medium for 3 days (at 30°C and in constant light), respectively. The cultures were collected through vacuum filtration and 0.5 g of *N. crassa* mycelia or 0.42 g of *T. reesei* mycelia were added to 100 ml 1% (w/v) cellulose with 1x Vogel's or 1x Mandels-Andreotti medium and the cultures were incubated at 25°C and 200 rpm for two days (*N. crassa*) or at 30°C and 200 rpm for three days (*T. reesei*), respectively.

For inoculation, generally a respective volume of conidial suspension was added after optical density measurements in order to achieve a starting concentration of  $10^6$  conidia/ml. All assays were done with biological triplicates for each strain per each condition.

### 3.8.3. Compositional analyses

Initially, the dried cellulose samples (~5 mg) were swollen in 50  $\mu$ l of 72% H<sub>2</sub>SO<sub>4</sub> for 1 h (Avicel, Alphacel, bacterial cellulose) or 4 h (ball-milled Emcocel) at RT. After addition of 1.45 ml water, the material was autoclaved for 1 h at 121 °C. Potential residual solids were subsequently removed by centrifugation, and the supernatant analyzed after appropriate dilution using an ICS-3000 liquid chromatography system (Dionex, Thermo Scientific) equipped with a pulsed amperometric detector. The columns used were a CarboPac® PA20 3x150 mm (Dionex, Thermo Scientific) and a CarboPac® PA200 3x250 mm (Dionex, Thermo Scientific), with column temperature of 30 °C and a flow rate of 0.4 ml/min. Mobile phase for detection of monosaccharides (PA20) was 5 mM NaOH isocratic for 15 min. For detection of cellodextrins (PA200), mobile phases were 0.1 M NaOH (A) and 0.1 M NaOH/1 M NaAc (B). Gradient used was: 2 min 0% B, 10 min 0-10% B and 3 min 0% B. The analyses were done with technical triplicates for each substrate.

### 3.8.4. Solid state nuclear magnetic resonance spectroscopy

Solid-state <sup>13</sup>C NMR spectra were obtained on a Bruker Avance™ III 200 spectrometer (Bruker BioSpin GmbH, Karlsruhe, Germany). Cross-polarization magic angle spinning (CPMAS) was applied with a <sup>13</sup>C-resonance frequency of 50.32 MHz and a spinning speed of 5 kHz. Contact time was 1 ms and recycle delay was 2 s. Approximately 5000 scans were accumulated and no line broadening was applied. For calibration of the <sup>13</sup>C chemical shifts, tetramethylsilane was used and set to 0 ppm. Spectral analysis were performed using the spectrometer software. The crystallinity index (CrI) was then calculated by the NMR C4 peak separation method, that assigns peaks at about 87 and 82 ppm in the NMR spectra to the C4 carbons in ordered cellulose structures ("crystalline"; C4c) and non-crystalline

domains (“amorphous”; C4a), respectively (Horii *et al.* 1984; Newman and Hemmingson 1990; Park *et al.* 2010).

We would like to note that the Crl might have been underestimated for Alphacel, since we used a simple drying process instead of solvent-exchange drying, which might have given numbers more representative of the swollen state in the liquid broth. However, the measured differences have found to be less of an issue at high Crls (Fan 1981). The Crls of the MCCs were thus probably less affected, and that of Avicel was well in line with previously reported values (Sun *et al.* 2012).

### **3.8.5. Surface area measurements**

The specific surface area of the substrates was determined by multi-point BET (Brunauer *et al.* 1938) with an Autosorb-1 analyzer (Quantachrome, Syosset, USA) using nitrogen gas as adsorbate at 77 K. The samples were outgassed before analysis in vacuum under helium flow at 60°C for 12 h.

### **3.8.6. Scanning electron microscopy**

All substrates were dried over immobilized on metal stubs using a double sided sticky tape and then sputter coated with gold. The scanning electron micrographs were taken with a JSM-IT100 (JEOL, Freising, Germany) at 8 kV accelerating voltage. The substrates were visualized in triplicates.

### **3.8.7. Enzymatic assays**

Azo-CMCase and Azo-xylanase activity assays were carried out according to the protocols of the manufacturer (Megazyme, Ireland) (S-ACMC and S-AXBL), slightly modified, since the reaction mixture was reduced to a quarter of the original volume. Assays were done with biological triplicates for each substrate per each strain.

### **3.8.8. RNA-extraction and RT-qPCR**

Quantification of gene expression was done by quantitative real-time PCR (RT-qPCR) performed on RNA samples that were harvested after a four-hour induction phase on the respective celluloses as described in Benz *et al.* (Peng *et al.* 2013). The RNA extraction was performed according to the TRIzol Reagent protocol (Fisher Scientific, Schwerte, Germany). RNA was then treated with DNase I (RNase-Free) according to manufacturer’s recommendations (New England Biolabs, Frankfurt am Main, Germany) and subsequently cleaned up with the GeneJET RNA Purification Kit (Fisher Scientific, Schwerte, Germany). A 96-well plate reader (Infinite 200 PRO, Tecan) was used to check RNA purity and

concentration. cDNA was obtained following instructions of the High-Capacity cDNA Reverse Transcription Kit (Applied Biosystems; Fisher Scientific, Schwerte, Germany). Finally, RT-qPCR was performed with the sensiFAST SYBR No-ROX Kit (Bioline, Luckenwalde, Germany) on a Mastercycler ep realplex<sup>2</sup> (Eppendorf, Wesseling-Berzdorf, Germany) and analyzed using the realplex 2.2 software. Actin gene (NCU04173) was used as a reference gene. Primers used are shown in Table 3-3. Expression analyses were done with biological and technical triplicates for each condition.

**Table 3-3. Sequences of primers used for RT-qPCR.**

gene	forward primer	reverse primer
<i>actin</i> (NCU04173)	CATCGACAATGGTTCGGGTATGT G	CCCATACCGATCATGATACC ATGATG
<i>cbt-1/clp-1</i> (NCU05853)	CGCCCTGACCTACACCTAC	GGCCAAACGACCAAAGAGC
<i>D-xylulose kinase</i> (NCU11353)	GGCACATCATCGCTTCACTG	CAAGGGAGATGCGCGAGG
<i>ce16-1</i> (NCU09416)	GGTGCTGCTCCCATCTACTAC	GTACTIONGGCGATGGCGAC

### 3.8.9. Statistical analyses

Statistical analyses were done by applying analysis of variance (ANOVA) followed by a Tukey test using the statistical computing software R (Team 2013).

---

## 4. Cross-talk of cellulose and mannan perception pathways leads to inhibition of cellulase production in several filamentous fungi

Lara Hassan, Liangcai Lin, Hagit Sorek, Laura Sperl, Thomas Goudoulas, Franz Hagn, Natalie Germann, Chaoguang Tian, and J. Philipp Benz

### 4.1. Authors' contributions

L.H., C.T., and J.P.B. designed the research. L.H., L.L., H.S., L.E.S., T.G., and J.P.B. performed research. L.H., L.L., H.S., L.E.S., F.H., T.G., N.G., C.T., and J.P.B. analyzed data. L.H. wrote the initial draft of the manuscript, J.P.B. made extensive edits. All authors reviewed and approved the final version of the manuscript.

### 4.2. Summary

The degradation of lignocellulolytic substrates by fungal enzymes is critical for the generation of fermentable sugars to be used in the production of biofuels and other high-value products. However, in Hassan et al. (2017) presented above, differences in substrates' crystallinity and hemicellulose impurities were found to be perceived by fungi and to affect their production of (hemi-)cellulases. Hence, in this study, genetics, biochemical and rheological approaches were used to address the fungal perception of hemicellulose impurities present in cellulosic substrates. In particular, the study focused on investigating the cross-talk between cellulose and mannan (hemicellulose) degradation pathways in *N. crassa*. The results indicated that this cross-talk is competitive both at the level of uptake by cellodextrin transporters and at the level of intracellular signaling, thereby causing inhibition of cellulase production. Moreover, an intracellular balance between the inducing and inhibiting molecules, cellodextrins and mannodextrins, respectively, was shown to be important for the wildtype cellulolytic response. Importantly, the inhibition was shown to be conserved in the industrially used strains *M. thermophila* and *T. reesei* RUT-C30.

### 4.3. Abstract

It is essential for microbes to acquire information about their environment. Fungi use soluble degradation products of plant cell wall components to understand the substrate composition they grow on. Individual perception pathways have been well described. However, the interconnections between pathways remain poorly understood. In the present work, we provide evidence of cross-talk between the perception pathways for cellulose and the hemicellulose mannan, being conserved in several filamentous fungi and leading to the inhibition of cellulase expression. We used the functional genomics tools available for *Neurospora crassa* to investigate this overlap at the molecular level. Cross-talk and competitive inhibition could be identified both during uptake by cellodextrin transporters and intracellularly. Importantly, the overlap is independent of CRE-1-mediated catabolite repression. These results provide novel insights into the regulatory networks of lignocellulolytic fungi and will contribute to the rational optimization of fungal enzyme production for efficient plant biomass depolymerization and utilization.

### 4.4. Introduction

Fungi are of ecological, economical, pharmaceutical and biotechnological importance. This group of microorganisms has a major commercial impact in product areas including food and feed, pulp and paper, textiles, detergents, bio-fuel and chemical production (Meyer *et al.* 2016). The importance of filamentous fungi in biotechnological applications lies in their potential to efficiently degrade plant cell wall material and release sugar monomers (Galbe and Zacchi 2002). They utilize their cellular resources for the production of a wide range of enzymes including cellulases and hemicellulases. The great heterogeneity and resulting chemical complexity of lignocellulosic feedstocks provides a range of fermentable carbohydrates for high value biological, chemical, and pharmaceutical products (Vaz Jr 2017). Yet, the production of the fungal cellulolytic and hemicellulolytic enzymes for hydrolysis of complex biomass remain a high cost factor (Bhattacharya *et al.* 2015). Research efforts to optimize enzyme production and remove unwanted constraints therefore are still warranted. Previous research has greatly focused on how filamentous fungi regulate the degradation of single polysaccharides as isolated cell wall components. However, relatively little is known about the cross-talk between separate signaling pathways for cellulose and hemicellulose perception during the utilization of complex carbon sources. In this study, we demonstrate that cross-talk not only occurs but can result in inhibition with detrimental effects for the production of hydrolytic enzymes.

Cellulose and hemicellulose are the major constituents of lignocellulosic biomass. While cellulose is a linear chain of glucose molecules connected by  $\beta$ -(1,4)-glycosidic

linkages (Marchessault 1983), hemicelluloses are a heterogeneous group of branched and linear polysaccharides (Sánchez 2009) consisting mainly of xylans and mannans in variable ratios depending on the source of the biomass. While xylans, such as glucuronoxylan, arabinoxylan, and arabinoglucuronoxylan (Ebringerova and Heinze 2000), are the most abundant hemicellulose in hardwoods, glucomannan represents the major hemicellulose in softwood (15%-20%) (Timell 1967). It consists of a  $\beta$ -(1,4) linked D-mannopyranose and D-glucopyranose backbone in a Man:Glc ratio of about 1.6:1 (Teramoto and Fuchigami 2000). Cellulose and glucomannan are hydrolyzed by glucanases and mannanases into cello- and (gluco-)mannodextrins, respectively, which are further processed into the simple constituent monosaccharides by intra- and extracellular  $\beta$ -glucosidases and  $\beta$ -mannosidases (Moreira 2008; Znameroski *et al.* 2012). The production of such enzymes is controlled by complex signaling networks including several transcriptional regulators. In *N. crassa*, CLR-1 and CLR-2 (cellulose degradation regulator 1 and 2) are essential transcription factors (TFs) responsible for the vast majority of the cellulolytic response (Coradetti *et al.* 2012). In the presence of cellulose or its degradation products (such as cellobiose) as an inducer (Znameroski *et al.* 2012), a signaling pathway results in the activation of CLR-1 which in turn induces the expression of  $\beta$ -glucosidases and the cellobiose transporter-encoding genes *cdt-1* and *cdt-2*. Both CDT-1 and CDT-2 are Major Facilitator Superfamily (MFS)-type transporters described to be capable of transporting cellobiose/cellobioses into the cell (Kim *et al.* 2014). Additionally, CLR-1 induces the expression of the transcription factor CLR-2, which in turn triggers the major cellulolytic response (Craig *et al.* 2015).

Homologs of these regulators are present in most filamentous Ascomycetes, albeit differing in their functional role (Huberman *et al.* 2016; Seibert *et al.* 2016; Benocci *et al.* 2017). For example, ManR, the CLR-2 ortholog in *Aspergillus oryzae*, is involved in the regulation of both cellulolytic and mannanolytic genes (Ogawa *et al.* 2012), a function that is partly conserved in *N. crassa* (Craig *et al.* 2015; Samal *et al.* 2017), while the function of the CLR-2 homolog in *Trichoderma reesei* (TR\_26163) for the production of cellulase and hemicellulase is less clear so far (Hakkinen *et al.* 2014). In *T. reesei* and *Aspergillus* spp., the regulator XYR1/XInR controls both the hemicellulolytic and the cellulolytic response (van Peij *et al.* 1998; Stricker *et al.* 2006; Kowalczyk *et al.* 2014; dos Santos Castro *et al.* 2016) which is divergent from the mechanism utilized by *N. crassa*. The XYR1-homolog in *N. crassa*, XLR-1, is more specific for the regulation of hemicellulose degradation, yet it only modulates cellulase induction (Sun *et al.* 2012). In the presence of a preferred carbon source, another highly conserved regulatory system, carbon catabolite repression (CCR), is activated to repress unnecessary metabolic routes and prevent the wasting of energy. A key component of CCR in filamentous fungi is the TF CreA/CRE1/CRE-1, which represses the expression of genes encoding enzymes involved in lignocellulose degradation (Bailey

and Arst 1975; Ronne 1995; Portnoy *et al.* 2011; Sun and Glass 2011; Ries *et al.* 2016). The presence of partially conserved regulatory mechanisms for lignocellulose degradation (Coradetti *et al.* 2013; Benocci *et al.* 2017) and the partially different functions assigned to homologous regulators in the various fungal species add another level of complexity to the regulation of lignocellulolytic genes. However, the elucidation of the underlying mechanisms in those fungi, despite (or precisely because of) existing differences and similarities, is likely the key to a better understanding of how fungi utilize transcriptional rewiring to enable efficient plant biomass degradation adapted to their specific ecological niche.

Most of our knowledge regarding the molecular details of the underlying regulatory pathways is based on the analysis of the fungal response to single polysaccharides. While this was important to delineate many of the known signaling components, the heterogeneous nature of lignocellulosic substrates demands an understanding of the molecular interplay between the separate regulatory pathways. Our observations of *N. crassa* growth on complex biomass suggested a relation between the cellulase activity and the mannan content of the biomass. We therefore used genetics, biochemical and rheological approaches to find that mannan and cellulose perception pathways involve common components and are interconnected. Surprisingly, this cross-talk does not lead to synergies but rather leads to competition on the molecular level with negative effects on cellulase production in several tested fungi. This study thereby provides insights that advance our fundamental understanding of the complex network behind the cross-talk between regulatory systems governing plant cell wall perception and can potentially be applied to produce industrially favorable fungal strains with a lower propensity to be inhibited in presence of complex biomass.

## 4.5. Results

### 4.5.1. Softwood substrates are inhibitory for cellulase production in *N. crassa*, and GH2-1 is its only $\beta$ -mannosidase

Comparing the cellulase activity of *N. crassa* WT growing on different carbon sources, we initially observed a consistently lower enzymatic activity on softwood-derived wood powders as carbon source than on hardwood-derived materials and grasses (Figure 4-1 A). A compositional analysis verified the main difference between hardwoods and softwoods being the content of hemicelluloses. Hardwoods usually have higher xylan content while the main hemicellulose in softwoods are mannans (SFigure 6-2 A) (Timell 1967; Pettersen 1984; Harada H 1985). We hypothesized that the higher amount of mannan present in softwoods might be involved in the inhibition of cellulase activity of *N. crassa*. To verify this hypothesis, we aimed to provoke a stronger effect of mannan by artificially altering its

intracellular metabolism. The genome of *N. crassa* encodes only one gene (NCU00890) encoding a predicted  $\beta$ -mannosidase for the processing of (gluco-)mannodextrins into monomers (Chhabra *et al.* 2001), a member of the glycosyl hydrolase family two (GH2-1) with no predicted N-terminal secretion signal peptide (Petersen *et al.* 2011).

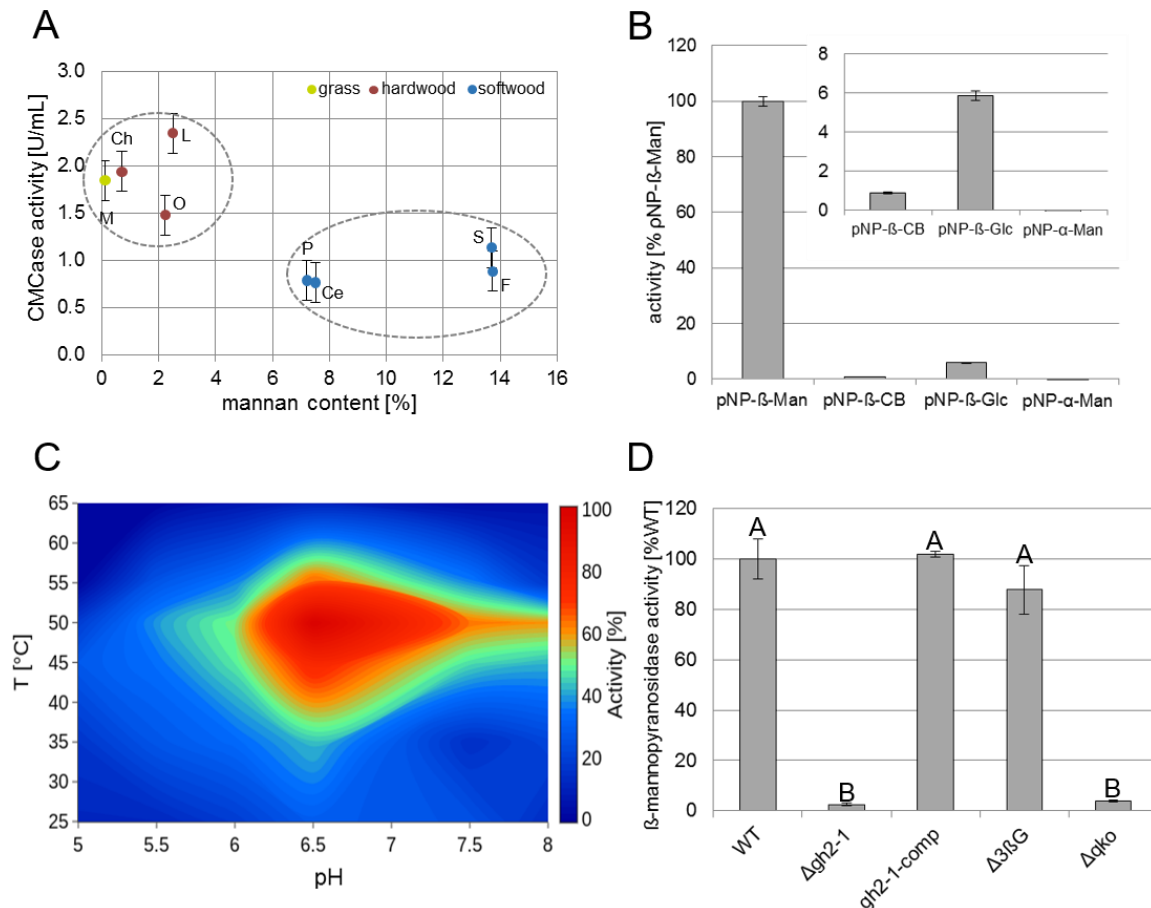


**Figure 4-1. Characterization of GH2-1.**

(A) CMCCase activity of enzymes secreted into WT culture supernatants after 3 days of growth in 1% (w/v) powdered biomass (M: *Miscanthus*, Ch: chestnut, O: oak, L: locust, P: pine, Ce: cedar, S: spruce and F: fir). (B) Substrate specificity assay of GH2-1 using  $\rho$ NP- $\beta$ -D-mannopyranoside ( $\rho$ NP- $\beta$ -Man),  $\rho$ NP- $\beta$ -D-cellopyranoside ( $\rho$ NP- $\beta$ -CB),  $\rho$ NP- $\beta$ -D-glucopyranoside ( $\rho$ NP- $\beta$ -Glc) and  $\rho$ NP- $\alpha$ -D-mannopyranoside ( $\rho$ NP- $\alpha$ -Man) as substrates. (C) Contour plot for GH2-1 activity, at different combinations of temperatures and pHs in parallel, using  $\rho$ NP- $\beta$ -Man as a substrate. (D)  $\beta$ -mannopyranosidase activity of the cytosolic protein extracts of the WT,  $\Delta gh2-1$ ,  $\Delta 3\beta G$  and  $\Delta qko$  (the  $\Delta 3\beta G$  strain crossed to  $\Delta gh2-1$ ) after growth in 1% (w/v) Avicel with 1x Vogel's salts for 3 days. Error bars represent standard deviations (n=3). Different lower and upper case letters indicate significant difference within data groups that are significantly different (one-way ANOVA followed by a post-hoc Tukey's test, p-values < 0.05 were considered significant).

To verify its predicted function, GH2-1 was heterologously expressed in *Pichia pastoris*. The purified enzyme showed strong activity on  $\rho$ NP- $\beta$ -D-mannopyranoside with high specificity compared to its activity on  $\rho$ NP- $\beta$ -D-cellopyranoside,  $\rho$ NP- $\beta$ -D-glucopyranoside, and  $\rho$ NP- $\alpha$ -D-mannopyranoside as substrates (Figure 4-1 B). Also a GFP-fusion construct displayed cytosolic localization *in vivo* in *N. crassa* (SFigure 6-3 A). When assayed at a combination

of different temperatures and pHs in parallel, GH2-1 showed the highest activity in a temperature range between 43 and 54 °C and a pH range between 6.25 and 7.5 (Figure 4-1 C) and a thermostability up to about 49 °C (SFigure 6-3 B). Moreover, to assess the possibility of mannodextrin cleavage by cross-reactivity of  $\beta$ -glucosidases, we tested the hydrolysis of  $p$ NP- $\beta$ -mannopyranoside by cytosolic protein extracts from WT,  $\Delta gh2-1$ ,  $\Delta 3\beta G$  (a strain carrying deletions for all three  $\beta$ -glucosidase genes (Samal *et al.* 2017)) and  $\Delta qko$  ( $\Delta gh1-1 \Delta gh3-4 \Delta gh3-3 \Delta gh2-1$ ) grown on 1% Avicel. Only strains possessing GH2-1 displayed  $\beta$ -mannopyranosidase activity (Figure 4-1 D). Also, when complementing the  $\Delta gh2-1$  strain with the *gh2-1* gene under control of its native promoter and terminator, strain *gh2-1-comp*, it showed WT-like  $\beta$ -mannosidase activity (Figure 4-1 D), indicating a functional complementation of the *gh2-1* deletion. In summary, these assays confirmed that GH2-1 is the main cytosolic hydrolase encoded in the *N. crassa* genome capable of cleaving mannodextrins.

#### **4.5.2. The presence of mannodextrins inhibits growth of *N. crassa* on cellulose**

To this end, we checked the cellulosic activity of both the WT and the GH2-1 deletion strain ( $\Delta gh2-1$ ) grown on the same complex carbon sources as used above. The  $\Delta gh2-1$  strain showed a sharp decrease in total cellulase activity which correlated well with an increased mannan content of the biomass, suggesting a connection between both parameters with a half maximal inhibitory concentration (IC<sub>50</sub>) of about 1.1% of mannan (Figure 4-2 A, SFigure 6-2 A, and SFigure 6-4 A-B). To further verify this result, we grew WT and  $\Delta gh2-1$  on mannan-free bacterial cellulose (SFigure 6-1 F) (Hassan *et al.* 2017) and added low concentrations (0.03% (w/v) corresponding to 3% (w/w) of the used bacterial cellulose) of commercially available mannans or mannobiose to roughly mimic the mannan content present in softwood (SFigure 6-2 A). The added mannan and even mannobiose was sufficient to inhibit cellulase production in the WT and provoked an even more severe phenotype in the  $\Delta gh2-1$  strain (Figure 4-2 B). To directly test which sugar molecules may cause the inhibition, both the WT and  $\Delta gh2-1$  mutant strain were grown on Avicel, a mannan-contaminated microcrystalline cellulose (SFigure 6-2 B) (Baehr and Puls 1991; Xiong *et al.* 2014; Hassan *et al.* 2017). Afterwards, the HSQC spectra for the anomeric region of the extracted intracellular sugars of both strains were observed by NMR (nuclear magnetic resonance). In comparison to WT, the  $\Delta gh2-1$  strain was found to accumulate mannose as part of a  $\beta$ -1,4-polymer, glucose as part of a  $\beta$ -1,4-polymer, and reducing-end  $\beta$ -mannopyranosyl in the cytosol (Figure 4-2 C). These results provide strong evidence for  $\beta$ -1,4-linked (gluco-)mannodextrins being the causative molecules for the observed inhibition.

Assaying the cellulase production by the WT,  $\Delta gh2-1$ , and  $gh2-1$ -comp strains grown in 1% Avicel showed that cellulase inhibition was relieved in the  $gh2-1$ -comp strain (Figure 4-2 D) indicating a functional complementation of the  $gh2-1$  deletion mutation.

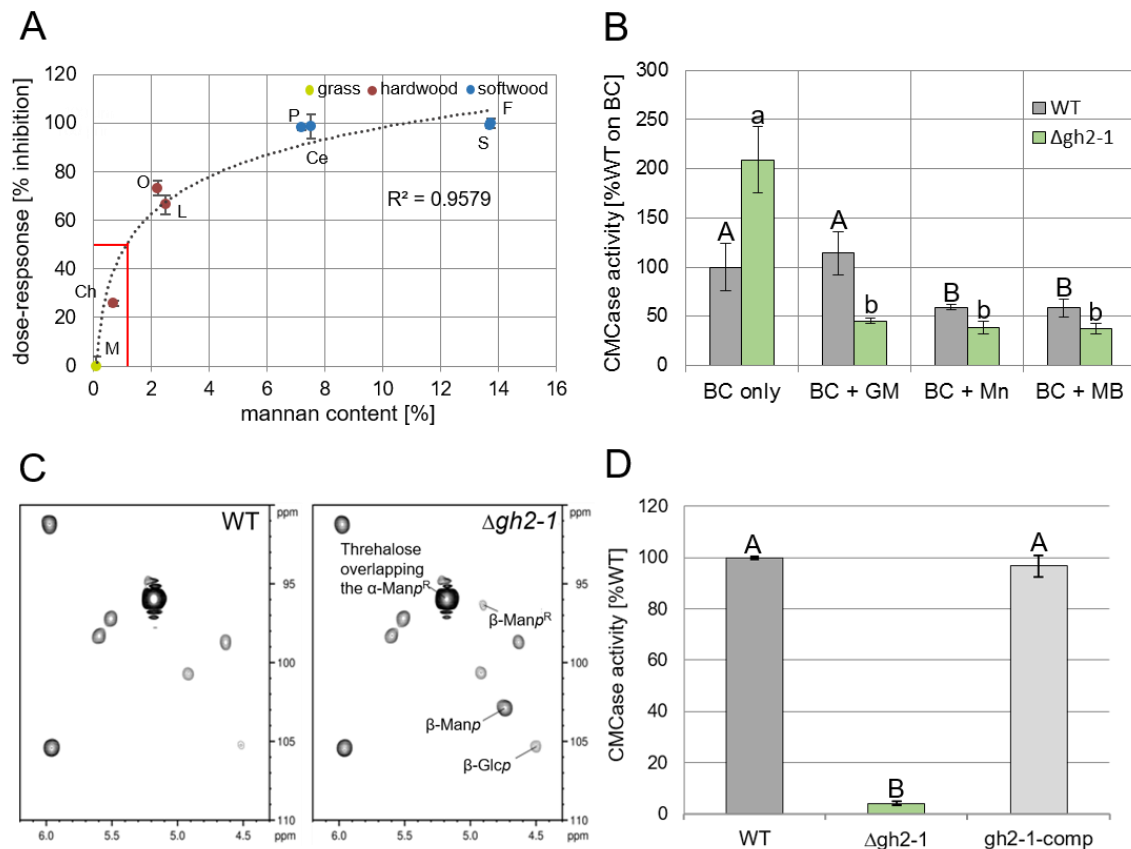


**Figure 4-2. High mannan content is inhibitory for cellulase activity.**

**(A)** CMCCase activity of enzymes secreted into the  $\Delta gh2-1$  culture supernatants after 3 days of growth in 1% (w/v) powdered biomass (M: *Miscanthus*, Ch: chestnut, O: oak, L: locust, P: pine, Ce: cedar, S: spruce and F: fir). The inhibition is indicated in percent relative to the inhibition on *Miscanthus* (uninhibited; 0%) and fir (highest inhibition; 100%) and the mannan content is calculated from the compositional analysis of the used biomass sources (see SFigure 6-2 A). **(B)** CMCCase activity of the WT and  $\Delta gh2-1$  cultures after growth in 1% (w/v) bacterial cellulose (BC) with the addition of 0.03% (w/v) glucomannan (GM) and mannan (Mn) or mannobiose (MB). **(C)** 2D- $[^1H^{13}C]$ -HSQC spectra for the anomeric region of the extracted intracellular sugars of the mycelia of both WT and the  $\Delta gh2-1$  strains after growth in 2% (w/v) Avicel for 24 h post transfer.  $\beta$ -Glc<sub>p</sub>: glucose as part of  $\beta$ -1,4-polymer,  $\beta$ -Man<sub>p</sub>: mannose as part of  $\beta$ -1,4-polymer, and  $\alpha/\beta$ -Man<sub>p</sub>R: reducing-end  $\alpha/\beta$ -mannopyranosyl. **(D)** CMCCase activity of the WT,  $\Delta gh2-1$ , and  $gh2-1$ -comp cultures after growth in 1% (w/v) Avicel with 1x Vogel's salts for 3 days. Error bars represent standard deviations (n=3). Different lower and upper case letters indicate significant difference within data groups that are significantly different (one-way ANOVA followed by a post-hoc Tukey's test, p-values < 0.05 were considered significant).

#### 4.5.3. A delicate intracellular balance between cello- and mannodextrins

Considering the substantial inhibition caused by intracellular accumulation of mannodextrins, the question arose whether this could be the result of a possible conflict with cellulose perception. We therefore wanted to assess the influence of the intracellular

cellodextrin levels on cellulase inhibition in the  $\Delta gh2-1$  strain. To this end, a cross with  $\Delta gh1-1$ , a deletion strain of the main intracellular  $\beta$ -glucosidase gene (Znameroski *et al.* 2012) was created. Deleting *gh1-1* in the  $\Delta gh2-1$  background completely rescued the  $\Delta gh2-1$  phenotype on mannan-contaminated cellulose (Avicel) (Figure 4-3 A). In addition, we directly checked the intracellular sugars of the double knockout strain after growth on Avicel by NMR. In comparison to WT and the single deletion strains, the HSQC spectra for the  $\Delta gh2-1 \Delta gh1-1$  extract displayed an accumulation of both mannodextrin and cellodextrin signals (SFigure 6-5).

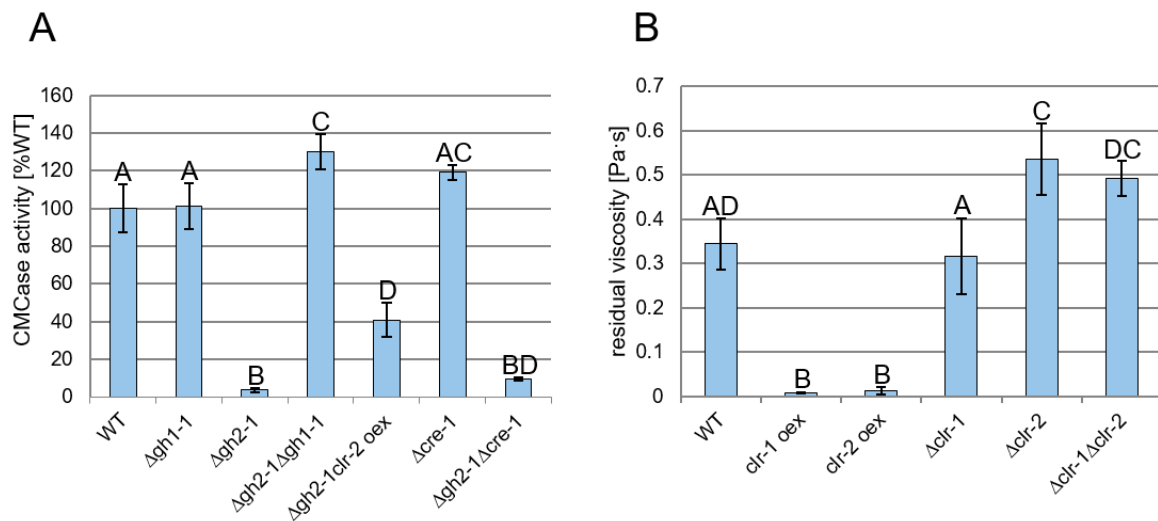


**Figure 4-3. Cello- and mannodextrins compete intracellularly, and the inhibition is independent of CCR by CRE-1.**

**(A)** CMCase activity of culture supernatants of the indicated strains after growth for 3 days in 1% (w/v) Avicel. **(B)** Viscosity of the culture supernatant of the indicated strains 8 h post-transfer to 1% (w/v) glucomannan. Error bars represent standard deviations (n=3). Different lower and upper case letters indicate significant difference within data groups that are significantly different (one-way ANOVA followed by a post-hoc Tukey's test, p-values < 0.05 were considered significant).

This indicated that the effect of accumulating mannodextrins could be counterbalanced by raising the intracellular concentration of cellodextrins. Since the presence of cellodextrins leads to the induction of CLR-2 via the activation of CLR-1 (Coradetti *et al.* 2013), we next tested the possibility to suppress the inhibited phenotype of  $\Delta gh2-1$  by constitutive expression of *clr-2*, rendering its protein levels independent of the levels of its inducing molecules (strain  $\Delta gh2-1 \Delta clr-2$  oex; (Coradetti *et al.* 2013)). Indeed, inducer-independent overexpression of *clr-2* was able to (partially) rescue the  $\Delta gh2-1$  phenotype on Avicel (Figure 4-3 A).

The accumulation of polysaccharide degradation products in  $\Delta gh2-1$  could theoretically also have led to activation of CCR. We thus tested the possibility that the observed inhibition might be due to repression by CRE-1 and studied the effect of a *cre-1* deletion on the phenotype. However, a de-repression due to the loss of CRE-1 in the  $\Delta gh2-1$  background

did not lead to a substantial relief of inhibition when grown on 1% Avicel (Figure 4-3 A), arguing against an involvement of CCR.

Taking into account that CLR-2 is an ortholog of ManR, the regulator of mannan degradation in *A. oryzae* (Coradetti *et al.* 2012; Ogawa *et al.* 2012), and that ChIP-seq data showed CLR-2 to be a direct regulator of *gh5-7* (Craig *et al.* 2015), the main predicted  $\beta$ -mannanase-encoding gene in *N. crassa*, we hypothesized that the regulatory pathway of mannan perception shares a common ancestor with the cellulolytic one. This led us to grow *clr-1* and *clr-2* deletion ( $\Delta clr-1$ ,  $\Delta clr-2$  and  $\Delta clr-1 \Delta clr-2$ ) and mis-expression (*clr-1 oex* and *clr-2 oex*) strains on glucomannan as sole carbon source. By measuring the culture viscosities over time, we aimed to detect the decrease in molecular weight of the hemicellulose polymer (Wang *et al.* 2012) due to mannanolytic degradation. Besides *clr-2 oex* also the *clr-1 oex* strain displayed a significantly stronger decrease in glucomannan viscosity than the WT strain (Figure 4-3 B), indicating an enhanced enzyme production on this substrate, which in the case of *clr-1 oex* however might have been an indirect effect via CLR-2. On the other hand,  $\Delta clr-2$  and  $\Delta clr-1 \Delta clr-2$  strains showed a significantly lower reduction in glucomannan viscosity (Figure 4-3 B), suggesting that CLR-2 is indeed involved in the regulation of mannan degradation in *N. crassa*.

#### 4.5.4. Cello- and mannodextrins also compete at the level of uptake

Since our data strongly indicate that mannodextrins are cleaved into their constituent monosaccharides only intracellularly by GH2-1, we investigated the transport of mannodextrins into the cell. The two MFS-type transporters CDT-1 and CDT-2 are known to facilitate the uptake of both cellodextrins and xylodextrins (Galazka *et al.* 2010; Cai *et al.* 2014). Due to structural similarity of (gluco-)mannodextrins, we hypothesized that CDT-1 and -2 might be involved in the uptake of mannodextrins as well. To this end, we tested the growth of the individual and double knockout strains ( $\Delta cdt-1$ ,  $\Delta cdt-2$  and  $\Delta cdt-1 \Delta cdt-2$ ) in 1% glucomannan. The individual deletion strains for *cdt-1* and *cdt-2* had 66.5% and 85.5% biomass compared to the WT strain, respectively. More significantly, the  $\Delta cdt-1 \Delta cdt-2$  strain had a biomass reduction of about 51% compared to WT (Figure 4-4 A), indicating an involvement in metabolism of glucomannan. We next tested whether the loss of either CDT-1 or CDT-2 would lead to an impaired uptake of mannobiose by *N. crassa*. For this, sucrose pre-grown cultures of WT,  $\Delta cdt-1$  and  $\Delta cdt-2$  were first induced on 2 mM cellobiose, and then transferred to mannobiose. Following the residual concentration of mannobiose in the culture supernatant, the uptake was found to be almost completely abolished in the  $\Delta cdt-1$  strain (Figure 4-4 B), whereas its transport was slightly reduced (by about 18 %) in the  $\Delta cdt-2$  strain compared to the WT. We further used *Saccharomyces cerevisiae* that is unable of endogenously transporting cellobiose, to heterologously express CDT-1 or CDT-2 (Galazka

*et al.* 2010). The yeast cells were incubated in either cellobiose or mannobiose for 30 minutes. Indeed, not only cellobiose was imported by both *S. cerevisiae* strains, but also mannobiose (Figure 4-4 C). Notably, CDT-1 even preferred mannobiose over cellobiose, with only about 18% of mannobiose remaining in the culture supernatant compared to about 40% of cellobiose over the background of empty-vector transformed cells. Moreover, when both sugars were present simultaneously, cellobiose and mannobiose import by CDT-1 was reduced by about 33% and 61%, respectively, indicating that there is a competition between both sugars at the level of uptake by CDT-1 (Figure 4-4 C).

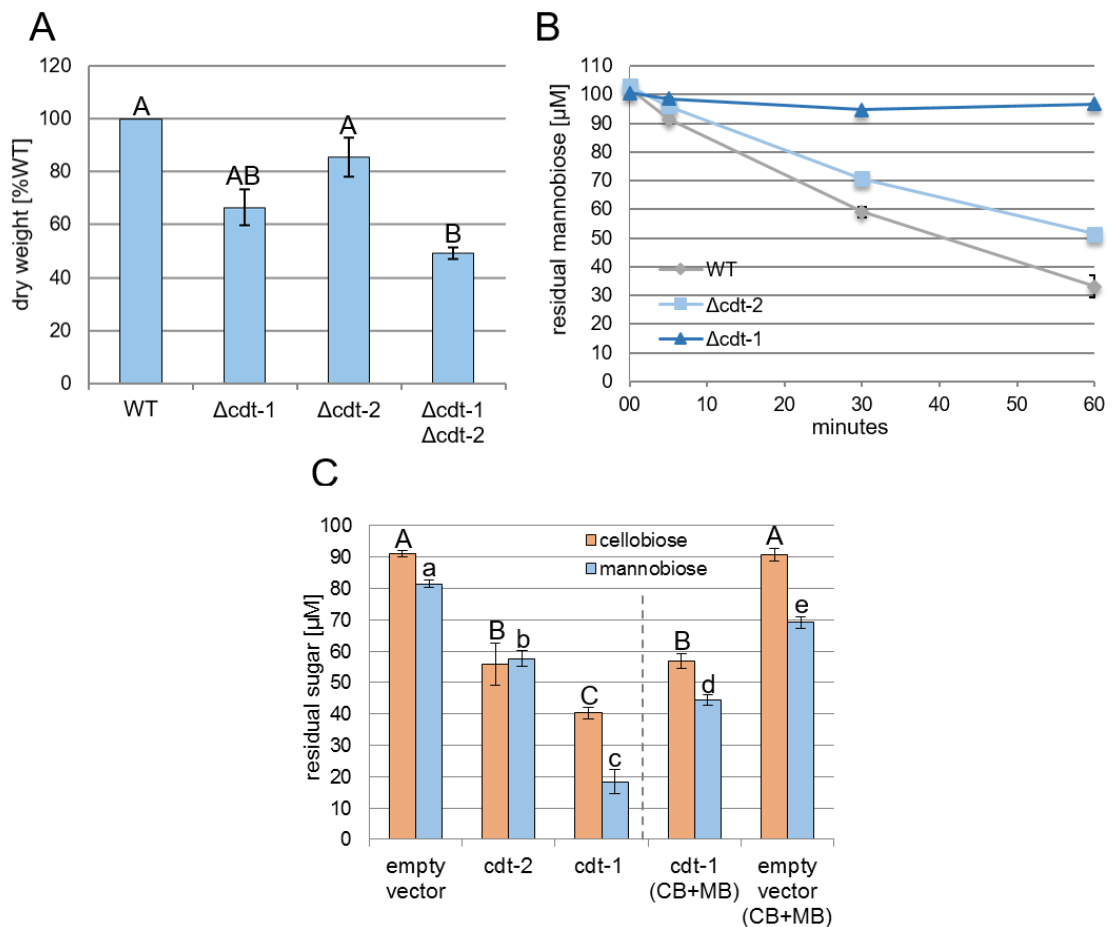


**Figure 4-4. Cello- and mannodextrins compete at the level of sugar uptake.**

**(A)** Mycelial dry weight of the indicated strains after growth for 3 days in 1% (w/v) glucomannan (indicated in % of WT). **(B)** Residual mannobiose in the supernatant of the indicated strains at indicated times post-transfer to the uptake solution (100  $\mu$ M mannobiose). **(C)** Residual sugars in the culture supernatants of *S. cerevisiae* heterologously expressing CDT-1 or -2 transporters, 30 minutes post-transfer to the 100  $\mu$ M uptake solutions (cellobiose (CB) or mannobiose (MB), or both disaccharides simultaneously). Error bars represent standard deviations (n=3). Different lower and upper case letters indicate significant difference within data groups that are significantly different (one-way ANOVA followed by a post-hoc Tukey's test, p-values < 0.05 were considered significant).

#### 4.5.5. The inhibitory effect of mannan is conserved in the industrially relevant species *Myceliophthora thermophila* and *Trichoderma reesei*

Lignocellulosic substrates are regularly composed of >1% of mannan. Given the potential impact of the mannan-elicited inhibition on industrial cellulase production, we wanted to test if the inhibition is also present in industrially relevant fungal species. For this, we grew the thermophilic fungus *M. thermophila* (Liu *et al.* 2017) on 1% hardwood-derived cellulose being naturally poor in mannan (Emcocel (Hassan *et al.* 2017)) with and without adding 0.05% glucomannan. Glucomannan addition clearly had an inhibitory effect on cellulase activity (Figure 4-5 A). Importantly, we checked if the effects are also present for the cellulase hyper-producing *T. reesei* strain RUT-C30 (having gone through rounds of classical mutagenesis and containing a truncated *cre1* gene) (Mello-de-Sousa *et al.* 2014). To this end, we grew both *N. crassa* WT and RUT-C30 on 1% Emcocel with and without the addition of 0.05% glucomannan. Similar to *N. crassa*, the low amount of glucomannan was therefore sufficient to significantly reduce total production of cellulases by RUT-C30 (Figure 4-5 B). This indicates that the overlap between cellulose and mannan perception pathways appears to be conserved, showing a similar inhibition of cellulase induction in both *M. thermophila* and *T. reesei* as well.

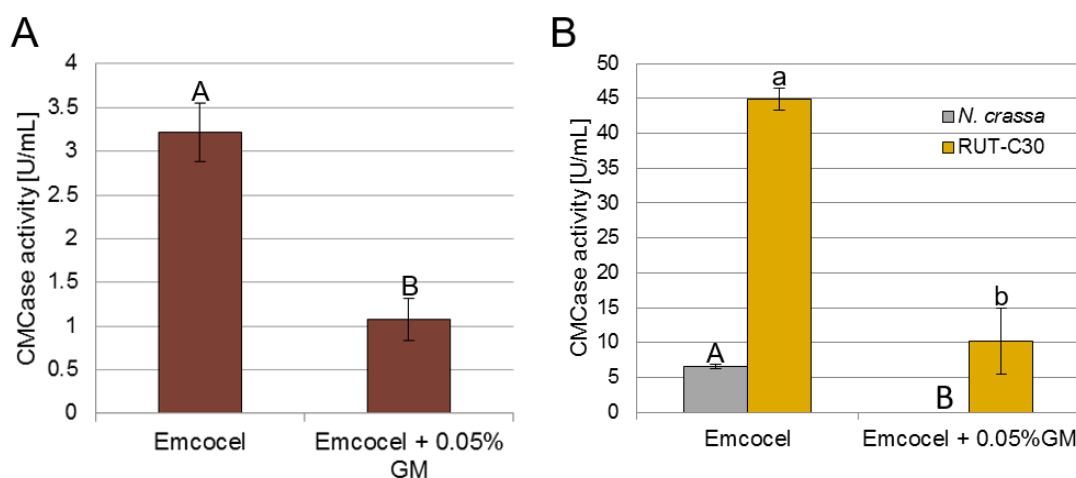


**Figure 4-5. Mannan addition is inhibitory to cellulase production in *T. reesei* and *M. thermophila* as well.**

CMCase activity of culture supernatants of **(A)** *M. thermophila* WT strain and **(B)** *N. crassa* WT and *T. reesei* RUT-C30 after 3 days growth in 1% (w/v) Emcocel with or without the addition of 0.05% (w/v) glucomannan (GM). Error bars represent standard deviations (n=3). Different lower and upper case letters indicate significant difference within data groups that are significantly different (one-way ANOVA followed by a post-hoc Tukey's test, p-values < 0.05 were considered significant).

## 4.6. Discussion

In the current model of plant cell wall degradation, starvation will lead to the production of low quantities of polysaccharide-degrading enzymes and sugar transporters to degrade

potential food sources present in the environment (Tian *et al.* 2009). When cellulose and glucomannan are present (Figure 4-6 A), secreted cellulases and mannanases degrade the polysaccharides into smaller cellodextrins (such as cellobiose) and mannodextrins (such as mannobiose), which are transported into the cytosol. While it is known that cellodextrin transporters CDT-1 and CDT-2 transport cellodextrins and might act as transceptors (Galazka *et al.* 2010; Znameroski *et al.* 2014), we found that both transporters are capable of transporting mannobiose as well (Figure 4-4). This provides evidence that both transporters are also involved in hemicellulose perception, in line with the previously reported xylo-dextrin transport activity for CDT-2 (Cai *et al.* 2014). Using *S. cerevisiae* as heterologous expression system, we were able to show that both molecules compete at the level of transport by CDT-1, which even prefers mannobiose over cellobiose (Figure 4-4 C). Cellobiose and mannobiose have a similar intramolecular  $\beta$ -(1,4)-glycosidic bond (Morris and Striegel 2014), and their constituent sugars (D-glucose and D-mannose, respectively) are C-2 epimers, possibly allowing them to interact with the same transporters. In line with this, the *N. crassa* transporters GAT-1 and XAT-1 were shown to be capable of transporting the uronic acids galacturonic/glucuronic acid (Benz *et al.* 2014) and the pentoses D-xylose/L-arabinose (Li *et al.* 2014), respectively. Also MstA in *Aspergillus* was shown to transport D-xylose, D-mannose and D-glucose (Diderich *et al.* 2004), and the fungal D-fructose permease RhtA also accepts L-rhamnose (both 6-deoxy-hexoses) (Sloothaak *et al.* 2016).

A multitude of previous and ongoing studies have been focusing on understanding the induction of fungal cellulase production by soluble sugars. Many oligosaccharides have been identified as inducers of cellulase production (Mandels *et al.* 1962; Sternberg and Mandels 1979; Gielkens *et al.* 1999; Seiboth *et al.* 2002; Znameroski *et al.* 2012). Yet little is known about an oligosaccharide to have a direct inhibitory effect on the production of such enzymes. *N. crassa* degrades mannodextrins further into glucose and mannose monomers by the action of the intracellular  $\beta$ -mannosidase GH2-1 (Figure 4-6A) (Moreira 2008; Znameroski *et al.* 2012). Our results indicate that the deletion of this  $\beta$ -mannosidase gene leads to the accumulation of substantial amounts of undigested (gluco-)mannodextrins in the cytosol of *N. crassa* (Figure 4-2 C). Our data furthermore provide evidence that these (gluco-)mannodextrins are causative for the strong repression of growth seen for example on mannan-contaminated Avicel (Figure 4-2 D). Considering the structural similarity between cello- and mannodextrins, their competition at the level of uptake via CDT-1 and the fact that mannodextrins can also inhibit cellobiohydrolase (Xin *et al.* 2015), it appears likely that they can also both interact with a (yet unknown) signaling component in the cell being slightly unspecific. The accumulation of (gluco-)mannodextrins is possibly skewing the original balance of signaling molecules in the cytosol and outcompeting the cellodextrins

(Figure 4-6 B). While these would be positively inducing, the interaction with (gluco-)mannodextrins however seems to be unproductive. Likely, this is causing antagonistic effects preventing the native response to cellobiose and interfering with the molecular events leading to the induction of cellulases. Generally, less cellulolytic activity results in less substrate degradation and thus lower availability of carbon source and inducing molecules (cellobiose). Eventually, this vicious circle leads to a strong overall signal loss and inhibition of cellulase production and growth (Figure 4-6B).

Our use of viscosity measurements as a sensitive tool to detect glucomannan degradation (Kojima *et al.* 2016) showed that CLR-2 indeed regulates glucomannan degradation, corroborating earlier findings (Craig *et al.* 2015; Samal *et al.* 2017). For instance, ChIP-Seq had identified the genes encoding the  $\beta$ -mannosidase *gh2-1*, the endo-mannanase *gh5-7* and the cellodextrin transporter *cdt-1* to be direct targets of CLR-2 (Craig *et al.* 2015). Homologs of this transcription factor are present in the genomes of many filamentous Ascomycetes including *T. reesei*, *M. thermophila*, and the Aspergilli (Coradetti *et al.* 2012; Benocci *et al.* 2017). In *A. oryzae*, ManR was described to regulate both cellulolytic and mannanolytic genes including the genes coding for the orthologs of the  $\beta$ -mannosidase *gh2-1*, the endo-mannanase *gh5-7* and the cellodextrin transporter *cdt-1* (Ogawa *et al.* 2013). A similar regulon was also determined for ClrB, the ortholog in *A. nidulans* (Coradetti *et al.* 2013). These results suggest that the dual function of CLR-2/ManR/ClrB as a combined mannanolytic and cellulolytic TF is conserved from the Aspergilli to *N. crassa*. The role of CLR-2 orthologs in *T. reesei* (Hakkinen *et al.* 2014) and *M. thermophila* is much less clear (Benocci *et al.* 2017). Nevertheless, the fact that mannodextrins can also induce cellulase inhibition in both strains (Figure 4-5) further supports the conserved role of CLR-2. The observation that an interaction between ClrA and ClrB in Aspergilli may not occur (Raulo *et al.* 2016) suggests a CLR-1-independent role of CLR-2 and its homologs. This is further supported by the ability of the *clr-1* deletion strain to utilize glucomannan in contrast to the *clr-2* deletion strain (Figure 4-3 B). Our results support the existence of an intracellular competition upstream of CLR-2, since a mis-expression of CLR-2 was able to at least partially rescue the inhibited phenotype (Figure 4-3 A).

Importantly, our results strongly suggest that there is a delicate intracellular balance between cellobiose and mannobiose which appears to be essential for full cellulase production. While the accumulation of mannodextrins inside the cell has a repressing effect, slowing down catabolism of the cellodextrins in the double deletion strain  $\Delta gh2-1 \Delta gh1-1$  counteracts the repression and restores a better cellulosic activity (Figure 4-6 C), presumably by raising the intracellular concentration of cellodextrins. This supports the necessity of a balance that affects the signaling pathway eventually leading to induction or repression of cellulases as presented in our model (Figure 4-6).

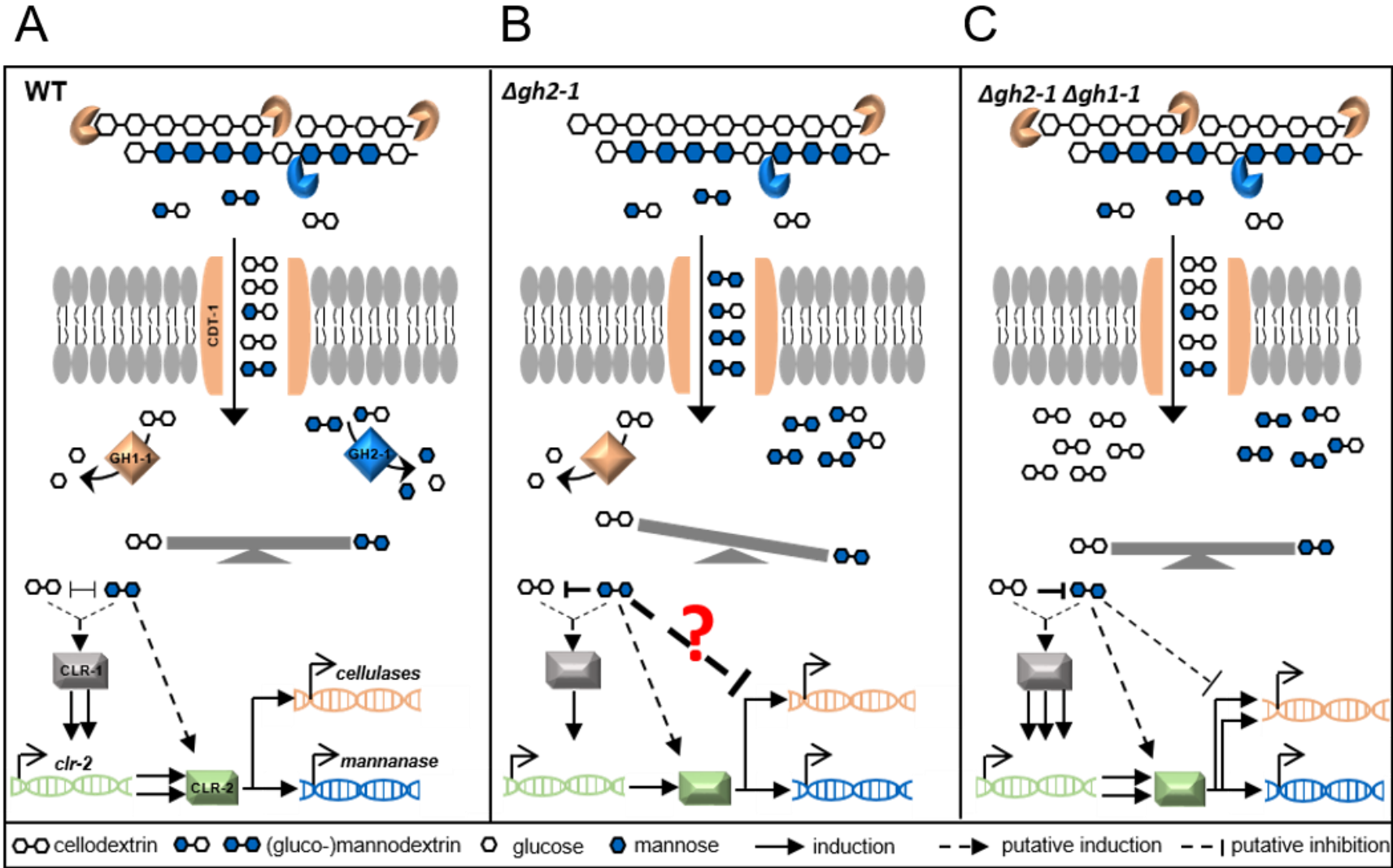


Figure 4-6. A model of the induction (A), inhibition (B) and relief of inhibition (C) of cellulase production in *N. crassa*.

**Figure 4 6. A model of the induction (A), inhibition (B) and relief of inhibition (C) of cellulase production in *N. crassa*.**

After the degradation of cellulose and glucomannan by cellulases (endo- and exo-acting glucanases, orange) and mannanase (blue), respectively, (gluco)mannodextrins outcompete cellodextrins extracellularly at the level of transport by the MFS-type transporter CDT-1. Intracellularly, cellodextrins and (gluco)mannodextrins are further cleaved into the corresponding glucose and mannose monomers by the action of the intracellular  $\beta$ -glucosidase (GH1-1) and  $\beta$ -mannosidase (GH2-1), respectively. In case of an intracellular balance between cello- and mannodextrins **(A)**, an unknown signaling cascade will lead to the activation of the upstream transcription factor CLR-1, which induces expression of the downstream transcription factor CLR-2, which then evokes the major cellulolytic and mannanolytic responses. In the  $\Delta gh2-1$  deletion strain **(B)**, undigested (gluco)mannodextrins accumulate in the cytosol, disrupting the intracellular balance of signaling molecules and outcompeting the positively inducing cellodextrins, in a way that the fungus is unable to determine the “adequate” amount of cellulase enzymes to be produced, eventually causing a reduced cellulase production. When *gh1-1* is deleted in the  $\Delta gh2-1$  background ( $\Delta gh2-1 \Delta gh1-1$  strain), **(C)**, the accumulating mannodextrins can be counterbalanced by the higher amount of undigested cellodextrins present in the cytosol, which re-inforce the induction of the cellulolytic response and relieve the inhibition.

The ability of molecules to induce or repress the production of cellulases and hemicellulases might be masked by CCR. In the  $\Delta gh2-1 \Delta cre-1$  strain, the major TF mediating CCR, *cre-1*, is deleted (Sun and Glass 2011). Nevertheless, the unaltered inhibition of cellulases in this strain and the fact that glucomannan was able to inhibit growth on cellulose also in the carbon catabolite de-repressed industrial strain *T. reesei* RUT-C30 (Portnoy *et al.* 2011; Mello-de-Sousa *et al.* 2014) confirms that mannodextrin inhibition is a novel process which is independent of CRE-1-induced CCR. Moreover, it is known that inducers/repressors are mostly oligomers or monomers that are derived from the polysaccharide itself, such as downstream metabolites and trans-glycosylation derivatives (Mandels *et al.* 1962; Eneyskaya *et al.* 2009). However, in the *N. crassa*  $\Delta gh2-1$  mutant, the  $\beta$ -mannosidase, which would be the likeliest enzyme to perform trans-glycosylation (Kubicek 2012), was deleted, suggesting that trans-glycosylation of the inhibitory mannodextrins is not a relevant step for the inhibition.

Although the degradation of cellulose and hemicellulose by filamentous fungi has been intensively studied on well defined, individual polysaccharides, only recently common components for cellulose and mannan perception pathways were described (Ogawa *et al.* 2012; Samal *et al.* 2017). The conservation of the common pathway components CLR-2, GH2-1 and CDT-1 described in this study suggests that the molecular communication between regulatory pathways of cellulose and mannan utilization is likely similarly conserved among filamentous fungi. Moreover, the presence of common signaling intermediates is probably a reflection of the environmental niche of plant-cell-wall degrading fungi, in which cellulose and mannan naturally co-exist (Whitney *et al.* 1998; Carpita *et al.* 2001), allowing to utilize both via common routes.

Finally, taking into account that the industrial production of cellulases is usually performed in presence of residual mannan (either as part of complex plant cell walls or in commercially available plant biomass-derived substrates such as Avicel), this study provides new targets for the improvement of industrial strains for higher cellulase production through the engineering of mannan-insensitivity in the future. This will benefit the development of better enzyme cocktails for the production of biofuels and biochemicals.

## 4.7. Materials and Methods

### 4.7.1. Strains and growth conditions

*N. crassa* strains were obtained from the Fungal Genetics Stock Center (FGSC; (McCluskey *et al.* 2010)) unless indicated otherwise. The  $\Delta cre-1$ ,  $3\beta G$  and *clr-2 oex* strains are a kind gift of N. L. Glass (UC Berkeley, USA). The other knock out strains  $\Delta qko$ ,  $\Delta gh2-1 \Delta gh1-1$ ,  $\Delta gh2-1 clr-2 oex$ ,  $\Delta gh2-1 \Delta cre-1$ ,  $\Delta clr-1 \Delta clr-2$  were created through crossings of the respective individual deletion strains as described in the FGSC protocols (McCluskey *et al.* 2010). The genotypes of the progeny were confirmed using a gene-specific primer and a common primer for the hygromycin phosphotransferase (*hph*) resistance cassette as described before (Znameroski *et al.* 2014).

All *N. crassa* strains and *T. reesei* RUT-C30 strain (kind gift of M. Schmoll, AIT, Austria) were maintained as described before (Hassan *et al.* 2017). *M. thermophila* WT strain (obtained from DSMZ, strain DSM1799) was maintained on 2% (w/v) sucrose Vogel's minimal medium (Vogel 1956) at 45 °C for 10 days to obtain conidia.

For *gh2-1* complementation strain (*gh2-1-comp*), the *gh2-1* gene amplified from gDNA was placed using *SacII* restriction site under the control of its native promoter and terminator in plasmid pCSR. The construct was transformed into the  $\Delta gh2-1$  (A) deletion strain by electrotransfection.

The *clr-1* mis-expression strain (*clr-1 oex*) was constructed as described in (Coradetti *et al.* 2013) but by using *SbfI* and *PacI* restriction sites to insert the *clr-1* gDNA in the pTSL126B plasmid placing the *clr-1* gene under the control of the *ccg-1* (clock-controlled gene 1) promoter. A  $\Delta clr-1$  (a) deletion background was used for transformation by electrotransfection.

*S. cerevisiae* strain used in this study was D452-2 transformed with pRS316-*CDT1*, -*CDT2* (67). Growth was performed as described by (Benz *et al.* 2014).

Growth experiments on complex biomasses and on bacterial cellulose were done in 3 ml of 1 × Vogel's salts plus 1% (w/v) of the corresponding carbon source in 24 deep well plates (at 25 °C, 200 rpm and in constant light). 0.03% (w/v) of commercially available mannans or mannobiose was added to cultures where indicated. Growth experiments for *N. crassa*

(at 25 °C and 200 rpm), *M. thermophila* (at 45 °C and 150 rpm), and *T. reesei* (at 30 °C and 200 rpm) were performed in flasks containing 100 ml 1% (w/v) carbon source as described with 1x Vogel's (*N. crassa* and *M. thermophila*) or 1x Mandels-Andreotti medium (Mandels and Andreotti 1978) in constant light. For inoculation, generally a respective volume of conidial suspension was added after optical density measurements in order to achieve a starting concentration of 10<sup>6</sup> conidia/ml.

#### 4.7.2. Biomass and enzymatic assays

Azo-CMCase activity assays from culture supernatants were done according to manufacturer's protocols (Megazyme, Ireland, S-ACMC), slightly modified according to (Hassan *et al.* 2017). For biomass determination after growth in glucomannan, the mycelial mass was first washed 3x with Vogel's NoC, then dried for 16 h in aluminum pans at 105 °C and measured afterwards.

For the  $\beta$ -mannopyranosidase activity, *N. crassa* strains were grown in flasks containing 100 ml 1% (w/v) Avicel with 1x Vogel's (at 25 °C, 200 rpm and in constant light). The mycelia were then harvested by using a Buchner funnel and glass fiber filters, washed 3 times by about 50 ml of 1x Vogel's solution, then frozen in liquid nitrogen. Frozen mycelia were ground into powder using freezing-milling method. About 250 mg of frozen mycelia were then lysed for protein extraction by adding 750  $\mu$ l lysis buffer (50 mM Na<sub>3</sub>PO<sub>4</sub>, 1 mM EDTA, 5 % glycerol and 1mM PMSF at pH 7.4). Samples were kept at -20 °C for 30 minutes, and then centrifuged (at 4 °C and 1300 rpm for 10 minutes). Protein concentration was measured with Roti<sup>®</sup>-Quant (Carl Roth, K015.1) as described by the manufacturer.

The  $\beta$ -mannopyranosidase activity was then assayed using 4-Nitrophenyl- $\beta$ -D-mannopyranoside (Megazyme, Ireland, O-PNPBM) as a substrate according to (Rangarajan *et al.* 2013) with the following modification: the reaction mixture (containing 50 mM KP buffer at pH 5.5, 80  $\mu$ g substrate and 1  $\mu$ g of intracellular protein solution) was incubated at 45 °C for 1 h, then stopped by the addition of 0.5 M Na<sub>2</sub>CO<sub>3</sub> (pH 11.5). The absorbance was then measured at an OD of 405 nm.

#### 4.7.3. Compositional analysis

Compositional analysis of biomass was performed as described previously (Bauer *et al.* 2012).

#### 4.7.4. Nuclear Magnetic Resonance (NMR) analyses

For NMR analysis, the indicated strains were grown in 2% (w/v) sucrose (Sigma Aldrich, S7903) for 16 h, then transferred to 2% (w/v) Avicel (PH-101; Sigma Aldrich, 11365) for 24

h. Then the mycelia were collected and their intracellular metabolites were extracted using a protocol modified from Tambellini *et al.* (Tambellini *et al.* 2013). Briefly, about 500 mg of homogenized mycelia were incubated for 30 minutes on ice with 24 ml cold CH<sub>3</sub>Cl:MeOH (1:1) and 6 ml dH<sub>2</sub>O. Samples were centrifuged at 4 °C, 4000 rpm for 15 minutes. Supernatants were collected and re-centrifuged at 4 °C, 12000 rpm for 30 minutes. Samples were dried down in a Speed Vacuum concentrator without heating.

For experiment in Figure 4-2 C, samples were dissolved in 440 µl D<sub>2</sub>O, 100 mM Na<sub>2</sub>HPO<sub>4</sub> of pH 7 and 10 µl DSS (internal standard) yielding clear solutions at approximately 60 mg/ml in 5 mm tubes. 2D NMR spectra were acquired at 25 °C on a Bruker AVANCE 600 MHz NMR spectrometer equipped with an inverse gradient 5-mm TXI cryoprobe. Spectra were referenced to DSS at δH 0.00 ppm, yielding HOD resonance at 4.78 ppm. <sup>13</sup>C-<sup>1</sup>H correlation spectra (HSQC) were measured with a Bruker standard pulse sequence “hsqcetgpsisp.2”. The data were recorded with the following parameters: spectral width of 16 ppm in F2 (<sup>1</sup>H) dimension with 2048 data points (TD1) and 240 ppm in F1 (<sup>13</sup>C) dimension with 256 data points (TD2); scan number (SN) of 128; interscan delay (D1) of 1 sec; acquisition time of 10 h. Assignments of the anomeric signals were assigned based on reference data from the literature. The NMR data processing and analysis were performed using Bruker’s Topspin 3.1 software. For the experiment in SFigure 6-5, samples and 30 mg/ml each of β-D-cellobiose (22150; Sigma, Germany), β-D-mannobiose (O-MBI; Megazyme, Ireland) and glucosyl-D-mannobiose (O-GMM; Megazyme, Ireland), used as references for the assignment of sugar resonances in the extract samples, were dissolved in 100 mM NaPi pH 7 in D<sub>2</sub>O. 2D-[<sup>1</sup>H<sup>13</sup>C]-HSQC spectra were recorded at 25 °C on Bruker AVANCE III HD spectrometers equipped with cryogenic TCI probes. The extract samples were measured at 950 MHz for 24 h with 160 increments in the indirect <sup>13</sup>C dimension and 2048 complex data points in the direct <sup>1</sup>H dimension. The spectral width was 16 ppm for <sup>1</sup>H with an offset of 4.7 ppm and 100 ppm for <sup>13</sup>C with an offset of 74 ppm, respectively. The references were recorded at 900 MHz for 4h (32 transients and 256 increments in the indirect dimension). The data was processed with the Bruker TopSpin 3.5 software and analyzed with NMRFAM-Sparky (Lee *et al.* 2014).

#### **4.7.5. GH2-1 heterologous expression**

For the heterologous expression of GH2-1, the *gh2-1* cDNA was inserted between EcoRI and XbaI restriction sites on the plasmid pGAPZ-B. The construct was transformed into *Pichia pastoris* X-33 strain by electrotransfection according to Invitrogen protocol ([https://assets.thermofisher.com/TFS-Assets/LSG/manuals/pgapz\\_man.pdf](https://assets.thermofisher.com/TFS-Assets/LSG/manuals/pgapz_man.pdf)). The growth of the transformed *Pichia* strain and the preparation of cell lysate were done according to the previously mentioned protocol. The cell lysate supernatant was used for GH2-1

purification by immobilized metal-affinity chromatography (IMAC) of the histidine affinity tag (Bornhorst and Falke 2000). Elution of the enzyme was performed via a pH gradient of 5.5, 5.0, and 4.5 (elution buffer: 50 mM NaH<sub>2</sub>PO<sub>4</sub>, 300 mM NaCl). Protein concentration was measured with Roti®-Quant (Carl Roth, K015.1) as described by the manufacturer.

#### 4.7.6. Substrate specificity of GH2-1

The substrate specificity of GH2-1 was determined by measuring its activities with 4 different substrates: 4-Nitrophenyl( $\rho$ NP)- $\beta$ -D-mannopyranoside,  $\rho$ NP- $\beta$ -D-cellopyranoside,  $\rho$ NP- $\beta$ -D-glucopyranoside, and  $\rho$ NP- $\alpha$ -D-mannopyranoside as substrates (Megazym). The reactions (50 mM KP buffer pH 5.5, 0.1  $\mu$ g enzyme and 80  $\mu$ g substrate) were incubated at 37 °C for 1 h, and stopped by the addition of 0.5 M Na<sub>2</sub>CO<sub>3</sub> (pH 11.5). The absorbance was then measured at an OD of 405 nm.

#### 4.7.7. Contour plot of GH2-1 activity

The optimal  $\beta$ -mannopyranosidase activity of GH2-1 at different combinations of temperatures and pHs, in parallel, was assayed according to the setup used before (Herlet *et al.* 2017) with modifications. The reactions consisted of 50 mM KP buffer at different pHs (5, 5.5, 6, 6.5, 7.5, and 8), 80  $\mu$ g 4-Nitrophenyl- $\beta$ -D-mannopyranoside (Megazyme, Ireland, O-PNPBM) and 0.0025  $\mu$ g of purified enzyme. The reactions were incubated for 15 minutes at different temperatures (25, 35, 45, 50, 55, and 65 °C) in a gradient PCR cycler. Then 0.5 M Na<sub>2</sub>CO<sub>3</sub> (pH 11.5) were added to stop the reaction. The absorbance was then measured at an OD of 405 nm. Blanked measurements were used to generate the contour plot using plotly (Inc. 2015).

#### 4.7.8. Viscosity measurements

For the Viscosity measurement, the indicated strains were grown in 2% (w/v) sucrose for 16 h then transferred to 1% (w/v) glucomannan. Culture supernatants were collected after 8 h. The viscosity measurements were carried out on an Anton Paar MCR502 rheometer. The control mode feature TruRate™ of the rheometer was enabled during all measurements. Sandblasted parallel plates with a diameter of 25 mm were used and the gap was varied between 0.5 and 1.1 mm, depending on the available amount of the solution. All experiments were carried out at 25 °C. The Peltier hood of the rheometer was used to cover the geometry and the sample. To avoid sample evaporation, the hood was used without applying the internal air circulation and the lower plate was equipped with a solvent trap filled with water, providing an enclosed volume inside the hood. A constant shear rate

of 10 sec<sup>-1</sup> was applied for 100 sec and sampling rate of the measurement was one point/1 sec. The average of the last 10 points was used for the calculation of viscosity.

#### **4.7.9. Uptake assays**

For the yeast-cell based uptake, yeast strain D452-2 cells transformed with pRS316-*CDT1* or -*CDT2* (Zhang *et al.* 2017) were used. Uptake assays in *S. cerevisiae* and *N. crassa* strains were performed as described before (Galazka *et al.* 2010; Benz *et al.* 2014) with the following modifications: the induction and uptake media contained 1x Vogel's salts plus 2 mM cellobiose and 0.5x Vogel's salts plus 100 µM mannobiose, respectively. Samples of the culture supernatants of each strain were taken at the indicated time points (0, 5, 30 and 60 minutes). The samples were centrifuged (at 12000 rpm for 1 minute) and 50 µl of the supernatant was diluted 1:10 with dH<sub>2</sub>O. Mannobiose concentration was quantified by High Performance Anion Exchange Chromatography coupled to Pulsed Amperometric Detection (HPAEC-PAD) on an ICS-3000 instrument (Thermo Scientific, USA). 25 µl sample was injected onto a Dionex CarboPac PA200 column (3 × 50 mm guard and 3 × 250 mm analytical columns) and eluted at 30 °C using a gradient of 50–170 mM sodium acetate in 0.1 M NaOH at 0.4 ml/min over 12 minutes.

#### **4.7.10. Statistical analyses**

Experiments were done in biological triplicate, and statistical significance was determined by applying analysis of variance followed by a Tukey test using the statistical computing software R (Team 2013). Values of bars and lines in bar and line graphs, respectively, are the mean of the biological replicates, and error bars in all figures are SDs (n=3).

---

## 5. General Discussion

Numerous studies have examined the degradation of plant cell wall substrates by fungi (Aro *et al.* 2005; Tian *et al.* 2009; Glass *et al.* 2013; Zhao *et al.* 2013; Huberman *et al.* 2016). In this context, this thesis followed two approaches to assess the substrates' influence on the fungal performance as well as the fungal differential perception in presence of impurities in the substrate (e.g. mannan). The first approach (chapter 3) focused on the bi-directional aspect of the substrate-fungus relationship. For this, the differences in critical properties of three celluloses (Avicel, Alphacel, and Emcocel) were examined and their effects on digestibility were evaluated. In addition, the effectiveness of the substrates for the induction of the (hemi-)cellulolytic perception pathways in the two biological systems *T. reesei* RUT-C30 and *N. crassa* were checked. Purified model substrates (e.g. MCCs) were used to limit the effects of macro-accessibility, lignin content and degree of polymerization on the digestion. The results highlighted that both crystallinity and hemicellulose content are major factors determining the suitability of the substrate for the production of cellulases from filamentous fungi. While crystallinity limits the substrate digestibility and liberation of inducer molecules, hemicellulose impurities are perceived by the fungus and translated into corresponding species-specific (hemi-)cellulolytic responses.

The second approach (chapter 4) took a closer look at the possible impact of the hemicellulose content present even in model substrates, such as Avicel, on the production of cellulases in filamentous fungi. For this, the functional genomics tools available for the model organism *N. crassa* was utilized to investigate the effect of mannan on the perception of cellulose at the molecular level. By applying genetics, biochemical, and rheological approaches, the results of chapter 4 reveal that mannan and cellulose perception pathways involve common components and are interconnected. Moreover, the connection between the two pathways is inhibitory for cellulase production. Overall, this thesis thereby provides both: 1) a set of criteria that can assist in the rational decision for cellulose substrates to be used in fermentation processes, and 2) insights that advance the fundamental understanding of the cross-talk between regulatory systems governing plant cell wall perception.

### 5.1. Substrate utilization is influenced by crystallinity, hemicellulose content, inducer bioavailability, and fungal regulatory networks

For the analysis of the structure-relevant parameters of celluloses for enzyme fermentation, three model substrates were compared: a hardwood-derived MCC (Emcocel) and a

softwood-derived MCC (Avicel) as well as a hardwood-derived powdered cellulose (Alphacel). This study revealed that Alphacel, with the highest specific surface area and lowest crystallinity, is the most readily digestible substrate (Figure 3-2, Figure 3-3). The observation that higher specific surface area (SSA) leads to an increase in substrate hydrolysis is well supported (Converse *et al.* 1990; Mooney *et al.* 1999; Zhu *et al.* 2009). For example, after the ball-milling of a MCC cellulose, the enzymatic hydrolysis rate of the substrate was greatly enhanced with an increase in its surface area (Yeh *et al.* 2010). Generally, enzymatic hydrolysis of cellulose requires enzymes to adsorb onto the polymer surface (Lee *et al.* 1982; Henrissat 1994; Arantes and Saddler 2010; Karimi and Taherzadeh 2016). The overall availability of cellulose binding sites to cellulases is called accessibility (Linder and Teeri 1997; Carrard *et al.* 2000). It should be noted that accessibility refers to both, macro- and micro-accessibilities. The first denotes the availability of cellulose in the presence of physical barriers in lignocellulosic biomass (e.g. lignin and hemicellulose), while the second denotes the availability of cellulase binding sites on cellulose (Kumar and Wyman 2013). In this study, however, the use of pure cellulose substrates eliminated the effect of cellulose macro-accessibility on cellulose digestion (Kothari *et al.* 2019). It is hypothesized that the accessible surface area is a critical factor limiting the digestibility of cellulose and is increased with the specific surface area (Sinitsyn *et al.* 1991; Zhao *et al.* 2012; Karimi and Taherzadeh 2016). However, this was not the case for Emcocel, where the increase in specific surface area after ball-milling was not sufficient to increase its performance as a substrate (SFigure 6-1). One explanation for this could be that ball-milling leads to an increase in the substrate external surface but not in the accessible pore surfaces, by which over 90% of the substrate enzymatic digestibility is contributed (Wang *et al.* 2012). This is in agreement with another investigation, where a further reduction of substrate particle size, to smaller than 590  $\mu\text{m}$ , did not significantly improve the enzymatic digestibility further (Wen *et al.* 2004). Another explanation for the behavior of Emcocel could be its high crystallinity (Figure 3-2). Several studies revealed that crystallinity is a key determinant for substrate digestibility (Fan 1981; Sinitsyn *et al.* 1991; Ramos *et al.* 1993; Mansfield *et al.* 1999; Yoshida *et al.* 2008; Zhu *et al.* 2008; Hall *et al.* 2010; Hall *et al.* 2010; Chundawat *et al.* 2011; Paes *et al.* 2019). Higher degrees of crystallinity confer higher recalcitrance, lower accessibility to cellulases, and consequently lower hydrolysis of cellulosic substrates (Hall *et al.* 2010; Kothari *et al.* 2019; Paes *et al.* 2019). Although it was observed that an increase in SSA is coupled with a decrease in crystallinity (Converse *et al.* 1990; Walker and Wilson 1991; Zhu *et al.* 2008), in a previous study, the ball-milling of a MCC substrate led to a significant reduction in particle size and increase in SSA, but only a little change in cellulose crystallinity (Yu and Wu 2011). This could have also been the case with Emcocel, in which the ball-milling possibly had no effect

on its internal surface area and crystallinity, and thus did not improve its accessibility to enzymes. Taken together, these observations show that although SSA is an important factor for cellulose digestibility, it likely becomes less critical at higher substrate crystallinity which itself becomes the more limiting factor.

In addition to the physical characteristics, the chemical composition of lignocellulosic substrates also influences their enzymatic hydrolysis. The nature of plant cell walls as a matrix of cross-linked polysaccharide networks and lignin convey structural heterogeneity and complexity to lignocellulosic materials (Ritter 2008). The presence of hemicellulose, and especially lignin in the substrates strongly interferes with the enzymatic activity of cellulases on cellulose (Yang and Wyman 2004; Zhang and Lynd 2004; Öhgren *et al.* 2007; Yoshida *et al.* 2008). However, the substrates evaluated in chapter 3 are commercially and reproducibly obtainable pure cellulosic substrates, which limits such interference. Nevertheless, the presence of low amounts of hemicellulose impurities (xylan and mannan) were detected in the examined substrates by compositional analysis. For example, Alphacel, as a hardwood-derived cellulose, had a higher xylan:mannan ratio than the softwood-derived Avicel (Table 3-1), which reflects their source material (Baehr and Puls 1991; Mitchell *et al.* 2014; Hassan *et al.* 2019). Yet, this was not the case for the hardwood-derived MCC Emcocel, showing the least xylan and mannan contents (Table 3-1). These differences in the hemicellulose composition are likely attributable to differences in plant species, age, growth stage, environmental conditions, and - importantly - substrate processing, since hemicelluloses can get washed out during this procedure (Laca *et al.* 2019).

In terms of sugar polymer perception by fungi, it was shown that different carbon sources induce different tailored transcriptional responses (Tian *et al.* 2009; Delmas *et al.* 2012; Häkkinen *et al.* 2012; Sun *et al.* 2012; Benz *et al.* 2014; Pullan *et al.* 2014). In the general model of such polysaccharide perception by fungi, it is proposed that when a fungus encounters starvation, a small set of hydrolases, called scouting enzymes, are released by which they sense the presence of nearby C-sources. Scouting enzymes then initiate a small-scale digestion of the available substrates to liberate small quantities of sugar monomers and oligomers. These molecules, in turn, act as inducers, triggering the tailored large-scale induction of the fungal lignocellulosic degradative machinery (Melo *et al.* 1997; Delmas *et al.* 2012; Benz *et al.* 2014; van Munster *et al.* 2014; Xiong *et al.* 2014; Daly *et al.* 2016). Therefore, the bioavailability of substrate-derived inducer molecules (Glass *et al.* 2013) is a critical step during the fungal response.

In the current study, the analysis of the inducibility of representative genes of the cellulolytic and hemicellulolytic pathways showed that *N. crassa* is able to detect even the presence of

minor hemicellulose impurities of the cellulose substrates (Figure 3-4). However, the differences in the overall substrate compositions were not always reflected by the induction levels of the respective pathways. For example, the induction of the D-xylulose kinase gene *xyk-1* on both Avicel and Emcocel was not proportional to the difference in xylan content between the two substrates. In contrast, the induction of the same gene on Alphacel was the strongest, reflecting the higher content (and potentially also bioavailability) of xylan of this substrate (Figure 3-4 B). A similar observation was made for the expression of the acetylmannan esterase-encoding gene *ce16-1*, which was more strongly upregulated on the softwood-derived Avicel compared to the hardwood-derived Emcocel, roughly reflecting the difference in their mannan content. As for the other genes, however, the induction of the *ce16-1* gene was the strongest on Alphacel, despite its lower mannan content compared to Avicel. Previous studies of lignocellulose degradation by *Neurospora* showed that *ce16-1* is a direct target of the cellulolytic regulator CLR-2 (Craig *et al.* 2015; Samal *et al.* 2017), possibly indicating a cross-induction of the acetylmannan esterase gene on Alphacel due to the cellulose-induction. Taken together, these results show that even when purified model substrates are used, compositional impurities are still detectable by the fungus and affect its cellular response. The results further corroborate that the hemicellulose content alone is not the only factor shaping the fungal response to polysaccharides. Additional factors, such as substrate crystallinity, inducer bioavailability, and overlap in perception pathways, are also determinant for the hydrolysis of substrates by fungi.

Enzymatic hydrolysis of cellulose is a heterogeneous reaction in which enzymes derived from biological systems, mainly fungi (Singhania *et al.* 2017), are used to breakdown cellulosic substrates. Many studies have been conducted to evaluate the influence of substrate characteristics on enzymes production and activity. However, the majority of these studies, except for few (Peciulyte *et al.* 2014; Thomas *et al.* 2017), used purified enzymes. In the approach followed in this thesis, the two biological systems *N. crassa* and *T. reesei* RUT-C30 were used to evaluate how differences in the physicochemical properties of substrates (as discussed above) affect the production of (hemi-)cellulases. Based on the results, Emcocel was shown to be the substrate with the lowest production of cellulase and xylanase for *N. crassa* (Figure 3-5 B-C), reflecting the recalcitrance of the substrate. Similarly, the higher crystallinity of Avicel compared to Alphacel could have been expected to render it less efficient for the production of cellulases. On the contrary however, *Neurospora* WT produced slightly, but significantly, more cellulase on Avicel than on Alphacel, although this difference was diminished at longer incubation times (6 days) (Figure 3-5 B). A possible explanation could be that the higher amount of xylan present in the hardwood-derived Alphacel induced the fungus to utilize the more amorphous

hemicellulose polymer first, and thus delaying the cellulolytic response (Laca *et al.* 2019). This is in agreement with another study, where *A. niger* showed an earlier hemicellulolytic response on heterogeneous biomass (van Munster *et al.* 2014). Intriguingly, although *N. crassa* displayed a differential (hemi-)cellulolytic response to the highly crystalline MCCs Avicel and Emcocel, *T. reesei* RUT-C30 did not phenocopy this. On the contrary, RUT-C30 showed low production of cellulase and xylanase on both Avicel and Emcocel compared to Alphacel (Figure 3-5 B-C), likely due to a higher sensitivity of the *T. reesei* strain to the differences in substrate crystallinity. Generally, the results revealed that Alphacel induced an overall higher enzyme production in *T. reesei* compared to *Neurospora* (Figure 3-5). Meaning that the fungus was able to take full advantage of the xylan impurities present in this substrate. The elevated cellulase levels produced by RUT-C30 on Alphacel despite its lower cellulose content could thus be the result of differences between the fungal intrinsic regulatory networks. In *Trichoderma*, the induction of both cellulase and hemicellulase genes mediated by their respective inducer molecules is mainly regulated by the same transcription factor, XYR1 (Stricker *et al.* 2006; Mach-Aigner *et al.* 2008; Stricker *et al.* 2008). Thus, a cross-induction of cellulases by the various inducer molecules present in Alphacel (e.g. derived from the high amounts of xylan in addition to cellulose) is likely to happen (Figure 3-5 B). In *Neurospora*, on the other hand, only the hemicellulolytic response is under the control of XLR-1, the ortholog of XYR1 (Sun *et al.* 2012; Benocci *et al.* 2017), while the cellulolytic response is mainly regulated by CLR-1 and CLR-2 (Coradetti *et al.* 2012; Coradetti *et al.* 2013; Craig *et al.* 2015). A cross-induction of cellulases by xylan is therefore unlikely. Indeed, transcriptional profiling showed that xylose has an insignificant role in inducing cellulase gene expression in *N. crassa* (Sun *et al.* 2012; Wu 2017).

As a further layer of regulatory control to consider, the ability of molecules to induce lignocellulolytic responses is masked by carbon catabolite repression (CCR). CCR is a universal regulatory mechanism by which the utilization of easily metabolized C-sources, such as glucose, is favored over complex polymers (Ronne 1995; Ruijter and Visser 1997; Ebbole 1998; Gancedo 1998). This mechanism has been described to influence fungal responses throughout the substrate perception (Bailey and Arst 1975; Sun and Glass 2011). Among others, CRE1/CRE-1/CreA is a major transcription factor governing CCR (Bailey and Arst 1975; Strauss *et al.* 1995; Ilmen *et al.* 1996; Ebbole 1998; de Vries *et al.* 1999; Portnoy *et al.* 2011; Sun and Glass 2011). One of the main differences between *N. crassa* and *T. reesei* RUT-C30 strains, is the presence of a truncated version of the *cre1* gene in RUT-C30 (Ilmen *et al.* 1996; Seidl *et al.* 2008; Le Crom *et al.* 2009), leading to a xylanase and cellulase de-repressed phenotype (Portnoy *et al.* 2011; Mello-de-Sousa *et al.* 2014). As shown in other studies, the *N. crassa*  $\Delta cre-1$  deletion strain had higher cellulolytic and

xylanolytic responses compared to the WT (Figure 3-7 A-B) (Sun and Glass 2011; Roche *et al.* 2014). Interestingly, the  $\Delta cre-1$  strain exhibited a different proportional response to the three substrates in comparison to the one seen for the WT strain. In the absence of the CRE-1-mediated CCR, *N. crassa* was able to respond positively to the xylan impurities present in Alphacel, and phenocopy the behavior of RUT-C30 (Figure 3-7 B-C).

In summary, these results show that both fungi are able to perceive the differences in crystallinity and hemicellulose content between Avicel, Emcocel and Alphacel. However, crystallinity seems to be a more important factor determining cellulolytic perception in *T. reesei* RUT-C30. The absence of a stringent CCR in this fungus allows it to take full advantage of the higher amount of inducer molecules being liberated from the least crystalline substrate Alphacel.

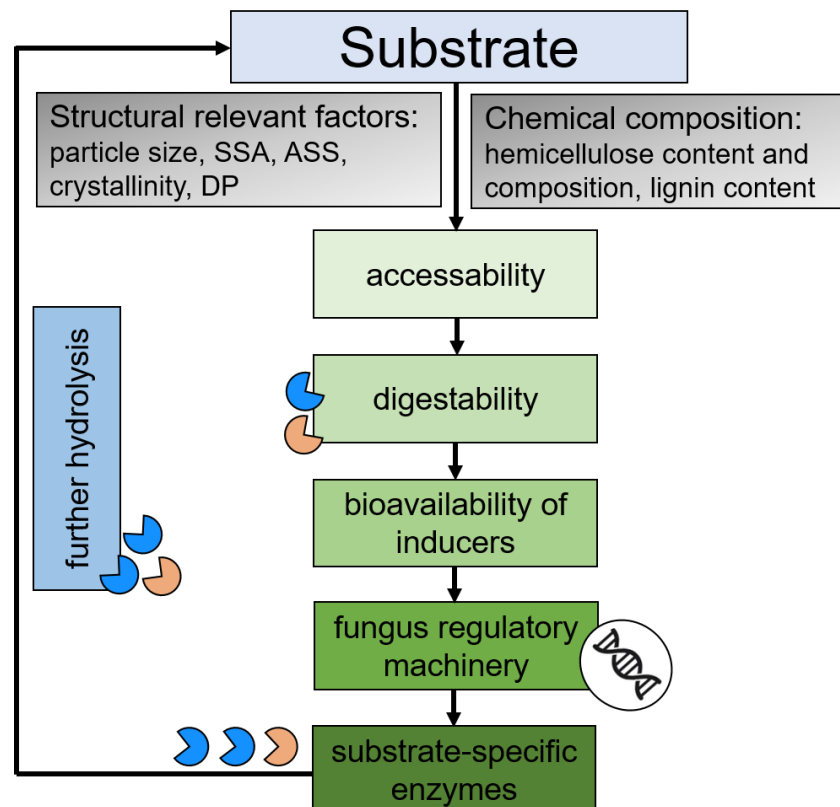


**Figure 5-1. Factors affecting the polysaccharide digestibility and perception fungi.**

The factors affecting the accessibility of cellulose substrate can be divided into structural relevant factors (e.g. particle size, specific surface area, accessible surface area, crystallinity and degree of polymerization) and chemical composition factor (e.g. acetyl group, hemicellulose and lignin contents). All these factors affect differently the accessibility of cellulose, the most crucial factor resulting in an increase or decrease in its digestibility. And thus directly influencing the release of inducer molecules from the substrate. Inducer bioavailability in the hydrolysate, the critical factor for fungal substrate perception, initiate the signal flow into the regulatory machinery of the fungus. Which in turn tailor the release of substrate specific enzymes to degrade the substrate in proximity. Further substrate hydrolysis influence it physicochemical properties and hence its hydrolysis and the release of inducers. Eventually, this vicious circle influence the strength of lignocellulolytic response of the fungus.

Taken together, the results of chapter 3 show that the physicochemical properties of the substrate, such as crystallinity and hemicellulose content, are important factors affecting substrate performance. These properties influence the availability of cellulase binding sites on cellulose (Arantes and Saddler 2010; Zhao *et al.* 2012), thus affecting its micro-accessibility to enzymes and subsequent digestibility (Figure 5-1). However, once hydrolysis is initiated, the bioavailability of inducer molecules comes into play to shape the fungal lignocellulolytic response. As the hydrolysis reaction proceeds, an increasing amount of hydrolytic products, such as mono- and oligomers, will be liberated and recognized by the fungus. Additionally, different utilization preferences for the released sugars might influence the order in which polysaccharides are perceived. As a result, the fungal regulatory machinery is activated, governing the expression of relevant sugar transporters and enzymes. The intrinsic regulatory networks of the fungus are then the dominant factor tailoring substrate utilization. However, the action of cellulases and hemicellulases also alters the inherent characteristics of the substrates (Ramos *et al.* 1993). For instance, the hemicellulose content, being readily degraded, is likely the first to be depleted (Zhang *et al.* 1999; Horn *et al.* 2012). In addition, crystallinity increases, making the substrate increasingly resistant to further hydrolysis (Sasaki *et al.* 1979; Fan *et al.* 1980; Pu *et al.* 2006; Chen *et al.* 2007; Hall *et al.* 2010; Cheng *et al.* 2019). Consequently, the factors affecting the substrate-fungus relationship are not only interrelated but also consecutive in a way that when a factor is no longer limiting, another factor then becomes dominant (Zhu *et al.* 2008). Therefore, it is important to understand the contributions that the substrate, the hydrolytic enzymes, as well as the degrading microorganisms make to the total saccharification of the substrate.

## **5.2. Mannan and cellulose perception pathways overlap and this overlap is inhibitive for cellulase production**

The transcriptional response of microorganisms to available C-sources is tuned by numerous regulatory networks, including nutrient sensing pathways, direct transcriptional regulation of enzymes, responses to the extracellular environment (e.g. pH and light), and regulatory feedback pathways (Huberman *et al.* 2016; Benocci *et al.* 2017). Many studies have been showing extensive overlaps in the induction of cellulolytic, hemicellulolytic and pectinolytic genes induced on different substrates (Benz *et al.* 2014; Gruben *et al.* 2017; Samal *et al.* 2017). These studies suggest potential overlaps in the utilization pathways of the different polysaccharides. In this thesis, the results of chapter 4 proposed two sites of overlap between mannan and cellulose degradation pathways. The first site is extracellular, at the level of uptake by the major facilitator super family (MFS) cellodextrin transporters



*oryzae*, by which the disruption/overexpression of the mannan regulator-encoding gene *manR* (Ogawa *et al.* 2012), a homolog of *clr-2* in *N. crassa*, resulted in a significant decrease/increase in the expression levels of four cellulolytic genes (*celC*, *celD*, *cbhD*, and *bgl5*) (Ogawa *et al.* 2013). Collectively, these observations confirm the involvement of CLR-2/ManR in the direct control or the modulation of the expression of genes involved in both, cellulolytic and mannanolytic pathways.

The involvement of a regulator in different perception pathways is not unexpected. In *T. reesei* for instance, the TFs ACE2 and XYR1 activate not only the expression of cellulases, but also of xylanases (Aro *et al.* 2001; Stricker *et al.* 2006; Portnoy *et al.* 2011; Bischof *et al.* 2013; Hakkinen *et al.* 2014; dos Santos Castro *et al.* 2016). The XYR1 homolog in *A. niger* and *A. oryzae*, XlnR, was also found to control genes of the cellulolytic and the xylanolytic pathways (van Peij *et al.* 1998; van Peij *et al.* 1998; Gielkens *et al.* 1999; Marui *et al.* 2002; Hasper *et al.* 2004; Noguchi *et al.* 2009). Nevertheless, a study by Hrmova *et al.* in *A. terreus* showed that homo-disaccharides of D-glucose (CB) and D-xylose (xylobiose) induced cellulases and xylanases separately, while the structurally similar hetero-disaccharide induced both xylanases and cellulases (Hrmová *et al.* 1991). Knowing that glucomannan is a linear chain of both D-mannose and D-glucose residues (see section 1.2) (Maeda *et al.* 1980), it is thus interesting to test if the signal overlap, presented in this study, is only valid for CB and MB homo-disaccharides, or it will also be present for the hetero-disaccharide glucomannodextrin. Moreover, in nature, mannan coats cellulose microfibrils and forms interstitial material between them (Whitney *et al.* 1998; Carpita *et al.* 2001; Hosoo *et al.* 2002), which puts the molecules in very close proximity (Zhang *et al.* 2014). Thus, the co-existence of cellulose and mannan could be a potential explanation that allows the fungus to use common routes during their utilization. Taken together, these findings suggest that the aforementioned structural similarity between cellulose and mannan degradation products (CB and MB, respectively) and the natural co-existence of both polymers allow them to be transported by the same transporters and to potentially interact with a downstream signaling component(s) leading to the TFs.

During lignocellulosic substrate degradation, mono- and oligosaccharides released by the action of scouting enzymes play a crucial role in the induction of the polysaccharide degradation machinery (see section 5.1). Inducer molecules capable of initiating the different (hemi-)cellulolytic pathways are researched extensively in different fungi (Amore *et al.* 2013). For example, in *T. reesei*, several saccharides can act as inducers such as lactose, sophorose, xylobiose and D-xylose (Mandels *et al.* 1962; Karaffa *et al.* 2006; Stricker *et al.* 2006; Kubicek *et al.* 2009; Herold *et al.* 2013; Ivanova *et al.* 2013). However

each inducer molecule can activate only part of the (hemi-)cellulolytic pathway (reviewed in Amore *et al.* 2013). Different inducers were also indicated for Aspergilli, such as sophorose in *A. terreus* (Hrmová *et al.* 1991) and D-xylose in *A. niger* (de Vries *et al.* 1999; Mach-Aigner *et al.* 2012; Amore *et al.* 2013). In *N. crassa*, cellobiose was assigned as the inducer molecule of the cellulolytic response (Znameroski *et al.* 2012). On the contrary, reports for similar molecules acting as inhibitors is extremely scarce. The results of chapter 4, however, show that a mannobiose acts as an inhibitor for cellulase production in *N. crassa*, *T. reesei* and *M. thermophila*. Upon the addition of either mannan or mannobiose to *N. crassa* WT cultures growing on pure cellulose (SFigure 6-2 B) cellulase production was significantly reduced (Figure 4-2 B). In *Neurospora*, mannobiose is degraded into sugar monomers by the action of the intracellular  $\beta$ -mannosidase GH2-1 characterized in this study (Figure 4-1 B-C and SFigure 6-3) (Moreira 2008; Znameroski *et al.* 2012). Compared to WT, the deletion of the *gh2-1* gene resulted in a strong inhibition in cellulase production upon mannobiose addition (Figure 4-2 B) and when grown on mannan-contaminated Avicel (Figure 4-2 C and SFigure 6-2 B) (Baehr and Puls 1991). Moreover, this strain accumulated undigested (gluco-)mannodextrins in the cytosol (Figure 4-2 C). Interestingly, a strain exhibiting the deletion of a gene encoding the intracellular  $\beta$ -glucosidase-encoding *gh1-1* in addition to the  $\Delta gh2-1$ , accumulated both, mannodextrins and cellodextrins, intracellularly (SFigure 6-5) and had a restored cellulosic production (Figure 4-3 C). These results show that the production of cellulases is sensitive to the intracellular balance between cellobiose and mannobiose. Therefore, a possible way to relieve the inhibition could be either by eliminating mannan catabolism or by enhancing intracellular metabolism of mannodextrins. Both approaches could be achieved by engineering a fungal strain that: either 1) lacks the extracellular  $\beta$ -mannanase (GH5-7), and thus is incapable of utilizing mannan, or 2) has elevated  $\beta$ -mannosidase activity (e.g. by overexpressing *gh2-1*) and is therefore metabolizing mannodextrins at higher rates. Shifting the intracellular balance in favor of CB could potentially favor cellulase induction over inhibition.

Structural analogs of inducing sugars have been used for multiple purposes, among which: 1) as enhanced inducers for induction of lignocellulolytic enzymes by different organisms such as ascomycetes (Mandels *et al.* 1962; Rho *et al.* 1982; Suto *et al.* 1991; Kurasawa *et al.* 1992; Agrawal *et al.* 2017), basidiomycetes (Yadav 2018), and bacteria (Rho *et al.* 1982; Nasser *et al.* 1991; Shiang *et al.* 1991; Haltrich *et al.* 1995), 2) as slowly metabolizable or non-metabolizable inducers for maintaining the production of high levels of enzymes in *T. reesei* (Huang and Wages 2016) and Aspergilli (Goto *et al.* 1998; Moreira *et al.* 2001), and 3) as inhibitors that selectively bind to the receptors of the inducing molecules and thus block the consequent generation of a positive signal (Meldrum 1985; Kozikowski *et al.* 2003; Wermuth 2006; Levy *et al.* 2007). The effect seen with MB in this thesis work appears highly

similar to the latter alternative. The accumulating non-inducing MB (Samal *et al.* 2017) is somehow interfering and competing with the binding of the inducing CB and thus appears to be blocking its role in the induction of a positive signal, leading to the inhibition of cellulase production. In line with this explanation, recent RNA-Seq data showed that mannobiose and mannan induce a starvation-like response in *N. crassa* (Samal *et al.* 2017; Wu 2017; Thieme 2019). The authors hypothesized that the disaccharide is not associated with any specific degradation response in the fungus. Therefore, it seems like *N. crassa* is blind to the presence of mannan so that it utilizes the cellulolytic response to induce the mannanolytic genes. Hence, the structural similarity of CB and MB (as discussed above) implies that both molecules are potentially competing for binding to the same, so far unknown, receptor or signaling component, but with different outcome: either 1) induction of cellulases upon the binding of CB, or 2) block of the induction with a non-productive binding of MB.

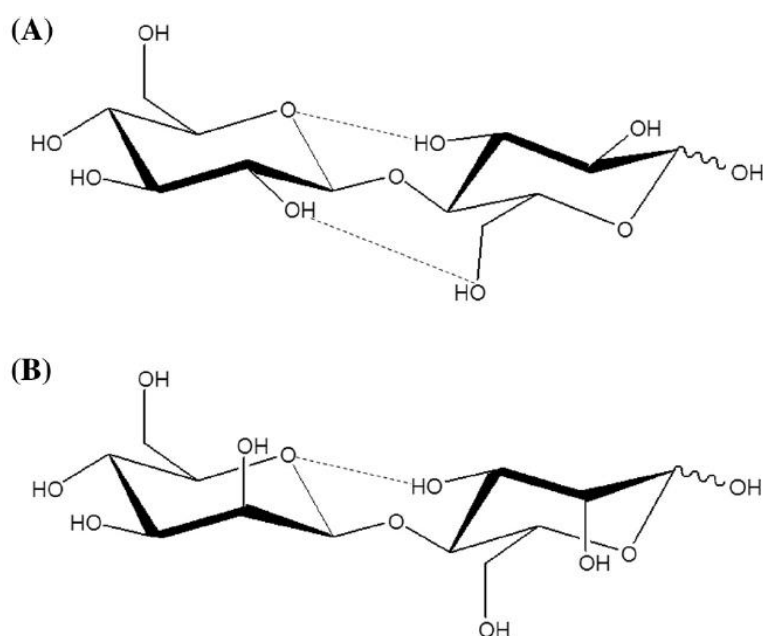


**Figure 5-2. Structures of (A) cellobiose and (B) mannobiose.**

Dashed lines denote intramolecular hydrogen bonds. This figure was modified from Morris and Striegel 2014.

Another structural characteristic might help MB to fit into certain binding pockets. The flexibility of disaccharides is usually restricted by the existence of intramolecular hydrogen bonds (H-bonds) (Morris and Striegel 2014). While CB possesses two H-bonds, one between HO<sub>3</sub> and O<sub>5</sub> and another between HO<sub>6</sub> and O<sub>2</sub> (Figure 5-2), the axial position of HO<sub>2</sub> on the mannose residue of MB prevents a second H-bond from forming (Mackie *et al.* 1986). Therefore, MB possesses a greater solution flexibility than CB (Moreira 2008; Morris and Striegel 2014) possibly allowing it to interact more easily with signaling components present in the cytosol. Further experiments, however, are necessary to elucidate the

involved signaling components, such as the actual receptor, which may subsequently result in the identification of new proteins involved in lignocellulose deconstruction.

In *Neurospora*, the presence of an inducer, e.g. CB, activates CLR-1 which induces the expression of a small number of genes, including some coding for  $\beta$ -glucosidases and the transcription factor *clr-2*. CLR-2 is then responsible for the induction of the majority of cellulase genes (Coradetti *et al.* 2012; Coradetti *et al.* 2013). An additional regulator, CLR-3, was described recently to act as a repressor of CLR-1 in the absence of an inducer (Huberman *et al.* 2017). The deletion of either *clr-1* or *clr-2* abolishes the production of cellulases and renders *N. crassa* unable to utilize cellulose as a C-source (Coradetti *et al.* 2013). In this study, however, *clr-1* deletion did not affect the hydrolysis of glucomannan (Figure 4-3 B). Also, ChIP-seq data by Craig *et al.* showed that both genes, the  $\beta$ -mannanase (*gh5-7*) and the  $\beta$ -mannosidase (*gh2-1*), are direct targets for CLR-2 (as mentioned above) while CLR-1 binds only to the *gh5-7* promoter region (Craig *et al.* 2015). Although CLR-2 is conserved in ascomycetes (Coradetti *et al.* 2012; Benocci *et al.* 2017), its interaction with CLR-1 is not necessary for its function in other species. In *A. nidulans*, for instance, the deletion of the *clr-2* ortholog, *clr-B*, resulted in a much more significant decrease in the expression of cellulolytic genes compared to the deletion of the *clr-1* ortholog, *clr-A* (Coradetti *et al.* 2013). Moreover, the ortholog of CLR-1 in *A. niger*, ClrA, was found not to be important for (hemi-)cellulolytic gene induction, and it was suggested that an interaction between it and the CLR-2 homolog, ClrB, may not occur (Raulo *et al.* 2016). Interestingly, in *T. reesei*, the deletion of the gene encoding the CLR-1 ortholog did not have a phenotype on cellulose (unpublished data, personal communication). Additionally, in this study, the *T. reesei* strain RUT-C30 showed a significant decrease in cellulase production upon the addition of glucomannan (Figure 4-5 B). Taken together, these observations suggest both a non-conserved role of CLR-1 (and thus CLR-3) as well as a CLR-1-independent role of CLR-2 and its homologs in ascomycete fungi.

Interestingly, the mis-expression of CLR-2 only partially restored the inhibition of cellulase production caused by the accumulating MB (Figure 4-3 B). This implies that the inhibitive competition between CB and MB might be upstream of CLR-2. In fungi, the precise transmission mechanism of the inducing signal from the membrane to the nucleus is still unclear. An increasing number of studies investigated the potential role of protein kinases and receptors in the induction of (hemi-)cellulolytic enzymes, such as mitogen-activated protein kinase (MAPK), cAMP-dependent protein kinase A (PKA), and G-protein coupled receptors (Brown *et al.* 2013; De Assis *et al.* 2015; de Paula *et al.* 2018; Kunitake *et al.* 2019; Ribeiro *et al.* 2019). A recent study described a new TF in *N. crassa* and *M.*

*thermophila*, CLR-4, as a regulator of the (hemi-)cellulolytic response by regulating both, genes of the cAMP signaling pathway and genes encoding the (hemi-)cellulolytic TFs *clr-1*, *Mtclr-2*, and *Mtxyr-1* (Liu *et al.* 2019). Most of these studies, however, focused on the involvement of the kinases in glucose sensing and in CCR, via CRE-1/Cre1/CreA. For example, in *A. nidulans*, PKA was described to mediate CCR either by increasing *creA* transcripts or by indirectly leading to CreA phosphorylation, and the consequent repression of hydrolases (Ribeiro *et al.* 2019). Interestingly, CCR was found not to be involved in the mannan-mediated inhibition (chapter 4). Since also *T. reesei* RUT-C30 is carbon catabolite de-repressed due to a *cre1* truncation (Figure 4-5) (Portnoy *et al.* 2011; Mello-de-Sousa *et al.* 2014), CRE-1-mediated CCR appears not to be involved in the inhibition of cellulase production by MB, and consequently PKA involvement described for *A. nidulans* could not be valid here as well. Nevertheless, a potential approach for the identification of involved protein kinases could be done through screening of the *N. crassa* mutant library for kinase deletion strains that have stronger (or reduced) growth and/or cellulase production on Avicel. Consequently, the effects of the deletions on the expression of (hemi-)cellulolytic TFs, particularly CLR-1 and -2, and on the cellulolytic response could be investigated.

For the induction of the (hemi-)cellulolytic response, genes encoding enzymes must be both released from repression (e.g. CCR) and activated by TFs that are regulated specifically by components of plant biomass. CCR is activated in the presence of a preferred C-source, when the latter is depleted, the fungus gets into a starvation phase during which scouting enzymes liberate inducing molecules that allow the fungus to sense polysaccharides nearby and utilize its regulatory machinery accordingly. The important questions valid here are: how is the inducer signal (e.g. CB) transduced to TFs (in *N. crassa*, *T. reesei*, and *Aspergilli*)? What are the molecular mechanisms involved in the activation of these TFs? To answer these questions, a further investigation at the transport level is to be considered, since many studies proposed a role of sugar transport during polysaccharide perception events. For instance, the *T. reesei* and *P. oxalicum* MFS transporters Crt1/Stp1 and CdtC/CdtD, respectively, were found to be involved in both, cellulose sensing and cellulolytic pathway induction (Ivanova *et al.* 2013; Li *et al.* 2013; Zhang *et al.* 2013). Similarly, cellodextrin transporters from *A. nidulans* and *N. crassa*, CltB and CDT-1/-2, respectively, might act as transceptors and thus might be involved in signal transduction (Znameroski *et al.* 2014; dos Reis *et al.* 2016). The first approach could be the uncoupling of the transport function of CDT-1/-2 from the possibility of their involvement in the intracellular signaling pathway. This could be possible by introducing site-directed mutations that abolish only one of the two functions. For instance, Znameroski *et al.* used defective transporters strains to report the involvement of CDT-1 and -2 in signaling (Znameroski *et*

*al.* 2014). Also, Kankipaty *et al.* used a similar approach in *Saccharomyces cerevisiae* to confirm that the sulfate binding to the corresponding transceptors initiates a series of conformational changes that triggers the signaling to the PKA pathway. In the aforementioned study, the transport function was assayed directly in cells using radiolabeled substrates, while the activation of signaling was detected by measuring an increase in trehalase activity, a well-established PKA target (Kankipati *et al.* 2015). A limitation, however, could be finding a substrate analog that is transported without triggering signaling (Diallinas 2017). Interestingly, this is not the case here, since the results showed that MB is transported by both transporters and that it induces a starvation-like response (Samal *et al.* 2017; Thieme 2019). Moreover, the uptake of MB was not completely abolished in the transporter deletion strains (Figure 4-4 B), implying that there could be additional factors involved.

In summary, based on the results reported here and in previous studies, it seems like *N. crassa* is not able to specifically perceive the presence of mannan, but is rather using its cellulolytic regulatory machinery in order to initiate its mannanolytic response. The results nevertheless clearly demonstrate that the mannan degradation products do have an effect and describe the possible sites of signaling molecule competition to be the perception events at which the recognition and differentiation between the two polysaccharides degradation products, cellobiose and mannobiose, would be possible: at the site of transport by the cellodextrin transporters, as well as intracellularly at the signaling stage reaching the TFs. This strongly suggests a possible “confusion” between both disaccharide molecules at those sites.

### 5.3. Conclusion and outlook

Based on the two approaches followed in this work to study the relationship between (hemi-)cellulosic substrates and fungi, this thesis could increase the understanding of the interplay between major physicochemical substrate characteristics and regulatory networks of their perception.

The analysis of the physicochemical properties of substrates and of their impact on perception by fungi revealed that both the crystallinity and the hemicellulose content are major factors determining the suitability of the substrates for the expression of cellulases in filamentous fungi as production hosts. Higher crystallinity restricts micro-accessibility, which reduces the enzymatic hydrolysis of the substrate and thus the release of inducer molecules. In addition, even minor hemicellulose impurities present in relatively pure substrates are perceived efficiently by fungi that translate those signals into corresponding cellulolytic and hemicellulolytic responses. The responses, however, are not always a

reflection of the overall chemical composition of the substrate. Eventually, this highlights the importance of inducer bioavailability, which triggers the species-specific regulatory pathways depending on the mechanisms and components of the regulatory pathways present in each fungus.

The second part of the thesis addressed the overlap between two seemingly unrelated perception pathways: that of cellulose and that of the hemicellulose (gluco-)mannan. Two potential sites of overlap were described in this thesis, the first being extracellular at the level of transport, and the second being intracellular, at the signaling stage leading to the activation of TFs. Moreover, this study identified a so far unknown competitive inhibition between the substrates' degradation products, cellobiose and mannobiose, potentially acting as inducers and inhibitors, respectively, and affecting the induction of cellulases. Importantly, the inhibition was shown to be conserved in *N. crassa*, *T. reesei* RUT-C30, and *M. thermophila*. This is the next aspect to be addressed which would allow a better understanding of the general molecular events involved in cellulase induction and of the conserved role of CLR-2 and its homologs in the three fungi (including *N. crassa*). In addition, the mechanistic results should be transferred from model organisms to industrial strains to facilitate the development of strains that are mannan-insensitive.

In conclusion, this thesis provides a set of criteria to consider when choosing substrates and strains for the fermentation processes and the production of enzymes. The substrate physicochemical characteristics, regulatory networks present for each fungus, the potential overlap in the perception pathways of different substrates, and the (in-)ability of the fungus to recognize certain substrates are among the important factors to be considered. Additionally, this thesis highlights possible targets for the overall improvement of the substrate-fungus relationship and thus the production of enzymes for different biotechnological applications. In this regard, future work could focus on two main areas: 1) enhancing digestibility and availability of inducer molecules through substrate improvement by increasing accessibility, reducing crystallinity, and controlling hemicellulose impurities by taking into account the regulatory machinery of the fermenting fungus, and 2) strain improvement by applying genetic engineering approaches to produce favorable fungal strains with a lower tendency to be inhibited by competitive pathway cross-talk in the presence of complex biomass. These results might help to accelerate the development of more effective substrates and improved industrial strains that are better suited for the efficient production of biofuels and biochemicals to ultimately overcome the current bottlenecks in those industries.

---

## 6. Appendix

### 6.1. Supplementary Methods

#### 6.1.1. Thermal stability assay

The thermal stability assay was carried out by incubating the enzyme at different temperatures (0, 25, 37, 45, 55, and 65 °C) for 1 h. Afterwards, the residual activity of 0.1 µg enzyme was assayed with 50 mM KP buffer (pH 5.5) and 80 µg 4-Nitrophenyl-β-D-mannopyranoside substrate (Megazyme, Ireland, O-PNPBM). The reaction was incubated at 37 °C for 5 minutes, then stopped by the addition of 0.5 M Na<sub>2</sub>CO<sub>3</sub> (pH 11.5). The absorbance was then measured at an OD of 405 nm.

#### 6.1.2. Microscopy

For *gh2-1-gfp* strain, the *gh2-1* gene amplified from gDNA was placed under the control of the constitutive promoter *ccg-1* (clock-controlled gene 1) using XbaI and BamHI restriction sites in plasmid pCCG-C-Gly-GFP. The construct was transformed into the WT *his-3<sup>-</sup>* strain by electrotransfection.

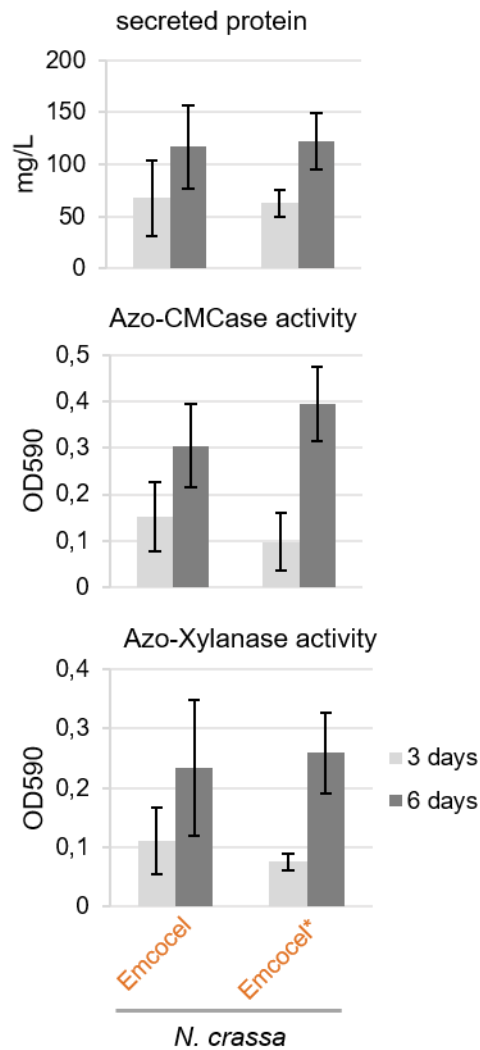
GFP fluorescence was visualized using an epifluorescence microscope with a 100x oil-immersion objective.

### 6.2. Abbreviations

Abbreviations	description
<b>BLAST</b>	Basic Local Alignment Search Tool
<b>Bp</b>	base pair
<b>BSA</b>	bovine serum albumin
<b>CAZY</b>	carbohydrate-active enzyme
<b>CB</b>	cellobiose
<b>CBM</b>	carbohydrate-binding modules (CAZY associated module class)
<i>ccg-1</i>	clock controlled gene 1
<b>CCR</b>	carbon catabolite repression
<b>cDNA</b>	complementary DNA
<b>Ce</b>	cedar
<b>Ch</b>	chestnut
<i>clr-1/2</i>	cellulose regulator 1 or 2
<b>CMC</b>	carboxymethyl cellulose
<i>cre-1</i>	carbon catabolite repressor protein 1
<b>C-source</b>	carbon source
<b>ddH<sub>2</sub>O</b>	double distilled water
<b>DNA</b>	deoxyribonucleic acid
<b>dNTP</b>	deoxynucleotide triphosphates
<b>e.g.</b>	<i>exempli gratia</i> (latin; translated to: for example)

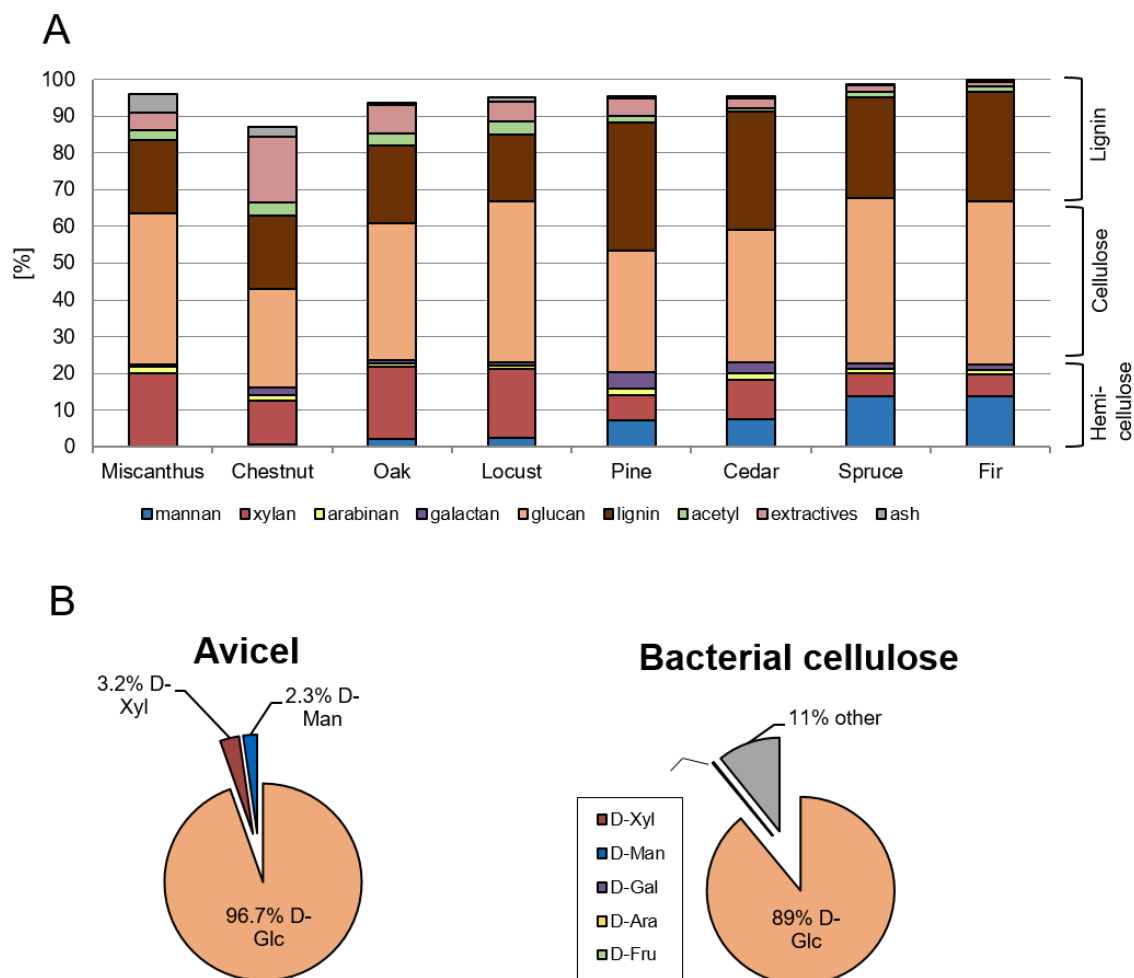
<b>EDTA</b>	ethylenediaminetetraacetic acid
<b>F</b>	fir
<b>FGSC</b>	Fungal Genetics Stock Center
<b>FungiDB</b>	fungal and oomycete genomics resources
<b>gDNA</b>	genomic DNA
<b>GFP</b>	green fluorescent protein
<b>GH</b>	glycoside hydrolases (CAZY class)
<b>h</b>	hour(s)
<b>H<sub>2</sub>SO<sub>4</sub></b>	sulfuric acid
<b>HFM</b>	Holzforchung München (german; translated to: Wood Research Munich)
<b><i>his-3</i></b>	histidine biosynthesis trifunctional protein coding gene
<b>L</b>	locust
<b>LB</b>	lysogeny broth
<b>M</b>	Miscanthus
<b>MB</b>	mannobiose
<b>MCC</b>	microcrystalline cellulose
<b>MCS</b>	multiple cloning site
<b>min</b>	minute(s)
<b>MM</b>	Vogel's Minimal Medium
<b>mRNA</b>	messenger RNA
<b>NMR</b>	nuclear magnetic resonance
<b>NoC</b>	no carbon source
<b>O</b>	oak
<b>OD</b>	optical density (used wavelengths in nm are added in subscript, e.g. OD <sub>600</sub> )
<b>oex</b>	overexpression
<b>P</b>	pine
<b>PCR</b>	polymerase chain reaction
<b>PDM</b>	plasmid DNA medium
<b>RNA</b>	ribonucleic acid
<b>RNA-Seq</b>	mRNA sequencing (used to create transcriptomics data)
<b>rpm</b>	revolutions per minute
<b>RT</b>	room temperature
<b>RT-qPCR</b>	quantitative real-time PCR
<b>S</b>	spruce
<b>SD</b>	standard deviation
<b>SFigure</b>	supplementary figure
<b>SOC</b>	super optimal broth with catabolite repression
<b>suc</b>	surcrose
<b>TA</b>	top agar
<b>TAE</b>	Tris acetate EDTA buffer
<b>TCDB</b>	Transporter Classification Database
<b>TF</b>	transcription factor
<b>WT</b>	Wild-type
<b>x g</b>	times gravity/gravitational acceleration
<b><i>xlr-1</i></b>	xylan regulator 1

### 6.3. Supplementary Figures



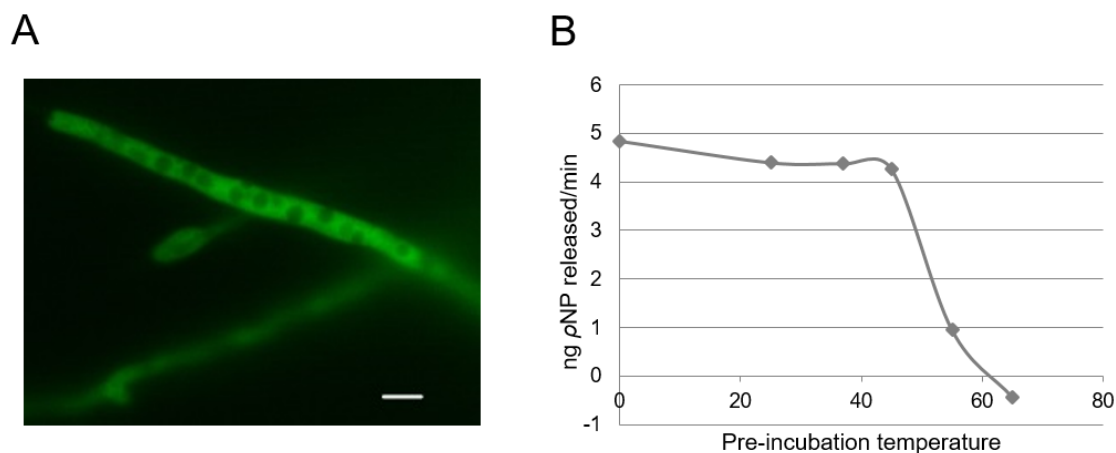
**SFigure 6-1. Cellulase and hemicellulase expression by *N. crassa* and *T. reesei* RUT-C30 on Emcocel with or without additional ball-milling.**

Performance was measured by analysis of culture supernatant aliquots taken after 3 and 6 days. Secreted protein was measured by Bradford assay, endo-glucanase activity by Azo-CMC assay and endo-xylanase activity by Azo-Xylanase assay as described in Methods. Emcocel\* denotes additionally ball-milled substrate. Values are the mean of biological triplicates. Error bars represent standard deviations (n=3; no statistical differences were detected by one-way ANOVA).



**SFigure 6-2. Compositional analysis of the different carbon sources.**

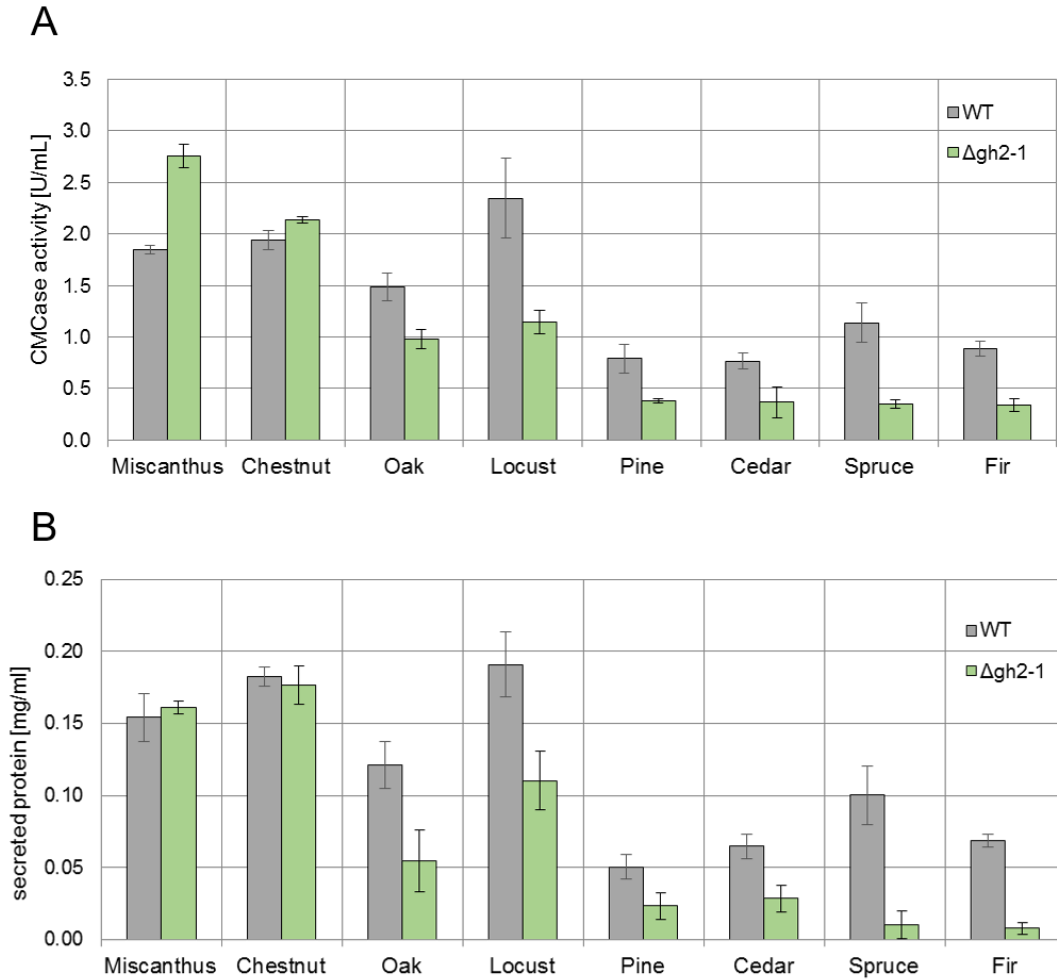
Results of compositional analysis of **(A)** complex powdered carbon sources (grass: Miscanthus, hardwood-derived: chestnut, oak, and locust, softwood-derived: pine, cedar, spruce and fir) and of **(B)** Avicel and bacterial cellulose after sulfuric acid hydrolysis (in %). Glc: glucose, Xyl: xylose, Man: mannose, Gal: galactose, Ara: arabinose, and Fru: fructose.



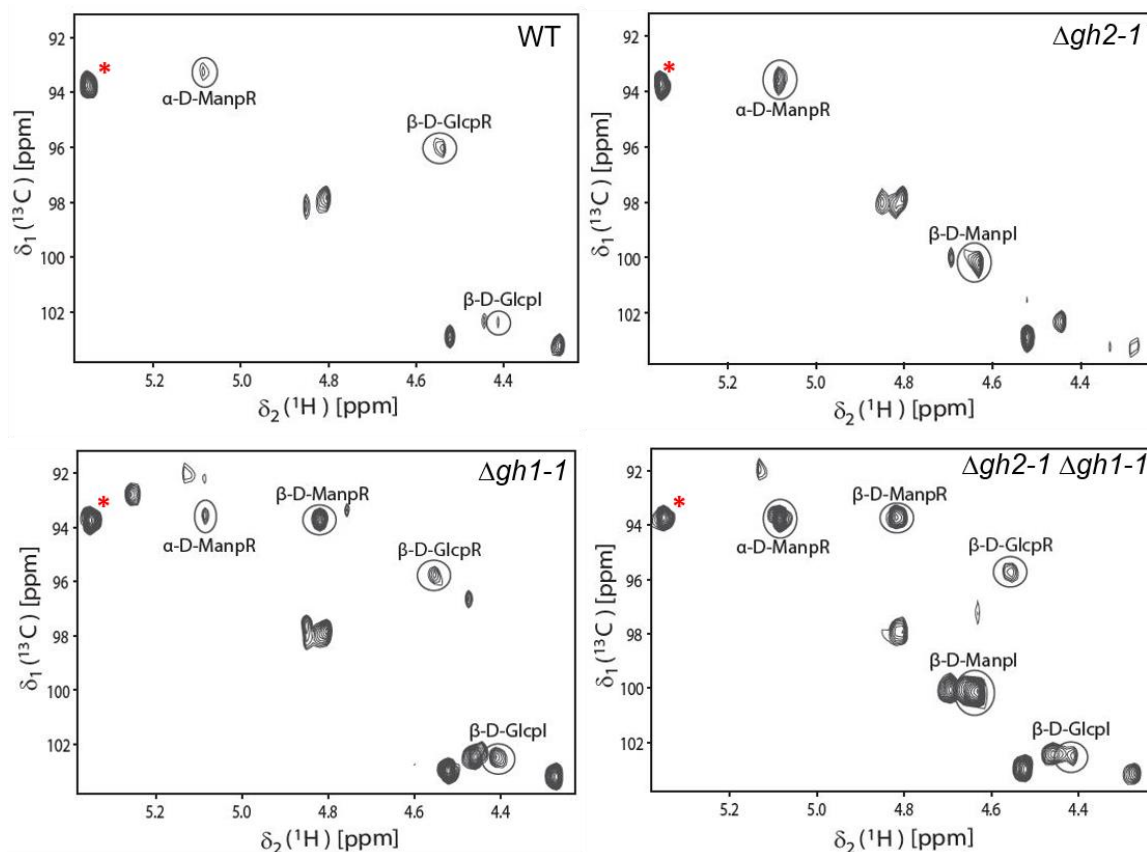
**SFigure 6-3. GH2-1 localization and thermostability.**

**SFigure 6 3. GH2-1 localization and thermostability.**

**(A)** GH2-1 intracellular localization. A gh2-1-gfp strain was used for the localization and visualization by fluorescence microscopy. Scale bar represents 10  $\mu\text{m}$ . **(B)** Thermal stability assay of GH2-1. Purified enzyme was pre-incubated for 1 h at the indicated temperatures, and then the  $\beta$ -mannopyranosidase activity was assayed at 37  $^{\circ}\text{C}$  for 5 minutes.

**SFigure 6-4. CMCase activity and protein secretion of *N. crassa* WT and  $\Delta\text{gh2-1}$  strains.**

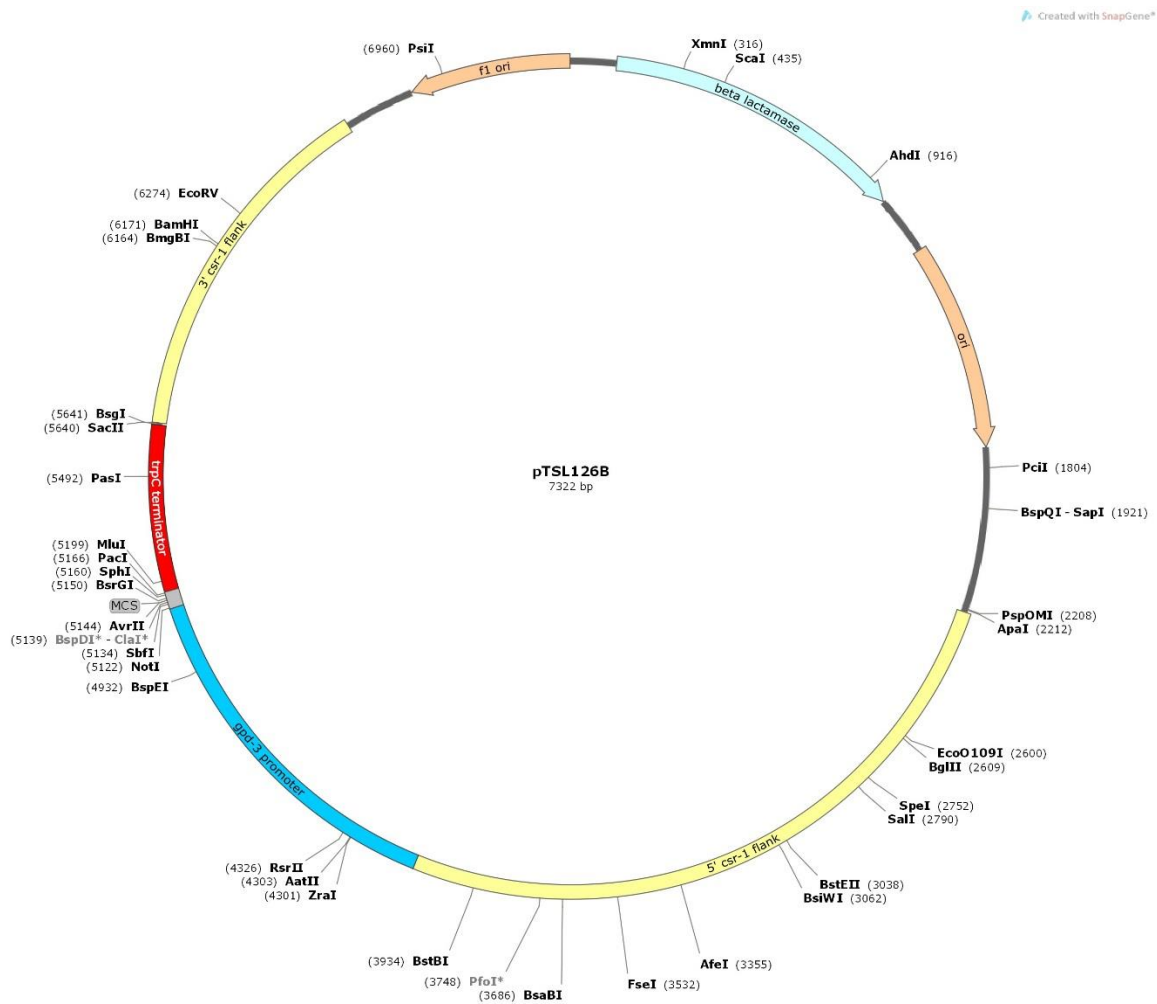
**(A)** CMCase activity of enzymes secreted into WT and  $\Delta\text{gh2-1}$  culture supernatants after 3 days of growth in 1% (w/v) powdered biomass with 1x Vogel's salts. **(B)** The concentration of secreted protein into culture supernatants. (M: Miscanthus, Ch: chestnut, O: oak, L: locust, P: pine, Ce: cedar, S: spruce and F: fir). Error bars represent standard deviations (n=3).



**SFigure 6-5. Analysis of the intracellular sugars of *N. crassa* WT,  $\Delta gh2-1$ ,  $\Delta gh1-1$ , and  $\Delta gh2-1$ ,  $\Delta gh1-1$  strains by NMR.**

2D-[ $^1\text{H}^{13}\text{C}$ ]-HSQC spectra for the anomeric region of the extracted intracellular sugars of the mycelia of WT,  $\Delta gh2-1$ ,  $\Delta gh1-1$ , and  $\Delta gh2-1$ ,  $\Delta gh1-1$  strains after growth in 2% (w/v) Avicel for 24 h. The spectra were measured at 25 °C for 24 h on a 950 MHz Bruker spectrometer and normalized to the signal marked with a red asterisk.  $\beta$ -D-GlcpI: glucose as part of  $\beta$ -1,4-polymer,  $\beta$ -D-GlcpR: reducing-end  $\beta$ -glucopyranosyl,  $\beta$ -D-ManpI: mannose as part of  $\beta$ -1,4-polymer, and  $\alpha/\beta$ -D-ManpR: reducing-end  $\alpha/\beta$ -mannopyranosyl.

## 6.4. Plasmid card



**SFigure 6-6. Map of pTSL126B plasmid.**

The important features of the plasmid are the 5' and 3' flanking regions of *csr-1*. This allow the cloning construct to be place into the *csr-1* locus by homologous recombination. Thus, the disruption of the *csr-1* gene in *N. crassa* cause its resistance to Cyclosporin A. The gene to be expressed in *N. crassa* is placed under the control of the constitutive promoter *gpd-3*. A MCS (multiple cloning site) and *trpC* terminator are also present within the 5' and 3' flanking regions of *csr-1*. Ampicillin resistance is another important feature and it is provided by the  $\beta$ -lactamase gene.

---

## References

1. Adel A. M., El-Wahab Z. H. A., Ibrahim A. A., Al-Shemy M. T. 2011. Characterization of microcrystalline cellulose prepared from lignocellulosic materials. Part II: Physicochemical properties. *Carbohydrate Polymers* 83:676-687.
2. Agrawal R., Satlewal A., Sharma B., Mathur A., Gupta R., Tuli D., Adsul M. 2017. Induction of cellulases by disaccharides or their derivatives in *Penicillium janthinellum* EMS-UV-8 mutant. *Biofuels* 8:615-622.
3. Alazi E., Niu J., Kowalczyk J. E., Peng M., Aguilar Pontes M. V., Van Kan J. A., Visser J., De Vries R. P., Ram A. F. 2016. The transcriptional activator GaaR of *Aspergillus niger* is required for release and utilization of D-galacturonic acid from pectin. *FEBS letters* 590:1804-1815.
4. Amore A., Giacobbe S., Faraco V. 2013. Regulation of cellulase and hemicellulase gene expression in fungi. *Current genomics* 14:230-249.
5. Antoniêto A. C. C., dos Santos Castro L., Silva-Rocha R., Persinoti G. F., Silva R. N. 2014. Defining the genome-wide role of CRE1 during carbon catabolite repression in *Trichoderma reesei* using RNA-Seq analysis. *Fungal genetics and biology* 73:93-103.
6. Arantes V., Saddler J. N. 2010. Access to cellulose limits the efficiency of enzymatic hydrolysis: the role of amorphogenesis. *Biotechnology for biofuels* 3:4.
7. Arevalo-Gallegos A., Ahmad Z., Asgher M., Parra-Saldivar R., Iqbal H. M. 2017. Lignocellulose: a sustainable material to produce value-added products with a zero waste approach - a review. *International journal of biological macromolecules* 99:308-318.
8. Aro N., Ilmén M., Saloheimo A., Penttilä M. 2003. ACEI of *Trichoderma reesei* is a repressor of cellulase and xylanase expression. *Appl Environ Microbiol* 69:56-65.
9. Aro N., Pakula T., Penttilä M. 2005. Transcriptional regulation of plant cell wall degradation by filamentous fungi. *FEMS microbiology reviews* 29:719-739.
10. Aro N., Saloheimo A., Ilmén M., Penttilä M. 2001. ACEII, a novel transcriptional activator involved in regulation of cellulase and xylanase genes of *Trichoderma reesei*. *Journal of Biological Chemistry* 276:24309-24314.
11. Baehr M., Puls J. 1991. Molecular weight distribution, hemicellulose content and batch conformity of pharmaceutical cellulose powders. *European Journal of Pharmaceutics and Biopharmaceutics (Germany, FR)*.
12. Bailey C., Arst H. N. 1975. Carbon catabolite repression in *Aspergillus nidulans*. *The FEBS Journal* 51:573-577.
13. Bastawde K. 1992. Xylan structure, microbial xylanases, and their mode of action. *World Journal of Microbiology and Biotechnology* 8:353-368.
14. Bationo A., Mokwunye A. 1991. Role of manures and crop residue in alleviating soil fertility constraints to crop production: With special reference to the Sahelian and Sudanian zones of West Africa. *Fertilizer research* 29:117-125.
15. Battaglia E., Hansen S. F., Leendertse A., Madrid S., Mulder H., Nikolaev I., de Vries R. P. 2011. Regulation of pentose utilisation by AraR, but not XlnR, differs in *Aspergillus nidulans* and *Aspergillus niger*. *Applied microbiology and biotechnology* 91:387-397.
16. Battista O. A., Smith P. A. 1961. Level-off DP cellulose products. Google Patents.
17. Bauer S., Sorek H., Mitchell V. D., Ibáñez A. B., Wemmer D. E. 2012. Characterization of *Miscanthus giganteus* lignin isolated by ethanol organosolv process under reflux condition. *Journal of agricultural and food chemistry* 60:8203-8212.
18. Bayer E. A., Chanzy H., Lamed R., Shoham Y. 1998. Cellulose, cellulases and cellulosomes. *Current opinion in structural biology* 8:548-557.

19. Beadle G. W., Tatum E. L. 1941. Genetic control of biochemical reactions in *Neurospora*. Proceedings of the National Academy of Sciences of the United States of America 27:499.
20. Benocci T., Aguilar-Pontes M. V., Zhou M., Seiboth B., Vries R. P. 2017. Regulators of plant biomass degradation in ascomycetous fungi. Biotechnology for biofuels 10:152.
21. Benocci T., Aguilar-Pontes M. V., Kun R. S., Seiboth B., de Vries R. P., Daly P. 2018. ARA1 regulates not only l-arabinose but also d-galactose catabolism in *Trichoderma reesei*. FEBS letters 592:60-70.
22. Benz J. P., Chau B. H., Zheng D., Bauer S., Glass N. L., Somerville C. R. 2014. A comparative systems analysis of polysaccharide-elicited responses in *Neurospora crassa* reveals carbon source-specific cellular adaptations. Mol Microbiol 91:275-99.
23. Benz J. P., Chau B. H., Zheng D., Bauer S., Glass N. L., Somerville C. R. 2014. A comparative systems analysis of polysaccharide-elicited responses in *Neurospora crassa* reveals carbon source-specific cellular adaptations. Molecular microbiology 91:275-299.
24. Benz J. P., Protzko R. J., Andrich J. M., Bauer S., Dueber J. E., Somerville C. R. 2014. Identification and characterization of a galacturonic acid transporter from *Neurospora crassa* and its application for *Saccharomyces cerevisiae* fermentation processes. Biotechnol Biofuels 7:20.
25. Bertani G. 1951. Studies on lysogenesis I.: the mode of phage liberation by lysogenic *Escherichia coli*1. Journal of bacteriology 62:293.
26. Bhattacharya A. S., Bhattacharya A., Pletschke B. I. 2015. Synergism of fungal and bacterial cellulases and hemicellulases: a novel perspective for enhanced bio-ethanol production. Biotechnology letters 37:1117-1129.
27. Bischof R., Fournis L., Limbeck A., Gamauf C., Seiboth B., Kubicek C. P. 2013. Comparative analysis of the *Trichoderma reesei* transcriptome during growth on the cellulase inducing substrates wheat straw and lactose. Biotechnology for biofuels 6:127.
28. Bornhorst J. A., Falke J. J. 2000. [16] Purification of proteins using polyhistidine affinity tags, p 245-254, Methods in enzymology, vol 326. Elsevier.
29. Brown N. A., De Gouvea P. F., Krohn N. G., Savoldi M., Goldman G. H. 2013. Functional characterisation of the non-essential protein kinases and phosphatases regulating *Aspergillus nidulans* hydrolytic enzyme production. Biotechnology for biofuels 6:91.
30. Brunauer S., Emmett P. H., Teller E. 1938. Adsorption of gases in multimolecular layers. Journal of the American chemical society 60:309-319.
31. Cai P., Gu R., Wang B., Li J., Wan L., Tian C., Ma Y. 2014. Evidence of a critical role for cellodextrin transport 2 (CDT-2) in both cellulose and hemicellulose degradation and utilization in *Neurospora crassa*. PLoS One 9:e89330.
32. Carpita N. C., Defernez M., Findlay K., Wells B., Shoue D. A., Catchpole G., Wilson R. H., McCann M. C. 2001. Cell wall architecture of the elongating maize coleoptile. Plant physiology 127:551-565.
33. Carrard G., Koivula A., Söderlund H., Béguin P. 2000. Cellulose-binding domains promote hydrolysis of different sites on crystalline cellulose. Proceedings of the National Academy of Sciences 97:10342-10347.
34. Chen S., Xiong B., Wei L., Wang Y., Yang Y., Liu Y., Zhang D., Guo S., Liu Q., Fang H. 2018. The Model Filamentous Fungus *Neurospora crassa*: Progress Toward a Systems Understanding of Plant Cell Wall Deconstruction, p 107-134, Fungal Cellulolytic Enzymes. Springer.
35. Chen Y., Stipanovic A. J., Winter W. T., Wilson D. B., Kim Y.-J. 2007. Effect of digestion by pure cellulases on crystallinity and average chain length for bacterial and microcrystalline celluloses. Cellulose 14:283.
36. Cheng L., Hu X., Gu Z., Hong Y., Li Z., Li C. 2019. Characterization of physicochemical properties of cellulose from potato pulp and their effects on

- enzymatic hydrolysis by cellulase. International journal of biological macromolecules.
37. Chhabra S., Parker K. N., Lam D., Callen W., Snead M. A., Mathur E. J., Short J. M., Kelly R. M. 2001.  $\beta$ -Mannanases from *Thermotoga* species, p 224-238, Methods in enzymology, vol 330. Elsevier.
  38. Chundawat S. P., Bellesia G., Uppugundla N., da Costa Sousa L., Gao D., Cheh A. M., Agarwal U. P., Bianchetti C. M., Phillips G. N., Jr., Langan P., Balan V., Gnanakaran S., Dale B. E. 2011. Restructuring the crystalline cellulose hydrogen bond network enhances its depolymerization rate. *J Am Chem Soc* 133:11163-74.
  39. Collins T., Gerday C., Feller G. 2005. Xylanases, xylanase families and extremophilic xylanases. *FEMS microbiology reviews* 29:3-23.
  40. Colot H. V., Park G., Turner G. E., Ringelberg C., Crew C. M., Litvinkova L., Weiss R. L., Borkovich K. A., Dunlap J. C. 2006. A high-throughput gene knockout procedure for *Neurospora* reveals functions for multiple transcription factors. *Proceedings of the National Academy of Sciences* 103:10352-10357.
  41. Converse A., Ooshima H., Burns D. 1990. Kinetics of enzymatic hydrolysis of lignocellulosic materials based on surface area of cellulose accessible to enzyme and enzyme adsorption on lignin and cellulose. *Applied Biochemistry and Biotechnology* 24:67-73.
  42. Coradetti S. T., Craig J. P., Xiong Y., Shock T., Tian C., Glass N. L. 2012. Conserved and essential transcription factors for cellulase gene expression in ascomycete fungi. *Proc Natl Acad Sci U S A* 109:7397-402.
  43. Coradetti S. T., Xiong Y., Glass N. L. 2013. Analysis of a conserved cellulase transcriptional regulator reveals inducer-independent production of cellulolytic enzymes in *Neurospora crassa*. *Microbiologyopen* 2:595-609.
  44. Craig J. P., Coradetti S. T., Starr T. L., Glass N. L. 2015. Direct target network of the *Neurospora crassa* plant cell wall deconstruction regulators CLR-1, CLR-2, and XLR-1. *MBio* 6:e01452-15.
  45. Cullen D. 2007. The genome of an industrial workhorse. *Nature biotechnology* 25:189.
  46. Daly P., van Munster J. M., Raulo R., Archer D. B. 2016. Transcriptional regulation and responses in filamentous fungi exposed to lignocellulose. Silva R, editor *Fungal Biotechnology for Biofuels Sharjah, UAE: Bentham ebooks*:82-127.
  47. Davis R. H., Perkins D. D. 2002. *Neurospora*: a model of model microbes. *Nature Reviews Genetics* 3:397.
  48. De Assis L. J., Ries L. N. A., Savoldi M., Dos Reis T. F., Brown N. A., Goldman G. H. 2015. *Aspergillus nidulans* protein kinase A plays an important role in cellulase production. *Biotechnology for biofuels* 8:213.
  49. de la Serna I., Ng D., Tyler B. M. 1999. Carbon regulation of ribosomal genes in *Neurospora crassa* occurs by a mechanism which does not require Cre-1, the homologue of the *Aspergillus* carbon catabolite repressor, CreA. *Fungal Genetics and Biology* 26:253-269.
  50. de Paula R. G., Antoniêto A. C. C., Carraro C. B., Lopes D. C. B., Persinoti G. F., Peres N. T. A., Martinez-Rossi N. M., Silva-Rocha R., Silva R. N. 2018. The Duality of the MAPK Signaling Pathway in the Control of Metabolic Processes and Cellulase Production in *Trichoderma reesei*. *Scientific reports* 8:14931.
  51. de Vries R. P., Jansen J., Aguilar G., Pařenicová L., Joosten V., Wulfert F., Benen J. A., Visser J. 2002. Expression profiling of pectinolytic genes from *Aspergillus niger*. *FEBS letters* 530:41-47.
  52. de Vries R. P., Visser J., de Graaff L. H. 1999. CreA modulates the XlnR-induced expression on xylose of *Aspergillus niger* genes involved in xylan degradation. *Research in Microbiology* 150:281-285.
  53. Delmas S., Pullan S. T., Gaddipati S., Kokolski M., Malla S., Blythe M. J., Ibbett R., Campbell M., Liddell S., Aboobaker A. 2012. Uncovering the genome-wide

- transcriptional responses of the filamentous fungus *Aspergillus niger* to lignocellulose using RNA sequencing. *PLoS genetics* 8:e1002875.
54. Demirbas A. 2009. Biofuels securing the planet's future energy needs. *Energy conversion and management* 50:2239-2249.
  55. Demirbas A., Arin G. 2002. An overview of biomass pyrolysis. *Energy sources* 24:471-482.
  56. Diallinas G. 2017. Transceptors as a functional link of transporters and receptors. *Microbial Cell* 4:69.
  57. Diderich J. A., MacCABE A. P., HERERRO O., RUIJTER G. J., VISSER J. 2004. *Aspergillus niger* mstA encodes a high-affinity sugar/H<sup>+</sup> symporter which is regulated in response to extracellular pH. *Biochemical Journal* 379:375-383.
  58. Ding S.-Y., Himmel M. E. 2006. The maize primary cell wall microfibril: a new model derived from direct visualization. *Journal of Agricultural and Food Chemistry* 54:597-606.
  59. dos Reis T. F., de Lima P. B. A., Parachin N. S., Mingossi F. B., de Castro Oliveira J. V., Ries L. N. A., Goldman G. H. 2016. Identification and characterization of putative xylose and cellobiose transporters in *Aspergillus nidulans*. *Biotechnology for biofuels* 9:204.
  60. dos Santos Castro L., de Paula R. G., Antoniêto A. C., Persinoti G. F., Silva-Rocha R., Silva R. N. 2016. Understanding the role of the master regulator XYR1 in *Trichoderma reesei* by global transcriptional analysis. *Frontiers in microbiology* 7:175.
  61. Dunlap J. C., Borkovich K. A., Henn M. R., Turner G. E., Sachs M. S., Glass N. L., McCluskey K., Plamann M., Galagan J. E., Birren B. W. 2007. Enabling a community to dissect an organism: overview of the *Neurospora* functional genomics project. *Advances in genetics* 57:49-96.
  62. Ebbole D. J. 1998. Carbon catabolite repression of gene expression and conidiation in *Neurospora crassa*. *Fungal Genetics and Biology* 25:15-21.
  63. Ebringerova A., Heinze T. 2000. Xylan and xylan derivatives—biopolymers with valuable properties, 1. Naturally occurring xylans structures, isolation procedures and properties. *Macromolecular rapid communications* 21:542-556.
  64. Eneyskaya E. V., Sundqvist G., Golubev A. M., Ibatullin F. M., Ivanen D. R., Shabalin K. A., Brumer H., Kulminskaya A. A. 2009. Transglycosylating and hydrolytic activities of the  $\beta$ -mannosidase from *Trichoderma reesei*. *Biochimie* 91:632-638.
  65. Fan L., Lee Y. H., Beardmore D. H. 1980. Mechanism of the enzymatic hydrolysis of cellulose: effects of major structural features of cellulose on enzymatic hydrolysis. *Biotechnology and Bioengineering* 22:177-199.
  66. Fan L. T. L. Y. H. B., David 1981. The influence of major structural features of cellulose on rate of enzymatic hydrolysis. *Biotechnology and Bioengineering* 23: 419-424.
  67. Fitzpatrick D. A., Logue M. E., Stajich J. E., Butler G. 2006. A fungal phylogeny based on 42 complete genomes derived from supertree and combined gene analysis. *BMC evolutionary biology* 6:99.
  68. Forment J. V., Flipphi M., Ramón D., Ventura L., MacCabe A. P. 2006. Identification of the mstE gene encoding a glucose-inducible, low affinity glucose transporter in *Aspergillus nidulans*. *Journal of Biological Chemistry* 281:8339-8346.
  69. Forment J. V., Flipphi M., Ventura L., González R., Ramón D., MacCabe A. P. 2014. High-affinity glucose transport in *Aspergillus nidulans* is mediated by the products of two related but differentially expressed genes. *PLoS One* 9:e94662.
  70. Fox J. M., Levine S. E., Clark D. S., Blanch H. W. 2011. Initial-and processive-cut products reveal cellobiohydrolase rate limitations and the role of companion enzymes. *Biochemistry* 51:442-452.
  71. Frey-Wyssling A. 1954. The fine structure of cellulose microfibrils. *Science* 119:80-82.

72. Galagan J. E., Calvo S. E., Borkovich K. A., Selker E. U., Read N. D., Jaffe D., FitzHugh W., Ma L.-J., Smirnov S., Purcell S. 2003. The genome sequence of the filamentous fungus *Neurospora crassa*. *Nature* 422:859.
73. Galazka J. M., Tian C., Beeson W. T., Martinez B., Glass N. L., Cate J. H. 2010. Cellodextrin transport in yeast for improved biofuel production. *Science* 330:84-6.
74. Galbe M., Zacchi G. 2002. A review of the production of ethanol from softwood. *Applied microbiology and biotechnology* 59:618-628.
75. Gancedo J. M. 1998. Yeast carbon catabolite repression. *Microbiol Mol Biol Rev* 62:334-361.
76. Gardner K., Blackwell J. 1974. The structure of native cellulose. *Biopolymers: Original Research on Biomolecules* 13:1975-2001.
77. Gibson L. J. 2012. The hierarchical structure and mechanics of plant materials. *Journal of the royal society interface* 9:2749-2766.
78. Gielkens M. M., Dekkers E., Visser J., de Graaff L. H. 1999. Two cellobiohydrolase-encoding genes from *Aspergillus niger* require D-xylose and the xylanolytic transcriptional activator XlnR for their expression. *Appl Environ Microbiol* 65:4340-4345.
79. Gielkens M. M., Dekkers E., Visser J., de Graaff L. H. 1999. Two cellobiohydrolase-encoding genes from *Aspergillus niger* require D-xylose and the xylanolytic transcriptional activator XlnR for their expression. *Applied and Environmental Microbiology* 65:4340-4345.
80. Gladieux P., Wilson B. A., Perraudeau F., Montoya L. A., Kowbel D., Hann-Soden C., Fischer M., Sylvain I., Jacobson D. J., Taylor J. W. 2015. Genomic sequencing reveals historical, demographic and selective factors associated with the diversification of the fire-associated fungus *Neurospora discreta*. *Molecular ecology* 24:5657-5675.
81. Glass N. L., Schmoll M., Cate J. H., Coradetti S. 2013. Plant cell wall deconstruction by ascomycete fungi. *Annu Rev Microbiol* 67:477-98.
82. Goto C. E., Barbosa E. P., Kistner L. s. C., Moreira F. G., Lenartovicz V., Peralta R. M. 1998. Production of amylase by *Aspergillus fumigatus* utilizing  $\alpha$ -methyl-D-glycoside, a synthetic analogue of maltose, as substrate. *FEMS microbiology letters* 167:139-143.
83. Goyal A., Ghosh B., Eveleigh D. 1991. Characteristics of fungal cellulases. *Bioresource Technology* 36:37-50.
84. Gruben B. S., Mäkelä M. R., Kowalczyk J. E., Zhou M., Benoit-Gelber I., De Vries R. P. 2017. Expression-based clustering of CAZyme-encoding genes of *Aspergillus niger*. *BMC genomics* 18:900.
85. Gruben B. S., Zhou M., Wiebenga A., Ballering J., Overkamp K. M., Punt P. J., De Vries R. P. 2014. *Aspergillus niger* RhaR, a regulator involved in L-rhamnose release and catabolism. *Applied microbiology and biotechnology* 98:5531-5540.
86. Habibi Y., Lucia L. A., Rojas O. J. 2010. Cellulose nanocrystals: chemistry, self-assembly, and applications. *Chemical reviews* 110:3479-3500.
87. Häkkinen M., Arvas M., Oja M., Aro N., Penttilä M., Saloheimo M., Pakula T. M. 2012. Re-annotation of the CAZy genes of *Trichoderma reesei* and transcription in the presence of lignocellulosic substrates. *Microbial cell factories* 11:134.
88. Hakkinen M., Valkonen M. J., Westerholm-Parvinen A., Aro N., Arvas M., Vitikainen M., Penttilä M., Saloheimo M., Pakula T. M. 2014. Screening of candidate regulators for cellulase and hemicellulase production in *Trichoderma reesei* and identification of a factor essential for cellulase production. *Biotechnol Biofuels* 7:14.
89. Häkkinen M., Valkonen M. J., Westerholm-Parvinen A., Aro N., Arvas M., Vitikainen M., Penttilä M., Saloheimo M., Pakula T. M. 2014. Screening of candidate regulators for cellulase and hemicellulase production in *Trichoderma reesei* and identification of a factor essential for cellulase production. *Biotechnology for biofuels* 7:14.
90. Hall M., Bansal P., Lee J. H., Realff M. J., Bommarius A. S. 2010. Cellulose crystallinity--a key predictor of the enzymatic hydrolysis rate. *Febs j* 277:1571-82.

91. Hall M., Bansal P., Lee J. H., Realf M. J., Bommarium A. S. 2010. Cellulose crystallinity—a key predictor of the enzymatic hydrolysis rate. *The FEBS journal* 277:1571-1582.
92. Haltrich D., Sebesta B., Steiner W. Induction of xylanase and cellulase in *Schizophyllum commune*, p 305-318. *In* (ed), ACS Publications,
93. Hanahan D. 1983. Studies on transformation of *Escherichia coli* with plasmids. *Journal of molecular biology* 166:557-580.
94. Hanna M., Biby G., Miladinov V. 2001. Production of microcrystalline cellulose by reactive extrusion. Google Patents.
95. Harada H C. W. 1985. Structure of wood. Orlando: Academic Press Biosynthesis and biodegradation of wood components:1–42.
96. Hasper A. A., Trindade L. M., van der Veen D., van Ooyen A. J., de Graaff L. H. 2004. Functional analysis of the transcriptional activator XlnR from *Aspergillus niger*. *Microbiology* 150:1367-1375.
97. Hassan L., Lin L., Sorek H., Goudoulas T., Germann N., Tian C., Benz J. P. 2019. Cross-talk of cellulose and mannan perception pathways leads to inhibition of cellulase production in several filamentous fungi. *bioRxiv*:520130.
98. Hassan L., Lin L., Sorek H., Sperl L. E., Goudoulas T., Hagn F., Germann N., Tian C., Benz J. P. 2019. Crosstalk of cellulose and mannan perception pathways leads to inhibition of cellulase production in several Filamentous fungi. *MBio* 10:e00277-19.
99. Hassan L., Reppke M. J., Thieme N., Schweizer S. A., Mueller C. W., Benz J. P. 2017. Comparing the physiochemical parameters of three celluloses reveals new insights into substrate suitability for fungal enzyme production. *Fungal Biology and Biotechnology* 4:10.
100. Hatakeyama H., Hatakeyama T. 2009. Lignin structure, properties, and applications, p 1-63, *Biopolymers*. Springer.
101. Hatti-Kaul R., Törnvall U., Gustafsson L., Börjesson P. 2007. Industrial biotechnology for the production of bio-based chemicals—a cradle-to-grave perspective. *Trends in biotechnology* 25:119-124.
102. Henrissat B. 1994. Cellulases and their interaction with cellulose. *Cellulose* 1:169-196.
103. Herlet J., Kornberger P., Roessler B., Glanz J., Schwarz W., Liebl W., Zverlov V. 2017. A new method to evaluate temperature vs. pH activity profiles for biotechnological relevant enzymes. *Biotechnology for biofuels* 10:234.
104. Herold S., Bischof R., Metz B., Seiboth B., Kubicek C. P. 2013. Xylanase gene transcription in *Trichoderma reesei* is triggered by different inducers representing different hemicellulosic pentose polymers. *Eukaryotic cell* 12:390-398.
105. Himmel M. E., Ding S.-Y., Johnson D. K., Adney W. S., Nimlos M. R., Brady J. W., Foust T. D. 2007. Biomass recalcitrance: engineering plants and enzymes for biofuels production. *science* 315:804-807.
106. Horii F., Hirai A., Kitamaru R. 1984. CP/MAS carbon-13 NMR study of spin relaxation phenomena of cellulose containing crystalline and noncrystalline components. *Journal of Carbohydrate Chemistry* 3:641-662.
107. Horn S. J., Vaaje-Kolstad G., Westereng B., Eijsink V. 2012. Novel enzymes for the degradation of cellulose. *Biotechnology for biofuels* 5:45.
108. Hosoo Y., Yoshida M., Imai T., Okuyama T. 2002. Diurnal difference in the amount of immunogold-labeled glucomannans detected with field emission scanning electron microscopy at the innermost surface of developing secondary walls of differentiating conifer tracheids. *Planta* 215:1006-1012.
109. Hrmová M., Petráková E., Biely P. 1991. Induction of cellulose- and xylan-degrading enzyme systems in *Aspergillus terreus* by homo- and heterodisaccharides composed of glucose and xylose. *Microbiology* 137:541-547.

110. Huang T. T., Wages J. M. 2016. New-to-nature sophorose analog: a potent inducer for gene expression in *Trichoderma reesei*. *Enzyme and microbial technology* 85:44-50.
111. Huang Z.-B., Chen X.-Z., Qin L.-N., Wu H.-Q., Su X.-Y., Dong Z.-Y. 2015. A novel major facilitator transporter TrSTR1 is essential for pentose utilization and involved in xylanase induction in *Trichoderma reesei*. *Biochemical and biophysical research communications* 460:663-669.
112. Huberman L. B., Coradetti S. T., Glass N. L. 2017. Network of nutrient-sensing pathways and a conserved kinase cascade integrate osmolarity and carbon sensing in *Neurospora crassa*. *Proceedings of the National Academy of Sciences* 114:E8665-E8674.
113. Huberman L. B., Liu J., Qin L., Glass N. L. 2016. Regulation of the lignocellulolytic response in filamentous fungi. *Fungal Biology Reviews* 30:101-111.
114. Ilmen M., Thrane C., Penttilä M. 1996. The glucose repressor *genecre1* of *Trichoderma*: Isolation and expression of a full-length and a truncated mutant form. *Molecular and General Genetics MGG* 251:451-460.
115. Inc. P. T. 2015. Collaborative data science, 2015 ed. Plotly Technologies Inc. , Montreal, QC.
116. Isikgor F. H., Becer C. R. 2015. Lignocellulosic biomass: a sustainable platform for the production of bio-based chemicals and polymers. *Polymer Chemistry* 6:4497-4559.
117. Ivanova C., Bååth J. A., Seiboth B., Kubicek C. P. 2013. Systems analysis of lactose metabolism in *Trichoderma reesei* identifies a lactose permease that is essential for cellulase induction. *PloS one* 8:e62631.
118. Jacobson D. J., Powell A. J., Dettman J. R., Saenz G. S., Barton M. M., Hiltz M. D., Dvorachek Jr W. H., Glass N. L., Taylor J. W., Natvig D. O. 2004. *Neurospora* in temperate forests of western North America. *Mycologia* 96:66-74.
119. Joseleau J.-P., Pérez S. 2016. The Plant Cell Walls: Complex Polysaccharide Nano-Composites.
120. Kankipati H. N., Rubio-Teixeira M., Castermans D., Diallinas G., Thevelein J. M. 2015. Sul1 and Sul2 sulfate transceptors signal to protein kinase A upon exit of sulfur starvation. *Journal of Biological Chemistry* 290:10430-10446.
121. Karaffa L., Fekete E., Gamauf C., Szentirmai A., Kubicek C. P., Seiboth B. 2006. D-Galactose induces cellulase gene expression in *Hypocrea jecorina* at low growth rates. *Microbiology* 152:1507-1514.
122. Karimi K., Taherzadeh M. J. 2016. A critical review on analysis in pretreatment of lignocelluloses: degree of polymerization, adsorption/desorption, and accessibility. *Bioresource Technology* 203:348-356.
123. Kato K., Matsuda K. 1969. Studies on the chemical structure of konjac mannan: part I. Isolation and characterization of oligosaccharides from the partial acid hydrolyzate of the mannan. *Agricultural and Biological Chemistry* 33:1446-1453.
124. Kenney K. L., Smith W. A., Gresham G. L., Westover T. L. 2013. Understanding biomass feedstock variability. *Biofuels* 4:111-127.
125. Kim H., Lee W.-H., Galazka J. M., Cate J. H., Jin Y.-S. 2014. Analysis of cellodextrin transporters from *Neurospora crassa* in *Saccharomyces cerevisiae* for cellobiose fermentation. *Applied microbiology and biotechnology* 98:1087-1094.
126. Klaubauf S., Zhou M., Lebrun M. H., de Vries R. P., Battaglia E. 2016. A novel l-arabinose-responsive regulator discovered in the rice-blast fungus *Pyricularia oryzae* (*Magnaporthe oryzae*). *FEBS letters* 590:550-558.
127. Klemm D., Heublein B., Fink H. P., Bohn A. 2005. Cellulose: fascinating biopolymer and sustainable raw material. *Angewandte Chemie International Edition* 44:3358-3393.
128. Kojima Y., Várnai A., Ishida T., Sunagawa N., Petrovic D. M., Igarashi K., Jellison J., Goodell B., Alfredsen G., Westereng B. 2016. Characterization of an LPMO from the brown-rot fungus *Gloeophyllum trabeum* with broad xyloglucan specificity, and

- its action on cellulose-xyloglucan complexes. Applied and Environmental Microbiology:AEM. 01768-16.
129. Kothari N., Bhagia S., Zaher M., Pu Y., Mittal A., Yoo C. G., Himmel M. E., Ragauskas A., Kumar R., Wyman C. E. 2019. Cellulose hydrolysis by *Clostridium thermocellum* is agnostic to substrate structural properties in contrast to fungal cellulases. Green Chemistry.
  130. Kowalczyk J. E., Benoit I., de Vries R. P. 2014. Regulation of plant biomass utilization in *Aspergillus*, p 31-56, Advances in applied microbiology, vol 88. Elsevier.
  131. Kozikowski A. P., Sun H., Brognard J., Dennis P. A. 2003. Novel PI analogues selectively block activation of the pro-survival serine/threonine kinase Akt. Journal of the American Chemical Society 125:1144-1145.
  132. Kubicek C. P. 2012. Fungi and lignocellulosic biomass. John Wiley & Sons.
  133. Kubicek C. P. 2013. Systems biological approaches towards understanding cellulase production by *Trichoderma reesei*. Journal of biotechnology 163:133-142.
  134. Kubicek C. P., Mikus M., Schuster A., Schmoll M., Seiboth B. 2009. Metabolic engineering strategies for the improvement of cellulase production by *Hypocrea jecorina*. Biotechnology for biofuels 2:19.
  135. Kuhad R. C., Gupta R., Singh A. 2011. Microbial cellulases and their industrial applications. Enzyme research 2011.
  136. Kuhad R. C., Singh A. 1993. Lignocellulose biotechnology: current and future prospects. Critical Reviews in Biotechnology 13:151-172.
  137. Kumar R., Singh S., Singh O. V. 2008. Bioconversion of lignocellulosic biomass: biochemical and molecular perspectives. Journal of industrial microbiology & biotechnology 35:377-391.
  138. Kumar R., Wyman C. E. 2013. Physical and chemical features of pretreated biomass that influence macro-/micro-accessibility and biological processing. Aqueous pretreatment of plant biomass for biological and chemical conversion to fuels and chemicals:281-310.
  139. Kunitake E., Li Y., Uchida R., Nohara T., Asano K., Hattori A., Kimura T., Kanamaru K., Kimura M., Kobayashi T. 2019. CreA-independent carbon catabolite repression of cellulase genes by trimeric G-protein and protein kinase A in *Aspergillus nidulans*. Current genetics:1-12.
  140. Kuo H.-C., Hui S., Choi J., Asiegbu F. O., Valkonen J. P., Lee Y.-H. 2014. Secret lifestyles of *Neurospora crassa*. Scientific reports 4:5135.
  141. Kurasawa T., Yachi M., Suto M., Kamagata Y., Takao S., Tomita F. 1992. Induction of cellulase by gentiobiose and its sulfur-containing analog in *Penicillium purpurogenum*. Appl Environ Microbiol 58:106-110.
  142. Laca A., Laca A., Díaz M. 2019. Hydrolysis: From cellulose and hemicellulose to simple sugars, p 213-240, Second and Third Generation of Feedstocks. Elsevier.
  143. Lampugnani E. R., Khan G. A., Somssich M., Persson S. 2018. Building a plant cell wall at a glance. J Cell Sci 131:jcs207373.
  144. Landin M., Martinez-Pacheco R., Gomez-Amoza J., Souto C., Concheiro A., Rowe R. 1993. Effect of batch variation and source of pulp on the properties of microcrystalline cellulose. International journal of pharmaceuticals 91:133-141.
  145. Landin M., Martinez-Pacheco R., Gomez-Amoza J., Souto C., Concheiro A., Rowe R. 1993. Effect of country of origin on the properties of microcrystalline cellulose. International journal of pharmaceuticals 91:123-131.
  146. Le Crom S., Schackwitz W., Pennacchio L., Magnuson J. K., Culley D. E., Collett J. R., Martin J., Druzhinina I. S., Mathis H., Monot F., Seiboth B., Cherry B., Rey M., Berka R., Kubicek C. P., Baker S. E., Margeot A. 2009. Tracking the roots of cellulase hyperproduction by the fungus *Trichoderma reesei* using massively parallel DNA sequencing. Proc Natl Acad Sci U S A 106:16151-6.
  147. Lee S. B., Shin H., Ryu D. D., Mandels M. 1982. Adsorption of cellulase on cellulose: effect of physicochemical properties of cellulose on adsorption and rate of hydrolysis. Biotechnology and Bioengineering 24:2137-2153.

148. Lee W., Tonelli M., Markley J. L. 2014. NMRFAM-SPARKY: enhanced software for biomolecular NMR spectroscopy. *Bioinformatics* 31:1325-1327.
149. Levine S. E., Fox J. M., Blanch H. W., Clark D. S. 2010. A mechanistic model of the enzymatic hydrolysis of cellulose. *Biotechnology and bioengineering* 107:37-51.
150. Levy B. D., Lukacs N. W., Berlin A. A., Schmidt B., Guilford W. J., Serhan C. N., Parkinson J. F. 2007. Lipoxin A4 stable analogs reduce allergic airway responses via mechanisms distinct from CysLT1 receptor antagonism. *The FASEB Journal* 21:3877-3884.
151. Li J., Lin L., Li H., Tian C., Ma Y. 2014. Transcriptional comparison of the filamentous fungus *Neurospora crassa* growing on three major monosaccharides D-glucose, D-xylose and L-arabinose. *Biotechnol Biofuels* 7:31.
152. Li J., Lin L., Li H., Tian C., Ma Y. 2014. Transcriptional comparison of the filamentous fungus *Neurospora crassa* growing on three major monosaccharides D-glucose, D-xylose and L-arabinose. *Biotechnology for biofuels* 7:31.
153. Li J., Liu G., Chen M., Li Z., Qin Y., Qu Y. 2013. Cellodextrin transporters play important roles in cellulase induction in the cellulolytic fungus *Penicillium oxalicum*. *Applied microbiology and biotechnology* 97:10479-10488.
154. Li L., Zhou W., Wu H., Yu Y., Liu F., Zhu D. 2014. Relationship between crystallinity index and enzymatic hydrolysis performance of celluloses separated from aquatic and terrestrial plant materials. *BioResources* 9:3993-4005.
155. Linder M., Teeri T. T. 1997. The roles and function of cellulose-binding domains. *Journal of biotechnology* 57:15-28.
156. Liu Q., Gao R., Li J., Lin L., Zhao J., Sun W., Tian C. 2017. Development of a genome-editing CRISPR/Cas9 system in thermophilic fungal *Myceliophthora* species and its application to hyper-cellulase production strain engineering. *Biotechnology for biofuels* 10:1.
157. Liu Q., Li J., Gao R., Li J., Ma G., Tian C. 2019. CLR-4, a novel conserved transcription factor for cellulase gene expression in ascomycete fungi. *Molecular microbiology* 111:373-394.
158. Mach-Aigner A. R., Omony J., Jovanovic B., van Boxtel A. J., de Graaff L. H. 2012. D-Xylose concentration-dependent hydrolase expression profiles and the function of CreA and XlnR in *Aspergillus niger*. *Appl Environ Microbiol* 78:3145-3155.
159. Mach-Aigner A. R., Pucher M. E., Steiger M. G., Bauer G. E., Preis S. J., Mach R. L. 2008. Transcriptional regulation of *xyr1*, encoding the main regulator of the xylanolytic and cellulolytic enzyme system in *Hypocrea jecorina*. *Appl Environ Microbiol* 74:6554-6562.
160. Mach-Aigner A. R., Pucher M. E., Steiger M. G., Bauer G. E., Preis S. J., Mach R. L. 2008. Transcriptional regulation of *xyr1*, encoding the main regulator of the xylanolytic and cellulolytic enzyme system in *Hypocrea jecorina*. *Appl Environ Microbiol* 74:6554-62.
161. Mackie W., Shieldrick B., Akrigg D., Perez S. 1986. Crystal and molecular structure of mannotriose and its relationship to the conformations and packing of mannan and glucomannan chains and mannobiose. *International Journal of Biological Macromolecules* 8:43-51.
162. Maeda M., Shimahara H., Sugiyama N. 1980. Detailed examination of the branched structure of konjac glucomannan. *Agricultural and Biological Chemistry* 44:245-252.
163. Mandels M., Andreotti R. 1978. Problems and challenges in the cellulose to cellulase fermentation. *Process Biochemistry*.
164. Mandels M., Parrish F. W., Reese E. T. 1962. Sophorose as an inducer of cellulase in *Trichoderma viride*. *Journal of Bacteriology* 83:400-408.
165. Mandels M., Reese E. T. 1957. Induction of cellulase in *Trichoderma viride* as influenced by carbon sources and metals. *Journal of Bacteriology* 73:269.
166. Mandels M., Weber J., Parizek R. 1971. Enhanced cellulase production by a mutant of *Trichoderma viride*. *Applied microbiology* 21:152.

167. Mansfield S. D., Mooney C., Saddler J. N. 1999. Substrate and enzyme characteristics that limit cellulose hydrolysis. *Biotechnology progress* 15:804-816.
168. Marchessault R. H. a. S., P. R. 1983. In *Cellulose, in the Polysaccharides*. New York: Academic Press:11.
169. Martinez D., Berka R. M., Henrissat B., Saloheimo M., Arvas M., Baker S. E., Chapman J., Chertkov O., Coutinho P. M., Cullen D. 2008. Genome sequencing and analysis of the biomass-degrading fungus *Trichoderma reesei* (syn. *Hypocrea jecorina*). *Nature biotechnology* 26:553.
170. Marui J., Kitamoto N., Kato M., Kobayashi T., Tsukagoshi N. 2002. Transcriptional activator, AoXlnR, mediates cellulose-inductive expression of the xylanolytic and cellulolytic genes in *Aspergillus oryzae*. *FEBS letters* 528:279-282.
171. Matthews J. F., Skopec C. E., Mason P. E., Zuccato P., Torget R. W., Sugiyama J., Himmel M. E., Brady J. W. 2006. Computer simulation studies of microcrystalline cellulose I $\beta$ . *Carbohydrate research* 341:138-152.
172. McCluskey K., Wiest A., Plamann M. 2010. The Fungal Genetics Stock Center: a repository for 50 years of fungal genetics research. *Journal of biosciences* 35:119-126.
173. Meldrum B. 1985. Possible therapeutic applications of antagonists of excitatory amino acid neurotransmitters. *Clinical Science* 68:113-122.
174. Mello-de-Sousa T. M., Gorsche R., Rassinger A., Pocas-Fonseca M. J., Mach R. L., Mach-Aigner A. R. 2014. A truncated form of the Carbon catabolite repressor 1 increases cellulase production in *Trichoderma reesei*. *Biotechnol Biofuels* 7:129.
175. Melo I., Faull J., Graeme-Cook K. 1997. Relationship between in vitro cellulase production of UV-induced mutants of *Trichoderma harzianum* and their bean rhizosphere competence. *Mycological Research* 101:1389-1392.
176. Meyer V., Andersen M. R., Brakhage A. A., Braus G. H., Caddick M. X., Cairns T. C., de Vries R. P., Haarmann T., Hansen K., Hertz-Fowler C. 2016. Current challenges of research on filamentous fungi in relation to human welfare and a sustainable bio-economy: a white paper. *Fungal biology and biotechnology* 3:6.
177. Meyer V., Wu B., Ram A. F. 2011. *Aspergillus* as a multi-purpose cell factory: current status and perspectives. *Biotechnology letters* 33:469-476.
178. Mitchell V. D., Taylor C. M., Bauer S. 2014. Comprehensive analysis of monomeric phenolics in dilute acid plant hydrolysates. *BioEnergy Research* 7:654-669.
179. Mohnen D. 2008. Pectin structure and biosynthesis. *Current opinion in plant biology* 11:266-277.
180. Montenecourt B. S., Eveleigh D. E. 1977. Preparation of mutants of *Trichoderma reesei* with enhanced cellulase production. *Appl Environ Microbiol* 34:777-782.
181. Montenecourt B. S., Eveleigh D. E. 1977. Semiquantitative plate assay for determination of cellulase production by *Trichoderma viride*. *Appl Environ Microbiol* 33:178-183.
182. Mooney C. A., Mansfield S. D., Beatson R. P., Saddler J. N. 1999. The effect of fiber characteristics on hydrolysis and cellulase accessibility to softwood substrates. *Enzyme and Microbial Technology* 25:644-650.
183. Moreira F. G., Lenartovicz V., de Souza C. G., Ramos E. P., Peralta R. M. 2001. The use of alpha-methyl-D-glucoside, a synthetic analogue of maltose, as inducer of amylase by *Aspergillus* sp in solid-state and submerged fermentations. *Brazilian Journal of Microbiology* 32:15-19.
184. Moreira L. 2008. An overview of mannan structure and mannan-degrading enzyme systems. *Applied microbiology and biotechnology* 79:165.
185. Morris M. J., Striegel A. M. 2014. Determining the solution conformational entropy of oligosaccharides by SEC with on-line viscometry detection. *Carbohydrate polymers* 106:230-237.
186. Morris M. J., Striegel A. M. 2014. Influence of glycosidic linkage on the solution conformational entropy of gluco- and mannobioses. *Carbohydrate research* 398:31-35.

187. Mussatto S. I., Teixeira J. A. 2010. Lignocellulose as raw material in fermentation processes.
188. Naik S. N., Goud V. V., Rout P. K., Dalai A. K. 2010. Production of first and second generation biofuels: a comprehensive review. *Renewable and sustainable energy reviews* 14:578-597.
189. Nasser W., Condemine G., Plantier R., Anker D., Robert-Baudouy J. 1991. Inducing properties of analogs of 2-keto-3-deoxygluconate on the expression of pectinase genes of *Erwinia chrysanthemi*. *FEMS microbiology letters* 81:73-78.
190. Newman R., Hemmingson J. 1990. Determination of the degree of cellulose crystallinity in wood by carbon-13 nuclear magnetic resonance spectroscopy. *Holzforschung-International Journal of the Biology, Chemistry, Physics and Technology of Wood* 44:351-356.
191. Newman R. H. 1994. Crystalline forms of cellulose in softwoods and hardwoods. *Journal of wood chemistry and technology* 14:451-466.
192. Newman R. H. 2004. Homogeneity in cellulose crystallinity between samples of *Pinus radiata* wood. *Walter de Gruyter*.
193. Nigam P. S., Singh A. 2011. Production of liquid biofuels from renewable resources. *Progress in energy and combustion science* 37:52-68.
194. Noguchi Y., Sano M., Kanamaru K., Ko T., Takeuchi M., Kato M., Kobayashi T. 2009. Genes regulated by AoXlnR, the xylanolytic and cellulolytic transcriptional regulator, in *Aspergillus oryzae*. *Applied microbiology and biotechnology* 85:141.
195. O'sullivan A. C. 1997. Cellulose: the structure slowly unravels. *Cellulose* 4:173-207.
196. Ogawa M., Kobayashi T., Koyama Y. 2012. ManR, a novel Zn (II) 2 Cys 6 transcriptional activator, controls the  $\beta$ -mannan utilization system in *Aspergillus oryzae*. *Fungal genetics and biology* 49:987-995.
197. Ogawa M., Kobayashi T., Koyama Y. 2013. ManR, a transcriptional regulator of the  $\beta$ -mannan utilization system, controls the cellulose utilization system in *Aspergillus oryzae*. *Bioscience, biotechnology, and biochemistry* 77:426-429.
198. Öhgren K., Bura R., Saddler J., Zacchi G. 2007. Effect of hemicellulose and lignin removal on enzymatic hydrolysis of steam pretreated corn stover. *Bioresource technology* 98:2503-2510.
199. Paes G., Navarro D., Benoit Y., Blanquet S., Chabbert B., Chaussepied B., Coutinho P. M., Durand S., Grigoriev I. V., Haon M., Heux L., Launay C., Margeot A., Nishiyama Y., Raouche S., Rosso M. N., Bonnin E., Berrin J. G. 2019. Tracking of enzymatic biomass deconstruction by fungal secretomes highlights markers of lignocellulose recalcitrance. *Biotechnol Biofuels* 12:76.
200. Palmqvist B. 2014. Processing Lignocellulosic Biomass into Ethanol-Implications of High Solid Loadings. *Lund University*.
201. Paloheimo M., Haarmann T., Mäkinen S., Vehmaanperä J. 2016. Production of industrial enzymes in *Trichoderma reesei*, p 23-57, *Gene expression systems in fungi: advancements and applications*. Springer.
202. Park S., Baker J. O., Himmel M. E., Parilla P. A., Johnson D. K. 2010. Cellulose crystallinity index: measurement techniques and their impact on interpreting cellulase performance. *Biotechnology for biofuels* 3:10.
203. Payne C. M., Knott B. C., Mayes H. B., Hansson H., Himmel M. E., Sandgren M., Stahlberg J., Beckham G. T. 2015. Fungal cellulases. *Chemical reviews* 115:1308-1448.
204. Peciulyte A., Anasontzis G. E., Karlstrom K., Larsson P. T., Olsson L. 2014. Morphology and enzyme production of *Trichoderma reesei* Rut C-30 are affected by the physical and structural characteristics of cellulosic substrates. *Fungal Genet Biol* 72:64-72.
205. Peng H., Li H., Luo H., Xu J. 2013. A novel combined pretreatment of ball milling and microwave irradiation for enhancing enzymatic hydrolysis of microcrystalline cellulose. *Bioresource technology* 130:81-87.

206. PÉrez S., Samain D. 2010. Structure and engineering of celluloses, p 25-116, *Advances in carbohydrate chemistry and biochemistry*, vol 64. Elsevier.
207. Peters L., Walker L., Wilson D., Irwin D. 1991. The impact of initial particle size on the fragmentation of cellulose by the cellulase of *Thermomonospora fusca*. *Bioresource technology* 35:313-319.
208. Petersen T. N., Brunak S., Von Heijne G., Nielsen H. 2011. SignalP 4.0: discriminating signal peptides from transmembrane regions. *Nature methods* 8:785.
209. Peterson R., Nevalainen H. 2012. *Trichoderma reesei* RUT-C30--thirty years of strain improvement. *Microbiology* 158:58-68.
210. Pettersen R. C. 1984. The chemical composition of wood. Washington: American Chemical Society 207:57–126.
211. Phillips C. M., Beeson IV W. T., Cate J. H., Marletta M. A. 2011. Cellobiose dehydrogenase and a copper-dependent polysaccharide monooxygenase potentiate cellulose degradation by *Neurospora crassa*. *ACS chemical biology* 6:1399-1406.
212. Polizeli M., Rizzatti A., Monti R., Terenzi H., Jorge J. A., Amorim D. 2005. Xylanases from fungi: properties and industrial applications. *Applied microbiology and biotechnology* 67:577-591.
213. Portnoy T., Margeot A., Linke R., Atanasova L., Fekete E., Sándor E., Hartl L., Karaffa L., Druzhinina I. S., Seiboth B. 2011. The CRE1 carbon catabolite repressor of the fungus *Trichoderma reesei*: a master regulator of carbon assimilation. *BMC genomics* 12:269.
214. Portnoy T., Margeot A., Seidl-Seiboth V., Le Crom S., Chaabane F. B., Linke R., Seiboth B., Kubicek C. P. 2011. Differential regulation of the cellulase transcription factors XYR1, ACE2, and ACE1 in *Trichoderma reesei* strains producing high and low levels of cellulase. *Eukaryotic cell* 10:262-271.
215. Pu Y., Ziemer C., Ragauskas A. J. 2006. CP/MAS <sup>13</sup>C NMR analysis of cellulase treated bleached softwood kraft pulp. *Carbohydrate Research* 341:591-597.
216. Pullan S. T., Daly P., Delmas S., Ibbett R., Kokolski M., Neiteler A., van Munster J. M., Wilson R., Blythe M. J., Gaddipati S. 2014. RNA-sequencing reveals the complexities of the transcriptional response to lignocellulosic biofuel substrates in *Aspergillus niger*. *Fungal biology and biotechnology* 1:3.
217. Puri V. P. 1984. Effect of crystallinity and degree of polymerization of cellulose on enzymatic saccharification. *Biotechnology and Bioengineering* 26:1219-1222.
218. Qi F., Jing T., Zhan Y. 2012. Characterization of endophytic fungi from *Acer ginnala Maxim.* in an artificial plantation: media effect and tissue-dependent variation. *PLoS One* 7:e46785.
219. Ragauskas A. J., Williams C. K., Davison B. H., Britovsek G., Cairney J., Eckert C. A., Frederick W. J., Hallett J. P., Leak D. J., Liotta C. L. 2006. The path forward for biofuels and biomaterials. *science* 311:484-489.
220. Ramos L., Nazhad M., Saddler J. 1993. Effect of enzymatic hydrolysis on the morphology and fine structure of pretreated cellulosic residues. *Enzyme and Microbial Technology* 15:821-831.
221. Rangarajan M., Aduse-Opoku J., Hashim A., Paramonov N., Curtis M. A. 2013. Characterization of the  $\alpha$ - and  $\beta$ -mannosidases of *Porphyromonas gingivalis*. *Journal of bacteriology* 195:5297-5307.
222. Rassinger A., Gacek-Matthews A., Strauss J., Mach R. L., Mach-Aigner A. R. 2018. Truncation of the transcriptional repressor protein Cre1 in *Trichoderma reesei* Rut-C30 turns it into an activator. *Fungal biology and biotechnology* 5:15.
223. Raulo R., Kokolski M., Archer D. B. 2016. The roles of the zinc finger transcription factors XlnR, ClrA and ClrB in the breakdown of lignocellulose by *Aspergillus niger*. *Amb Express* 6:5.
224. Reese E. History of the cellulase program at the US army Natick Development Center, p. *In* (ed), Army Natick Development Center, MA,

225. Report. 2016. Technical Enzymes Market by Type (Cellulases, Amylases, Proteases, Lipases, Other Enzymes), Application (Bioethanol, Paper & Pulp, Textile & Leather, Starch Processing, Other Applications), & by Region - Global Forecasts to 2021., Markets Ra,
226. Rho D., Desrochers M., Jurasek L., Driguez H., Defaye J. 1982. Induction of cellulose in *Schizophyllum commune*: thiocellobiose as a new inducer. *Journal of bacteriology* 149:47-53.
227. Ribeiro L. F., Chelius C., Boppidi K. R., Naik N. S., Hossain S., Ramsey J. J., Kumar J., Ribeiro L. F., Ostermeier M., Tran B. 2019. Comprehensive Analysis of *Aspergillus nidulans* PKA Phosphorylome Identifies a Novel Mode of CreA Regulation. *mBio* 10:e02825-18.
228. Ries L. N., Beattie S. R., Espeso E. A., Cramer R. A., Goldman G. H. 2016. Diverse regulation of the CreA carbon catabolite repressor in *Aspergillus nidulans*. *Genetics* 203:335-352.
229. Ringpfeil M. 2001. Biobased industrial products and biorefinery systems— Industrielle Zukunft des 21 Jahrhunderts. *Brandenburgische Umwelt Berichte*.
230. Ritter S. K. 2008. Lignocellulose: A complex biomaterial. *Plant Biochemistry* 86:15.
231. Roche C. M., Glass N. L., Blanch H. W., Clark D. S. 2014. Engineering the filamentous fungus *Neurospora crassa* for lipid production from lignocellulosic biomass. *Biotechnology and bioengineering* 111:1097-1107.
232. Roche C. M., Loros J. J., McCluskey K., Glass N. L. 2014. *Neurospora crassa*: looking back and looking forward at a model microbe. *American journal of botany* 101:2022-2035.
233. Rollin J. A., Zhu Z., Sathitsuksanoh N., Zhang Y. H. P. 2011. Increasing cellulose accessibility is more important than removing lignin: A comparison of cellulose solvent-based lignocellulose fractionation and soaking in aqueous ammonia. *Biotechnology and bioengineering* 108:22-30.
234. Ronne H. 1995. Glucose repression in fungi. *Trends in Genetics* 11:12-17.
235. Rowe R., McKillop A., Bray D. 1994. The effect of batch and source variation on the crystallinity of microcrystalline cellulose. *International journal of pharmaceutics* 101:169-172.
236. Ruijter G. J., Visser J. 1997. Carbon repression in Aspergilli. *FEMS Microbiology Letters* 151:103-114.
237. Samal A., Craig J. P., Coradetti S. T., Benz J. P., Eddy J. A., Price N. D., Glass N. L. 2017. Network reconstruction and systems analysis of plant cell wall deconstruction by *Neurospora crassa*. *Biotechnol Biofuels* 10:225.
238. Sánchez C. 2009. Lignocellulosic residues: biodegradation and bioconversion by fungi. *Biotechnology advances* 27:185-194.
239. Sasaki T., Tanaka T., Nanbu N., Sato Y., Kainuma K. 1979. Correlation between X-ray diffraction measurements of cellulose crystalline structure and the susceptibility to microbial cellulase. *Biotechnology and Bioengineering* 21:1031-1042.
240. Scheller H. V., Ulvskov P. 2010. Hemicelluloses. *Annual review of plant biology* 61.
241. Schols H. A., Posthumus M. A., Voragen A. G. 1990. Structural features of hairy regions of pectins isolated from apple juice produced by the liquefaction process. *Carbohydrate Research* 206:117-129.
242. Schuster A., Schmoll M. 2010. Biology and biotechnology of *Trichoderma*. *Applied microbiology and biotechnology* 87:787-799.
243. Seibert T., Thieme N., Benz J. P. 2016. The renaissance of *Neurospora crassa*: how a classical model system is used for applied research, p 59-96, *Gene expression systems in fungi: advancements and applications*. Springer.
244. Seiboth B., Hofmann G., Kubicek C. 2002. Lactose metabolism and cellulase production in *Hypocrea jecorina*: the gal7 gene, encoding galactose-1-phosphate uridylyltransferase, is essential for growth on galactose but not for cellulase induction. *Molecular genetics and genomics* 267:124-132.

245. Seiboth B., Ivanova C., Seidl-Seiboth V. 2011. *Trichoderma reesei*: a fungal enzyme producer for cellulosic biofuels, Biofuel production-recent developments and prospects. InTech.
246. Seidl V., Gamauf C., Druzhinina I. S., Seiboth B., Hartl L., Kubicek C. P. 2008. The *Hypocrea jecorina* (*Trichoderma reesei*) hypercellulolytic mutant RUT C30 lacks a 85 kb (29 gene-encoding) region of the wild-type genome. BMC genomics 9:327.
247. Shiang M., Linden J. C., Mohagheghi A., Grohmann K., Himmel M. E. 1991. Regulation of cellulase synthesis in *Acidothermus cellulolyticus*. Biotechnology Progress 7:315-322.
248. Singhanian R. R., Agarwal R. A., Kumar R. P., Sukumaran R. K. 2017. Waste to Wealth. Springer.
249. Sinitsyn A., Gusakov A., Vlasenko E. Y. 1991. Effect of structural and physico-chemical features of cellulosic substrates on the efficiency of enzymatic hydrolysis. Applied Biochemistry and Biotechnology 30:43-59.
250. Sloothaak J., Odoni D. I., dos Santos V. A. M., Schaap P. J., Tamayo-Ramos J. A. 2016. Identification of a novel L-rhamnose uptake transporter in the filamentous fungus *Aspergillus niger*. PLoS genetics 12:e1006468.
251. Somerville C., Bauer S., Brininstool G., Facette M., Hamann T., Milne J., Osborne E., Paredez A., Persson S., Raab T. 2004. Toward a systems approach to understanding plant cell walls. Science 306:2206-2211.
252. Somerville C., Youngs H., Taylor C., Davis S. C., Long S. P. 2010. Feedstocks for lignocellulosic biofuels. science 329:790-792.
253. Sterk H., Sattler W., Janosi A., Paul D., Esterbauer H. 1987. Einsatz der Festkörper <sup>13</sup>C-NMR-Spektroskopie für die Bestimmung der Kristallinität in Cellulosen. Das Papier 41:664-667.
254. Sternberg D., Mandels G. R. 1979. Induction of cellulolytic enzymes in *Trichoderma reesei* by sophorose. Journal of bacteriology 139:761-769.
255. Strauss J., Mach R. L., Zeilinger S., Hartler G., Stöffler G., Wolschek M., Kubicek C. 1995. CreI, the carbon catabolite repressor protein from *Trichoderma reesei*. FEBS letters 376:103-107.
256. Stricker A. R., Grosstessner-Hain K., Würleitner E., Mach R. L. 2006. Xyr1 (xylanase regulator 1) regulates both the hydrolytic enzyme system and D-xylose metabolism in *Hypocrea jecorina*. Eukaryotic cell 5:2128-2137.
257. Stricker A. R., Mach R. L., De Graaff L. H. 2008. Regulation of transcription of cellulases-and hemicellulases-encoding genes in *Aspergillus niger* and *Hypocrea jecorina* (*Trichoderma reesei*). Applied microbiology and biotechnology 78:211.
258. Sun J., Glass N. L. 2011. Identification of the CRE-1 cellulolytic regulon in *Neurospora crassa*. PLoS One 6:e25654.
259. Sun J., Tian C., Diamond S., Glass N. L. 2012. Deciphering transcriptional regulatory mechanisms associated with hemicellulose degradation in *Neurospora crassa*. Eukaryot Cell 11:482-93.
260. Sun Y., Cheng J. 2002. Hydrolysis of lignocellulosic materials for ethanol production: a review. Bioresource technology 83:1-11.
261. Suto M., Yachi M., Kamagata Y., Sasaki H., Takao S., Tomita F. 1991. Cellulase induction by soluble acetyl cellobioses in *Penicillium purpurogenum*. Journal of fermentation and bioengineering 72:352-357.
262. Tamayo E. N., Villanueva A., Hasper A. A., de Graaff L. H., Ramón D., Orejas M. 2008. CreA mediates repression of the regulatory gene *xlnR* which controls the production of xylanolytic enzymes in *Aspergillus nidulans*. Fungal Genetics and Biology 45:984-993.
263. Tambellini N., Zarembek V., Turner R., Weljie A. 2013. Evaluation of extraction protocols for simultaneous polar and non-polar yeast metabolite analysis using multivariate projection methods. Metabolites 3:592-605.

- 
264. Tangnu S. K., Blanch H. W., Wilke C. R. 1981. Enhanced production of cellulase, hemicellulase, and  $\beta$ -glucosidase by *Trichoderma reesei* (Rut C-30). *Biotechnology and Bioengineering* 23:1837-1849.
265. Tani S., Kawaguchi T., Kobayashi T. 2014. Complex regulation of hydrolytic enzyme genes for cellulosic biomass degradation in filamentous fungi. *Applied microbiology and biotechnology* 98:4829-4837.
266. Team R. C. 2013. R: A language and environment for statistical computing.
267. Teramoto A., Fuchigami M. 2000. Changes in temperature, texture, and structure of Konnyaku (Konjac Glucomannan Gel) during high-pressure-freezing. *Journal of Food Science* 65:491-497.
268. Thieme N. 2019. Plant polysaccharide perception and its molecular regulation – with a focus on pectin degradation – in *Neurospora crassa* Technical University of Munich.
269. Thieme N., Wu V. W., Dietschmann A., Salamov A. A., Wang M., Johnson J., Singan V. R., Grigoriev I. V., Glass N. L., Somerville C. R. 2017. The transcription factor PDR-1 is a multi-functional regulator and key component of pectin deconstruction and catabolism in *Neurospora crassa*. *Biotechnology for biofuels* 10:149.
270. Thomas V. A., Kothari N., Bhagia S., Akinosho H., Li M., Pu Y., Yoo C. G., Pattathil S., Hahn M. G., Raguaskas A. J. 2017. Comparative evaluation of *Populus* variants total sugar release and structural features following pretreatment and digestion by two distinct biological systems. *Biotechnology for biofuels* 10:292.
271. Tian C., Beeson W. T., Iavarone A. T., Sun J., Marletta M. A., Cate J. H., Glass N. L. 2009. Systems analysis of plant cell wall degradation by the model filamentous fungus *Neurospora crassa*. *Proc Natl Acad Sci U S A* 106:22157-62.
272. Tian C., Beeson W. T., Iavarone A. T., Sun J., Marletta M. A., Cate J. H., Glass N. L. 2009. Systems analysis of plant cell wall degradation by the model filamentous fungus *Neurospora crassa*. *Proceedings of the National Academy of Sciences* 106:22157-22162.
273. Timell T. E. 1967. Recent progress in the chemistry of wood hemicelluloses. *Wood Science and Technology* 1:45-70.
274. Tumuluru J. S., Wright C. T., Hess J. R., Kenney K. L. 2011. A review of biomass densification systems to develop uniform feedstock commodities for bioenergy application. *Biofuels, Bioproducts and Biorefining* 5:683-707.
275. van Beilen J. B., Li Z. 2002. Enzyme technology: an overview. *Current opinion in Biotechnology* 13:338-344.
276. van den Brink J., de Vries R. P. 2011. Fungal enzyme sets for plant polysaccharide degradation. *Applied microbiology and biotechnology* 91:1477.
277. van Munster J. M., Daly P., Delmas S., Pullan S. T., Blythe M. J., Malla S., Kokolski M., Noltorp E. C., Wennberg K., Fetherston R. 2014. The role of carbon starvation in the induction of enzymes that degrade plant-derived carbohydrates in *Aspergillus niger*. *Fungal genetics and biology* 72:34-47.
278. van Peij N. N., Gielkens M. M., de Vries R. P., Visser J., de Graaff L. H. 1998. The transcriptional activator XlnR regulates both xylanolytic and endoglucanase gene expression in *Aspergillus niger*. *Applied and Environmental Microbiology* 64:3615-3619.
279. van Peij N. N., Visser J., De Graaff L. H. 1998. Isolation and analysis of xlnR, encoding a transcriptional activator co-ordinating xylanolytic expression in *Aspergillus niger*. *Molecular microbiology* 27:131-142.
280. Van Zyl W. H., Rose S. H., Trollope K., Görgens J. F. 2010. Fungal  $\beta$ -mannanases: mannan hydrolysis, heterologous production and biotechnological applications. *Process Biochemistry* 45:1203-1213.
281. Vanholme R., Demedts B., Morreel K., Ralph J., Boerjan W. 2010. Lignin biosynthesis and structure. *Plant physiology* 153:895-905.
282. Vaz Jr S. 2017. *Biomass and Green Chemistry: Building a Renewable Pathway*. Springer.
-

283. Viikari L., Vehmaanperä J., Koivula A. 2012. Lignocellulosic ethanol: from science to industry. *Biomass and Bioenergy* 46:13-24.
284. Vogel H. J. 1956. A convenient growth medium for *Neurospora crassa* (N medium). *Microb Genet Bull* 13:42-43.
285. Walker L., Wilson D. 1991. Enzymatic hydrolysis of cellulose: an overview. *Bioresource technology* 36:3-14.
286. Wang C., Xu M., Lv W.-p., Qiu P., Gong Y.-y., Li D.-s. 2012. Study on rheological behavior of konjac glucomannan. *Physics Procedia* 33:25-30.
287. Wang Q. Q., He Z., Zhu Z., Zhang Y. H., Ni Y., Luo X. L., Zhu J. Y. 2012. Evaluations of cellulose accessibilities of lignocelluloses by solute exclusion and protein adsorption techniques. *Biotechnol Bioeng* 109:381-9.
288. Wang S.-W., Xing M., Liu G., Yu S.-W., Wang J., Tian S.-L. 2012. Improving cellulase production in *Trichoderma koningii* through RNA interference on ace1 gene expression. *J Microbiol Biotechnol* 22:1133-1140.
289. Wen Z., Liao W., Chen S. 2004. Hydrolysis of animal manure lignocellulosics for reducing sugar production. *Bioresource Technology* 91:31-39.
290. Wermuth C. G. 2006. Similarity in drugs: reflections on analogue design. *Drug Discovery Today* 11:348-354.
291. Westergaard M., Mitchell H. K. 1947. *Neurospora V*. A synthetic medium favoring sexual reproduction. *American Journal of Botany* 34:573-577.
292. Whitney S. E., Brigham J. E., Darke A. H., Reid J. G., Gidley M. J. 1998. Structural aspects of the interaction of mannan-based polysaccharides with bacterial cellulose. *Carbohydrate Research* 307:299-309.
293. Willats W. G., Knox J. P., Mikkelsen J. D. 2006. Pectin: new insights into an old polymer are starting to gel. *Trends in Food Science & Technology* 17:97-104.
294. Willför S., Sundberg A., Pranovich A., Holmbom B. 2005. Polysaccharides in some industrially important hardwood species. *Wood Science and Technology* 39:601-617.
295. Williams C. L., Westover T. L., Emerson R. M., Tumuluru J. S., Li C. 2016. Sources of biomass feedstock variability and the potential impact on biofuels production. *BioEnergy Research* 9:1-14.
296. Wu V.-X. 2017. *Lessons in Plant Cell Wall Degradation by the Ascomycete Model Fungus, Neurospora crassa*. University of California, Berkeley.
297. Wu V. W., Thieme, Nils, Huberman, Lori B., Dietschmann, Axel, Bleek, Elias, Kowbel, David John, Lee, Juna, Calhoun, Sara, Singan, Vasanth R, Lipzen, Anna M, Xiong, Yi, Monti, Remo, Blow, Matthew J., Benz, Johan Philipp, O'Malley, Ronan C., Grigoriev, Igor V., Glass, N. Louise. 2019. The plant biomass ENCODE of a filamentous fungi (manuscript in preparation).
298. Xin D., Ge X., Sun Z., Viikari L., Zhang J. 2015. Competitive inhibition of cellobiohydrolase I by manno-oligosaccharides. *Enzyme and microbial technology* 68:62-68.
299. Xiong Y., Coradetti S. T., Li X., Gritsenko M. A., Clauss T., Petyuk V., Camp D., Smith R., Cate J. H., Yang F. 2014. The proteome and phosphoproteome of *Neurospora crassa* in response to cellulose, sucrose and carbon starvation. *Fungal Genetics and Biology* 72:21-33.
300. Xiong Y., Sun J., Glass N. L. 2014. VIB1, a link between glucose signaling and carbon catabolite repression, is essential for plant cell wall degradation by *Neurospora crassa*. *PLoS Genet* 10:e1004500.
301. Xiong Y., Wu V. W., Lubbe A., Qin L., Deng S., Kennedy M., Bauer D., Singan V. R., Barry K., Northen T. R. 2017. A fungal transcription factor essential for starch degradation affects integration of carbon and nitrogen metabolism. *PLoS genetics* 13:e1006737.
302. Yadav B. 2018. Induction of laccase in fungus, *Cyathus stercoreus* using some aromatic inducers. *Journal of Applied and Natural Science* 10:445-447.

303. Yang B., Wyman C. E. 2004. Effect of xylan and lignin removal by batch and flowthrough pretreatment on the enzymatic digestibility of corn stover cellulose. *Biotechnology and bioengineering* 86:88-98.
304. Yeh A.-I., Huang Y.-C., Chen S. H. 2010. Effect of particle size on the rate of enzymatic hydrolysis of cellulose. *Carbohydrate Polymers* 79:192-199.
305. Yoshida M., Liu Y., Uchida S., Kawarada K., Ukagami Y., Ichinose H., Kaneko S., Fukuda K. 2008. Effects of cellulose crystallinity, hemicellulose, and lignin on the enzymatic hydrolysis of *Miscanthus sinensis* to monosaccharides. *Biosci Biotechnol Biochem* 72:805-10.
306. Yu Y., Wu H. 2011. Effect of ball milling on the hydrolysis of microcrystalline cellulose in hot-compressed water. *AIChE journal* 57:793-800.
307. Zhang C., Acosta-Sampson L., Yu V. Y., Cate J. H. 2017. Screening of transporters to improve xylodextrin utilization in the yeast *Saccharomyces cerevisiae*. *PLoS one* 12:e0184730.
308. Zhang S., Wolfgang D. E., Wilson D. B. 1999. Substrate heterogeneity causes the nonlinear kinetics of insoluble cellulose hydrolysis. *Biotechnology and bioengineering* 66:35-41.
309. Zhang W., Kou Y., Xu J., Cao Y., Zhao G., Shao J., Wang H., Wang Z., Bao X., Chen G. 2013. Two major facilitator superfamily sugar transporters from *Trichoderma reesei* and their roles in induction of cellulase biosynthesis. *Journal of Biological Chemistry* 288:32861-32872.
310. Zhang X., Rogowski A., Zhao L., Hahn M. G., Avci U., Knox J. P., Gilbert H. J. 2014. Understanding how the complex molecular architecture of mannan-degrading hydrolases contributes to plant cell wall degradation. *Journal of Biological Chemistry* 289:2002-2012.
311. Zhang Y.-H. P., Himmel M. E., Mielenz J. R. 2006. Outlook for cellulase improvement: screening and selection strategies. *Biotechnology advances* 24:452-481.
312. Zhang Y. H. P., Lynd L. R. 2004. Toward an aggregated understanding of enzymatic hydrolysis of cellulose: noncomplexed cellulase systems. *Biotechnology and bioengineering* 88:797-824.
313. Zhao X., Zhang L., Liu D. 2012. Biomass recalcitrance. Part I: the chemical compositions and physical structures affecting the enzymatic hydrolysis of lignocellulose. *Biofuels, Bioproducts and Biorefining* 6:465-482.
314. Zhao Z., Liu H., Wang C., Xu J.-R. 2013. Comparative analysis of fungal genomes reveals different plant cell wall degrading capacity in fungi. *BMC genomics* 14:274.
315. Zhong R., Ye Z.-H. 2014. Secondary cell walls: biosynthesis, patterned deposition and transcriptional regulation. *Plant and Cell Physiology* 56:195-214.
316. Zhou C.-H., Xia X., Lin C.-X., Tong D.-S., Beltramini J. 2011. Catalytic conversion of lignocellulosic biomass to fine chemicals and fuels. *Chemical Society Reviews* 40:5588-5617.
317. Zhou Q., Xu J., Kou Y., Lv X., Zhang X., Zhao G., Zhang W., Chen G., Liu W. 2012. Differential involvement of  $\beta$ -glucosidases from *Hypocrea jecorina* in rapid induction of cellulase genes by cellulose and cellobiose. *Eukaryotic cell* 11:1371-1381.
318. Zhu J., Wang G., Pan X., Gleisner R. 2009. Specific surface to evaluate the efficiencies of milling and pretreatment of wood for enzymatic saccharification. *Chemical Engineering Science* 64:474-485.
319. Zhu L., O'Dwyer J. P., Chang V. S., Granda C. B., Holtzapple M. T. 2008. Structural features affecting biomass enzymatic digestibility. *Bioresour Technol* 99:3817-28.
320. Zhu L., O'Dwyer J. P., Chang V. S., Granda C. B., Holtzapple M. T. 2008. Structural features affecting biomass enzymatic digestibility. *Bioresour Technol* 99:3817-3828.
321. Znameroski E. A., Coradetti S. T., Roche C. M., Tsai J. C., Iavarone A. T., Cate J. H., Glass N. L. 2012. Induction of lignocellulose-degrading enzymes in *Neurospora crassa* by cellodextrins. *Proc Natl Acad Sci U S A* 109:6012-7.

## References

---

322. Znameroski E. A., Glass N. L. 2013. Using a model filamentous fungus to unravel mechanisms of lignocellulose deconstruction. *Biotechnol Biofuels* 6:6.
323. Znameroski E. A., Li X., Tsai J. C., Galazka J. M., Glass N. L., Cate J. H. 2014. Evidence for transceptor function of cellodextrin transporters in *Neurospora crassa*. *J Biol Chem* 289:2610-9.

## Acknowledgements

First of all, I would like to thank Prof. Dr. J. Philipp Benz for allowing me to carry out this doctoral thesis work in his research group, for always being available for helpful discussions, and for all the professional support he provided during the last years.

Furthermore, I would like to thank Prof. Dr. Jürgen Soll for being my mentor, and Prof. Dr. Caroline Gutjahr for agreeing to be my examiner. I would also like to thank Prof. Dr. Klaus Richter for taking over the chair of the examination and for the interesting discussions during my work.

During my work as part of the wood bioprocess team, I have met different interesting and helpful people that, in one way or another, contributed to the completion of this dissertation. Special thanks go to Petra and Sabrina for their technical and organizational support. Furthermore, I would like to extend my warmest thanks to Nils for always providing help and support from the early beginning till this moment. I would also like to thank the current members of the group: Maria, Kevin, Christina, Yuxin, Lisa and Manfred. I hope you all have a great time and that your research projects always go well.

I would also like to thank my former students Isabel, Verena, and Katha, and further extend my thanks to the former lab members Diana, Magdalena, and Max. Working together with you was always fun. I wish you success in your chosen paths.

Last but not least, I would like to thank my parents, Hassan and Bassima, my brothers Taleb, Hamodi, and my sisters Hana and Lili, for their endless love and care. I would like to thank my husband, Wassef, for his never ending support and motivation. Thank you for always being there and supporting me in everything!

**Name:** Lara Hassan  
**Adresse:** Lortzingstr. 5  
85057 Ingolstadt  
Deutschland  
**Telefon:** +49 172 7943058  
**E-Mail:** lara.hasan@ymail.com  
**Geboren am:** 20. November 1987 im Libanon  
**Staatsangehörigkeit:** Deutsch – Libanesisch



## Bildungsweg

---

- 05/2015 – 09/2019 **Promotion an der Technischen Universität München in der Professur für Holz-Bioprozesse; Freising**  
Titel: An investigation of the interaction between filamentous ascomycetes and lignocellulosic substrates
- 09/2012 - 09/2014 **Masterabschluss in Applied Plant Biotechnology an der Libanesischen Universität; Beirut, Libanon**  
Schwerpunkte: Biotechnologie, Zellbiologie, Mikrobiologie, Pflanzengenetik
- 10/2008 – 03/2012 **Biologiestudium an der Libanesischen Universität; Beirut, Libanon**  
Bachelor of Science, Biologie

## Praktische Erfahrung

---

- 02/2014 - 11/2014 **Masterarbeit an der Freien Universität Berlin, Institut für Angewandte Genetik; Berlin**  
Titel: Characterization of a putative cytokinin receptor CHARK in rice  
Department of Applied Genetics
- 07/2013 - 09/2013 **Praktikum am Libanesischen Institut für landwirtschaftliche Forschung; Tal Amara, Libanon**  
Titel: Micro propagation of Mulberry
- 03/2013 - 07/2013 **Masterprojekt an der Libanesischen Universität; Beirut, Libanon**

---

Titel: Micro propagation of *Olea Europaea* (Olivenbaum)

## Fortbildungen

---

12/2018	<b>Kurs:</b> Relational Leadership; TUM, Freising
07/2018	<b>Kurs:</b> Basics in Business Administration; TUM, Freising
06/2018	<b>Kurs:</b> Writing Scientific Proposal; TUM, Freising
02/2018	<b>Kurs:</b> Internationales Project Management, Alumni portal Deutschland
01/2018	<b>Kurs:</b> Women in science; TUM, Freising
11/2017	<b>Workshop:</b> Biotech quality management / regulatory affairs management; TUM, Freising
11/2017	<b>Workshop:</b> Project Management in Biotech Industries; TUM, Freising
11/2017	<b>Kurs:</b> Stress release for the scientific minded; TUM, Freising
05/2017	<b>Kurs:</b> Communication in teams in difficult situations; TUM, Freising
10/2015	<b>Seminar:</b> Time Management; TUM, Garching

## Sprachkenntnisse

---

<b>Arabisch</b>	Muttersprache
<b>Deutsch</b>	Gut in Wort und Schrift
<b>Englisch</b>	Fließend in Wort und Schrift

## EDV-Kenntnisse

---

<b>Microsoft Office:</b>	Sehr gute Kenntnisse in Word, Excel, PowerPoint und MS Project
<b>SPSS</b>	Sehr gute Kenntnisse
<b>ImageJ</b>	Gute Kenntnisse
<b>Datenbanknutzung</b>	Sehr gut

Lara Hassan

Ingolstadt, den .....

**This thesis is based on the following publications:**

1. Hassan Lara, Lin Liangcai, Sorek Hagit, Sperl Laura, Goudoulas Thomas, Hagn Franz, Germann Natalie, Tian Chaoguang, and Benz J. Philipp. Cross-talk of cellulose and mannan perception pathways leads to inhibition of cellulase production in several filamentous fungi. 2019. MBio, 10(4), e00277-19.
2. Hassan Lara, Reppke Manfred J, Thieme Nils, Schweizer Steffen A, Mueller Carsten W, Benz J Philipp. 2017. Comparing the physicochemical parameters of three celluloses reveals new insights into substrate suitability for fungal enzyme production. Fungal Biology and Biotechnology 4:10.